

SPECTRUM EFFICIENCY ENHANCEMENT USING NOMA AND COOPERATIVE SPECTRUM SHARING IN 5G NETWORKS

Thesis Submitted for the Award of the Degree of

DOCTOR OF PHILOSOPHY

in

(Electrical Engineering)

By

Mohamed Hassan Babikir Eisa

Registration No: 11816074

Supervision By

Dr. Manwinder Singh, 25231

**Electronics and Electrical Engineering
Wireless Communication**

Co-supervision By

Dr. Khalid Hamid, 176256

**Communication Engineering
Wireless Communication**



LOVELY PROFESSIONAL UNIVERSITY, PUNJAB 2023

DECLARATION

I hereby declared that the presented work in the thesis entitled "**Spectrum Efficiency Enhancement Using NOMA and Cooperative Spectrum Sharing in 5G Networks**" in fulfilment of the degree of **Doctor of Philosophy (Ph.D. Electronics and Electrical Engineering)** is the outcome of research work carried out by me under the supervision of Prof. Manwinder Singh, working as Professor, in the Department of Wireless Communication of Lovely Professional University, Punjab, India and under the co-supervision of Prof. Khalid Hamid from Professor, University of Science and Technology, Khartoum, Sudan. In keeping with the general practice of reporting scientific observations, due acknowledgements have been made whenever the work described here has been based on the findings of other investigators. This work has not been submitted in part or full to any other University or Institute for the award of any degree.



Name of the scholar: Mohamed Hassan Babikir Eisa.

Registration No: 11816074.

Department/School: Wireless Communication.

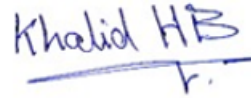
Lovely Professional University, Punjab, India.

CERTIFICATE

This is to certify that the work reported in the Ph.D. thesis entitled "Spectrum Efficiency Enhancement Using NOMA and Cooperative Spectrum Sharing in 5G Networks" submitted in fulfilment of the requirement for the reward of the degree of **Doctor of Philosophy (Ph.D. Electronics and Electrical Engineering)** in the Department of Wireless Communication, is a research work carried out by Mohamed Hassan Babikir Eisa, (Registration No.: 11816074), is bona fide record of his original work carried out under my supervision and that no part of the thesis has been submitted for any other degree diploma or equivalent course.



Name of supervisor: Dr. Manwinder Singh.
Designation: Professor.
Department/School: Wireless Communication.
University: Lovely Professional University.



Name of Co-supervisor: Dr. Khalid Hamid.
Designation: Professor.
Department/School: Communication.
University: University of Science and Technology.

Acknowledgement

All praise be to Allah, the Most Gracious and Merciful, for giving me life and the wisdom to pursue my Ph.D. (Electronics and Electrical Engineering) program at Lovely Professional University, Phagwara, Punjab, India. May Allah's peace and blessings be upon his messenger, Prophet Muhammad (S.A.W).

I would like to express my heartfelt appreciation to the Sudanese Embassy in India, represented by Mr. Mohamed Al-Fatih and Mr. Manish Kumar, International Admissions at LPU, for closely following them and finding solutions to all the problems I encountered. My heartfelt gratitude goes to Dr. Rashid Saeed at Taif University and Dr. Emad El-Din El-Sayed at the University of Malaysia Pahang for their unwavering support.

My sincere thanks go out to my wonderful friends and colleagues, especially Mr. Abubakar Sauti and Mr. Habibu Abdullahi, whose encouragement and contributions to this success have been enormous. Their names are too many to list here. Their contributions will be remembered forever.

Dedication

Dedicated to my parents and family.

Contents

Title page	I
Dedication	v

CHAPTER ONE

Introduction

1.1. Background.....	1
1.1.1. Cooperative for Spectrum Sharing.....	6
1.1.2. Uncooperative spectrum sharing	6
1.2. Problem Statement	7
1.3. Motivation for the Study	8
1.4. Objectives	8
1.5. Research Methodology	8
1.6. Scope and Limitations	9
1.7. Thesis Layout	9

CHAPTER TWO

Literature Review

2.1. Fundamental concepts	10
2.2. Orthogonal Multiple Access (OMA)	10
2.2.1. Time Division Multiple Access (TDMA)	11
2.2.2. Code Division Multiple Access (CDMA)	11
2.2.3. Orthogonal Frequency Division Multiple Access (OFDMA)	12
2.3. Non-Orthogonal Multiple Access (NOMA)	13
2.3.1. Power Domain (PD) NOMA	15
2.3.2. Transmission Downlink With NOMA	15
2.3.3. NOMA for the Uplink	16
2.3.4. Superposition Coding (SC)	17
2.3.5. Successive Interference Cancellation (SIC)	18
2.4. NOMA Downlink	20
2.5. Cooperative NOMA	22
2.6. 5G Concept	23
2.6.1. 5G Mobile Network Spectrum	24
2.7. Spectrum Efficiency Technique	25
2.8. The Principles of Cognitive Radios	26
2.8.1. Critical roles of CR	26
2.8.2. Benefits of Cognitive Radio	26
2.8.3. Sensing of the Spectrum (SS)	27

2.8.4. The Spectrum Analyzer (SA)	28
2.8.5. The Spectrum Decision (SD)	29
2.8.6. Mobility of the Spectrum	29
2.8.7. Sharing of the Spectrum	30
2.9. Cognitive Radio NOMA (CR-NOMA)	32
2.10. Multiple Input Multiple Output (MIMO)	33
2.11. Massive MIMO	34
2.12. Obstructive Parameters of the Surrounding Environment for Wireless Communications	35
2.12.1. Noise	35
2.12.2. Fading	36
2.12.3. Inter Symbol Interference (ISI)	36
2.13. Quality of Service (QoS)	36
2.13.1. Spectral efficiency	37
2.13.1.1 Spectral efficiency (SE) of 5G NR	37
2.13.2. Throughput	37
2.13.3. Bandwidth (BW)	38
2.13.4. Channel Capacity.....	39
2.13.5. Signal-to-noise ratio (SNR)	39
2.13.6. Bit Error Rate (BER)	39
2.13.7. Outage Probability (OP)	39
2.14. Related Works	40

CHAPTER THREE

Modeling of NOMA-MIMO Based Power Domain for 5G Network Under Selective Rayleigh Fading Channels

3.1. Introduction	45
3.2. DL PD-NOMA Model	45
3.3. UL PD-NOMA Model	47
3.3.1. UL NOMA Capacity Rates attained by Four Users	48
3.3.2. The UL NOMA OP of Four Users	49
3.4. Parameters for Simulation	50
3.5. Computer Model	51
3.6. Results and Discussion	54
3.6.1. The DL NOMA Model's Outcomes	54
3.6.2. The UL NOMA Model's Outcomes	60
3.7 Summary	67

CHAPTER FOUR
Average Rate Performance for Pairing Downlink
NOMA Networks Schemes

4.1. Introduction		68
4.2. System Model		69
4.2.1. NOMA, the first strategy to match nearby and far users (N-F)		70
4.2.2. NOMA Using the Alternate Approach of Close-to-Close or Remote-to-Remote Pairing (C-C, R-R)		71
4.3. Simulation Parameters		72
4.4. Computer Model		73
4.5. Result and Discussions		74
4.7. Summary		76

CHAPTER FIVE
Outage Probability Enhancement for DL Cooperative NOMA in 5G
Network

5.1. Introduction		77
5.2. System Model		78
5.2.1. Models of the DL PD NOMA and DL PD Cooperative NOMA Method.....		78
5.2.2. Models of the DL PD Cooperative NOMA with MIMO and Massive MIMO.....		79
5.2.3. Slot for Direct Transmission		81
5.2.4. The Slot for Relaying		81
5.2.5 Combining Diversity.....		81
5.3. Simulation Parameters		82
5.4. Results and Discussions		82
5.5. Summary		87

CHAPTER SIX
Spectrum Efficiency in 5G Networks Using Cooperative
Cognitive Radio NOMA

6.1. Introduction		89
6.2. System Model		90
6.2.1. DL-NOMA		90
6.2.1.1. Competitive Channel (C-CH) CCRN-NOMA		91
6.2.1.2. Dedicated Channel (D-CH) CCRN-NOMA		94
6.2.2. MIMO DL PD NOMA		94

6.2.3. Massive MIMO DL PD NOMA	95
6.3. Simulation Parameters	96
6.4. Computer Model	96
6.5. Results and Discussions	99
6.5.1. DL-NOMA Scenario Results	99
6.5.2. MIMO-DL-NOMA Scenario Results	108
6.5.3. Massive MIMO-DL-NOMA Scenario Results	116
6.6. Summary	124

CHAPTER SEVEN
Summary and Conclusion

7.1. Introduction	126
7.2. Summary	126
7.3. Conclusion	127
7.4. Future Research	128
List of Publications	130
References	135

List of Tables

2.1. The 5G Frequency Classification	25
2.2 Author's Contribution Table.....	44
3.1. DL Scenario Simulator Parameters	50
3.2. UL Scenario Simulator Parameters	51
4.1 Details the Simulation Settings	72
5.1. The List of Variables Used in the Simulation	82
6.1. Simulation settings for scenarios 1, 2, and 3.....	96

List of Figures

2.1. Construction of the NOMA System.....	14
2.2. The NOMA scheme's TP levels	15
2.3. NOMA for N-user DL transmissions	16
2.4. NOMA for N-user UL	17
2.5. Depicts the SIC procedure and the techniques in the N-user DL scenario.....	19
2.6. Methods of the SIC in the N-user DL Scenario.....	20
2.7. Displays the various application KPIs requirements.....	24
2.8. 5G Network Spectrum.....	25
2.9. The Cognitive Radio Process.....	27
2.10. The MIMO system utilizing NT transmitters and NR receivers.....	34
2.11. The BW of the channel.....	38
3.1. The wireless network has four users with 64x64 MIMO PD DL-NOMA	46
3.2. Shows the four-user 64x64 MIMO UL PD-NOMA wireless network.....	48
3.3. DL-NOMA Flowchart Scenario.....	52
3.4. UL-NOMA Flowchart Scenario.....	53
3.5. DL NOMA at 80 MHz BW: BER against TP for four 4 users located at 55 different distances	55
3.6. DL NOMA at 200 MHz BW: BER versus TP for four users at varying 55 distances.....	55
3.7. BER for four users in DL-NOMA against TP for 64x64 MIMO at 80 MHz 56 BW	56
3.8. BER versus TP in DL NOMA with 4 Users and 200 MHz BW using 64x64 MIMO	57
3.9. Four users at various distances, SE versus TP, 80 MHz BW for DL NOMA....	58
3.10. DL NOMA SE compared to TP for four users located at different distances with the BW of 200 MHz	58
3.11. SE versus TP for four users at varying distances, using 64x64 MIMO and the BW of 80 MHz in DL NOMA	59
3.12. SE versus TP for four users at varying distances, with 64x64 MIMO and BW 200 MHz for DL NOMA.....	60
3.13. Average capacity against SNR for four UL NOMA users at varied distances and BW 80 MHz	61
3.14. The relationship between average capacity and SNR for four users at various distances and BW 200 MHz in UL NOMA	62
3.15. The average capacity vs SNR for UL NOMA with 64x64 MIMO and 80 MHz BW for four users at different distances....	63
3.16. The average capacity against SNR for UL NOMA with 64x64 MIMO and 200 MHz BW for four users at varied distances.	63

3.17. Four users at varying distances and a bandwidth of 80 MHz are considered for UL NOMA's OP versus SNR.....	64
3.18. The UL NOMA's OP vs. SNR takes into account four users at different distances and the 200 MHz BW.....	65
3.19. UL NOMA with 64x64 MIMO and the 80 MHz BW pits OP vs SNR for four users at varying distances.....	66
3.20. For four users at different distances, UL NOMA with 64x64 MIMO and the 200 MHz BW compares OP and SNR.....	66
4.1. Displays how users are assigned to various multiple access methods.....	69
4.2. Shows a model of the downlink transmission system with six users at varying distances.....	70
4.3. Flowchart of PD DL-NOMA for four cases.....	73
4.4. Presents six users' average sum rates vs. SNR at varying distances using three distinct multiple-access approaches (NOMA using the initial scheme of pairing, SC-NOMA, and TDMA).....	74
4.5. The average total vs. SNR for six users at three different distances utilizing three distinct multiple access approaches is depicted (NOMA with the second scheme of pairing, SC-NOMA, TDMA).....	75
5.1. Transmitting DL PD NOMA network.....	78
5.2. Transmission in the DL for the cooperative NOMA.....	79
5.3. Cooperative NOMA network DL transmission using 16x16, 32x23, and 64x64 MIMO	79
5.4. DL transmission in a cooperative NOMA network utilizing 128x128, 256x256, and 512x512 M-MIMO	80
5.5. DL OP versus SNR for distant cooperative NOMA users with 0.8, 0.6 PLCs.....	83
5.6. DL OP vs. SNR for remote cooperative NOMA users with 0.8, 0.6 PLCs	84
5.7. DL OP versus SNR for NOMA and cooperative NOMA distant users using various PLCs	85
5.8. A DL OP vs. SNR analysis of cooperative NOMA distant users using various MIMO techniques.....	86
5.9. Comparing the DL OP vs SNR for cooperative NOMA distant users with and without varying massive MIMO configurations.	87
6.1. Displays the DL-NOMA PD network configured with (N) users.....	90
6.2. Model of the system with DL- PD NOMA and CCRN for N users.....	92
6.3. Transmission of CR is possible during a brief window.....	93
6.4. Flowchart of PD DL-NOMA for three scenarios.....	98

6.5. SE against TP for four DL PD NOMA users.....	100
6.6. SE versus TP for four DL CCR- PD NOMA users with C-CH.....	101
6.7. SE vs. TP for four DL CCR- PD NOMA users using D-CH.....	101
6.8. Four DL PD NOMA users' average capacity against TP	103
6.9. Four DL CCR- PD NOMA users average capacity versus TP with C-CH	104
6.10. Four DL CCR- PD NOMA users average capacity vs TP with D-CH	104
6.11. BER vs. TP for four DL NOMA PD users.....	106
6.12. BER against TP for four DL CCR-NOMA PD users with C-CH.....	107
6.13. BER versus TP for four DL CCR-NOMA PD users with D-CH.....	107
6.14. SE against TP for four MIMO DL PD NOMA users	109
6.15. SE versus TP for four MIMO DL CCR- PD NOMA users with C-CH.....	110
6.16. SE vs. TP for four MIMO DL CCR- PD NOMA users using D-CH.....	110
6.17. Average capacity versus TP for four MIMO DL PD NOMA users.....	112
6.18. Average capacity versus TP for four users MIMO DL CCR- PD NOMA with C-CH.....	113
6.19. Average capacity versus TP for four users MIMO DL CCR- PD NOMA with D-CH	113
6.20. BER vs. TP for four MIMO DL NOMA PD users.....	115
6.21. BER against TP for four MIMO DL CCR-NOMA PD users with C-CH.....	116
6.22. BER versus TP for four MIMO DL CCR-NOMA PD users with D-CH.....	116
6.23. SE against TP for four M-MIMO DL PD NOMA users.....	118
6.24. SE versus TP for four M-MIMO DL CCR- PD NOMA users with C-CH.....	118
6.25. SE vs. TP for four M-MIMO DL CCR- PD NOMA users using D-CH.....	119
6.26. Average capacity versus TP for four M-MIMO DL PD NOMA users.....	120
6.27. Average capacity versus TP for four users M-MIMO DL CCR- PD NOMA with C-CH.....	121
6.28. Average capacity versus TP for four users M-MIMO DL CCR- PD NOMA with D-CH.....	121
6.29. BER vs. TP for four M-MIMO DL NOMA PD users.....	123
6.30. BER against TP for four M-MIMO DL CCR-NOMA PD users with C-CH.	123
6.31. BER versus TP for four M-MIMO DL CCR-NOMA PD users with D-CH..	124

Abstract

One of the best strategies for maximizing the capacity of 5G and future-generation networks is non-orthogonal multiple access (NOMA). By integrating NOMA into the cognitive radio network (CRN), a new era of communications is on the horizon. There has been a rise in the importance of wireless connectivity metrics like spectrum efficiency (SE), average capacity, and bit error rate (BER) due to the proliferation of mobile service use, particularly for real-time applications. Modeling and designing power domain (PD) NOMA technologies and analyzing the impact that varying the bandwidth (BW) and the number of antennas has on the 5G network's BER, SE of the downlink (DL), average capacity, and outage probability (OP) are all reevaluated and introduced in Chapter three. In Chapter Four, two coupling strategies for DL NOMA networks are proposed: near-far (NF) coupling and close-and-close (C-C), or far-and-far (f-f) coupling. The overall average rate versus SNR of six users is determined using the proposed methods of single carrier NOMA (SC-NOMA) and time division multiple access (TDMA) at different intervals and distances. The cooperative NOMA methods have a huge amount of potential to solve several problems with the next generation of wireless networks by providing unprecedented levels of connectivity and speed. In Chapter Five, it was demonstrated how the power location coefficient (PLC) affects the performance of NOMA, cooperative DL NOMA, multiple-input multiple-output (MIMO) cooperative DL NOMA, and massive MIMO (M-MIMO) cooperative DL NOMA for far users in 5G networks by measuring the coefficient OP. In Chapter six, the SE, average capacity, and BER of DL PD NOMA combined with a new approach to the cooperative cognitive radio network (CCRN) through a competitive channel (C-CH) or a dedicated channel (D-CH), 64x64 MIMO, 128x128 M-MIMO separation distances in the 5G network were evaluated and explored. The analysis of the proposed systems is performed under the assumptions of additive white Gaussian noise (AWGN) and Rayleigh fading, and it also takes into account successive interference cancellation (SIC) and unstable channel conditions. Implement all simulations using the MATLAB software program. When comparing the obtained results with previous works, the outcomes of the presented methods are significantly improved.

CHAPTER ONE

Introduction

This chapter offers a concise overview of the study's motivation, scope and constraints, methodology, and some fundamental definitions, as well as a few ways to increase Spectrum Efficiency (SE) for Non-Orthogonal Multiple Access (NOMA) in 5G networks.

1.1 Background

Wireless networks have undergone several advancements in recent decades. Multiplexing techniques are a crucial advance in access methods, enabling numerous users to communicate over a single wired or wireless channel. Multiplexing, sometimes referred to as access, is essential for radio stations to optimize their utilization of tools and resources by collaborating effectively. The technologies may be categorised into two distinct classes: orthogonal multiple access (OMA) and NOMA [1]-[2]-[3].

Various access technologies, such as orthogonal frequency division multiple access (OFDMA), code division multiple access (CDMA), time division multiple access (TDMA), and frequency division multiple access (FDMA), have been utilised by wireless network technologies spanning from the first generation to the fifth generation. Conventional orthogonal multiple access (OMA) methods enable the broad provision of orthogonal radio services in the time, frequency, and/or coding domains [4]-[5]-[6].

Users just need to broadcast a single signal utilizing their FDMA frequency resource, and the receiver can readily decode information from any user regardless of the frequency range it was broadcast on. By assigning orthogonal spread sequences to their transmitted symbols, users in a CDMA network can share the available bandwidth and processing time by designating orthogonal spread sequences for their transmitted symbols. OFDMA is a hybrid approach that uses a time-flow grid to allocate radio resources, similar to the way FDMA and TDMA operate [6]-[7].

Nevertheless, the limited quantity of orthogonal resources hampers the capacity of conventional OMA systems to accommodate a substantial number of connections. Additionally, theoretical research has demonstrated that OMA isn't always successful in reaching the maximum achievable rate in multi-user wireless networks. In addition, a set range of interference prevention

mechanisms must be implemented in all OMA technologies, which wastes resources, particularly the spectrum [8].

In contrast to NOMA, which is fundamentally different. In NOMA, the sole distinguishing factor among users is their relative output power within the power domain (PD) type. Every user has identical frequency and time slot allocations. The NOMA transmitter utilizes superposition coding (SC) to separate the downlink (DL) and uplink (UL) signals, enabling the receiver to conduct successive interference cancellation (SIC) to isolate individual users [9]-[10]-[11].

NOMA, in addition to its conventional multiple access applications, can be regarded as a spectrum-sharing solution because it allows parallel transmissions on the same frequency range. 4G used OFDM technology, which utilized a non-orthogonal characteristic to speed up power management (rapid transmission power (TP) control), to counteract the distance effect [12].

However, NOMA is in the power domain (PD). Each user must use a separate path loss to achieve multi-user multiplexing in a new domain of power. Using a novel technique based on path loss, NOMA can superimpose the transmission signals of many channels. Because of this, it's clear that stronger signals are advantageous. This means that all the mobile devices within the same cell tower's service area can theoretically share the same high-speed Internet connection. In NOMA, multiple users share a single block of resources like radio channels, time, or code distribution [13]-[14]-[15]-[16]-[17].

Transmission power (TP) is increased for user equipment (UE) that is further from the base station (BS) while using NOMA DL, UEs closer to the BS have a reduced value. Every piece of user equipment in a network receives an identical signal, which contains all the users' data. Before calculating the total received signal strength, each User UE determines which signal is the strongest and decodes it separately.

The SIC receiver uses iterative removal to locate the necessary signal. Nearby UEs can prevent signals from far UEs by interacting with the BS. The UE with the strongest signal will have its signal decoded first [18]-[19] because it has the greatest impact on the overall received signal strength.

The two types of NOMA implementations, UL and DL, have a few subtle distinctions. BS now makes use of SIC to identify and isolate individual user

signals. The BS on the receiving end is responsible for putting the SIC into action. That is to say, the signal of the closest user will be deciphered first.

Each new generation of mobile communication schemes introduces novel multiplexing techniques. Upon examining the historical development and intricate nature of mobile communications, it becomes evident that the initial generation (1G) was distinguished by a singular voice service known as FDMA. This technology facilitated rates of up to 2.4 kbps. The transition from 1G to second generation (2G) on his cellular phone was the first time he had made much progress. Understanding the difference between the analogue radio transmission used by 1G networks, and the digital signals used by 2G networks, is critical to understanding the distinction between the two generations of mobile networks.

The key factors that pushed this generation forward were the need for a safe and dependable communication system, a data exchange rate of 144 kbps, and TDMA being used as the channel access technique. Third-generation (3G) WCDMA devices are the benchmark for features like online and email access, video and photo downloads, sharing, and voice calls.

Four generation (4G) aims to provide its users with low latency in voice calls, multimedia presentations, and the Internet by leveraging the Internet protocol (IP). This will allow for faster data transfer speeds and higher-quality video. OFDM-based cloud computing enables state-of-the-art internet access on mobile devices, IP telephony, video conferencing, and more with a maximum speed of around 1 gigabit per second (Gbps) [20]-[21]-[22]-[23].

The fifth-generation (5G) wireless network is the most recent development in cellular technology. Thanks to the possibilities enabled by 5G networks, a variety of electronic gadgets, beyond only individuals and their smartphones, will be able to connect with each other[24]-[25]-[26].

The development of 5G wireless technology will enable peak data rates of several Gbps, extremely low latency, higher reliability, massive network capacity, improved availability, and a more consistent user experience. Improved functionality and efficiency enable new user experiences and industry ties. The highest capacity of 5G is predicted to be 20 Gbps, allowing for multi-giga-bitrates while delivering data through wireless internet connections. The latency of these connections is five milliseconds or less, making them superior

to landline networks and perfect for time-sensitive programs. With 5G's improved bandwidth (BW) and antenna enhancements, wireless data transmission capacity will increase dramatically. [27]-[28]-[29].

The effective deployment and acceptance of 5G technology necessitates the resolution of several technological obstacles. Several primary obstacles exist:

Challenges related to the allocation of frequency bands and the availability of spectrum: Securing appropriate frequency bands and spectrum poses a significant obstacle to the adoption of 5G technology. The assignment and release of spectrum require a significant amount of time and might involve intricate and expensive procedures.

Strategy for implementing 5G network: Implementing 5G networks necessitates a substantial investment in infrastructure, encompassing the construction of fresh BSs, antennas, and additional equipment. Deploying may be a difficult process, and it can also be rather expensive.

Enhancing mobile devices: It is necessary to upgrade mobile devices at the user end to ensure compatibility with 5G technology. This can provide a difficulty, particularly in regions where consumers may lack access to the most recent technology or may be unable to pay for upgrades.

Overseeing the costs associated with the implementation of 5G technology networks: The implementation of 5G networks necessitates substantial financial resources, and effectively managing these expenses might pose a difficulty. Operators must carefully manage the expenses associated with acquiring spectrum, building network infrastructure, and upgrading devices, while also considering the money earned from 5G services.

The 5G specs exhibit a high level of intricacy and variety. The 5G requirements are intricate and varied, posing challenges in the development and deployment of 5G technology. The spectrum allotment, investment in 5G technology, and implementation of 5G networks are progressing at a sluggish pace. This can impede the accessibility of 5G services and hinder the widespread adoption of 5G technology. The deployment of 5G technology requires significant investment in infrastructure, including the allocation of spectrum, and the utilization of high-speed switches and routers. Capabilities and difficulties of a

developing network, 5G technology offers the potential for new applications and services, but it also brings up problems with the availability of spectrum.

To summarise, the effective deployment and uptake of 5G technologies are hindered by many technological problems that must be resolved. The challenges encompass various aspects such as frequency band and spectrum availability, strategies for deploying 5G networks, upgrading mobile devices, managing expenses associated with 5G network deployment, allocating spectrum, making investments, and deploying the network.

Today's wireless networks suffer from limited range and inadequate BW. As a result, wireless networks will need to develop in the next decade so they can keep up with the growing demand for traffic and services before the spectrum is completely exhausted [30]. When multiple users in different locations and periods share the same frequency band, spectrum usage can be maximized while also accommodating the anticipated increase in demand (i.e., counter BW scarcity).

The issue of increased spectrum sharing might potentially be addressed using Professor Mitola's "Cognitive Radio (CR)" methodology. In order to provide radio and wireless services, it is essential to establish a system that allows users to (a) determine the type of connections they need and (b) obtain these connections through wireless digital assistants and associated networks.

Both of these objectives must be met simultaneously [31]-[32]. The CR is constantly monitoring its environment and adjusting its settings to make the most efficient use of available BW. For the most part, it's safe to reuse frequency channels that have already been in use for transmissions for around 90% of the time, so this tactic's main goal is to maximize spectrum utilization.

Depending on the circumstances, CR will either transmit all the available frequencies in a region or limit their use to a particular time and location. Don't bother the current user while they're using this blank tape, but feel free to take advantage of the tape's versatility for your purposes. Hence, it is crucial to distinguish between the primary user (PU) and the secondary user (SU) in the context of the cognitive radio (CR) architecture. Authorized user and primary user authentication are given top priority. Since BW has been enhanced, more material and faster transmission rates for services can be provided. To achieve

CR, one must first sense the spectrum, analyze the spectrum, and make decisions regarding the spectrum and how to move within the spectrum [33]-[34]-[35].

Spectrum sharing maximizes the usefulness of wireless radiofrequency, this method is essential for preventing interference between cognitive radio and primary licensing. There are two options for achieving this [36].

1.1.1 Cooperative for Spectrum Sharing

This spectrum accommodates both a centralized data hub and a decentralized network-wide control channel. The first approach is more precise, but it takes significantly longer, has a more complicated implementation, and uses more energy than the second approach [37]-[38]. Collaboration between PUs and SUs also has SE benefits.

1.1.2 Uncooperative Spectrum Sharing

There is no way for individual users to exchange data, but this is perfect for facilitating communication between a small number of cognitive user networks [37]-[38].

The CR endeavour can be ranked as such, depending on the spectrum utilization scenario:

Interweaving is the process by which one user (SU) can only broadcast when another user (PU) is not using the licensed spectrum.

If the impact on the primary network is kept to a minimum, data can be sent on both the primary and secondary levels simultaneously over an underlay. This is possible if the underlay is used.

Third, an SU sends its signal while also making use of the major network's transmission infrastructure.

When compared to conventional OMA, NOMA's central notion is to maximize spectral efficiency (SE) for multiple users over a shared network by multiplying their respective power inputs. NOMA and CR spectrum sharing have been combined in this innovative new field of study.

5G necessitates high performance, high connection, and low latency, all of which can be provided by a cooperative effort between NOMA and CR. Despite its immense potential, NOMA is a difficult problem to solve cognitively given that interference affects both NOMA and CR, the former leads to NOMA multiplexing in the latter's control domain, which in turn causes significant inter-network interference of the latter. There are several types of interference [39]-[40]-[41], including primary interference, secondary interference, and intra-network (or co-channel) interference.

For this reason, it is crucial to effectively integrate NOMA and CR to lessen interference and maximize the system's primary resources. Cognitive NOMA (C-NOMA) seeks to improve spectrum sharing through proactive means by merging CR and NOMA spectrum sharing. Enhanced SE, massive connectivity, low latency, and greater fairness are just a few of the many advantages of the cognitive shared NOMA spectrum.

For next-generation radio networks to lessen the possibility of interference while making the most efficient use of the spectrum, greater familiarity and coordination are required. Radio stations can't make the most of their resources and potential without strong teamwork. The most efficient use of the hybrid broadcasting spectrum also requires that intelligent radios in an integrated system can communicate with radios they have never seen before. These radios need to be built to communicate in crowded and contested areas, as well as to convey the frequency band that may be used by a diverse set of radios without requiring central coordination or pre-allocated airwaves [41].

1.2 Problem Statement

The problems of this research are:

1. The signal between the transmitter and receiver for cognitive NOMA network is impaired by different parameters such as imperfect channel information, noise, fading and interference which degrade network quality of service performance and spectrum efficiency.
2. NOMA schemes make the spectrum efficiency and channel capacity utilization well, however, there is a great interference between the users.
3. How can the dynamic spectrum access method significantly improve spectrum utilization efficiency without losing the advantages associated with the static spectrum allocation scheme?

1.3 Motivation for the Study

The relevance of the research is in its ability to totally utilize the spectrum, reduce the BER, and increase the capacity to improve the quality of service (QoS).

1.4 Objectives

The objectives of this research are:

1. To study and analyze the performance of NOMA-based cooperative spectrum sharing in 5G Networks.
2. To design and simulate a CR - NOMA-enabled 5G network.
3. To enhance the efficiency of NOMA using cooperative spectrum sharing.
4. To compare the proposed system with existing techniques using potential parameters for NOMA-enabled 5G Networks.

1.5 Research Methodology

Depends on the ideas of cooperative spectrum sharing and NOMA in the 5G network. In this framework, the following phases approach to describe the research methodology.

- **Phase one:** Description Methodology, Utilizing the survey literature in our study, that is, the current books and literature related to our topic will be studied to get the idea of model formulation and solution technique.
- **Phase two:** Analytical Methodology, to Analyze NOMA and cooperative spectrum sharing algorithms.
- **Phase three:** Modeling Methodology, for developing a new model, for proposed solutions.
- **Phase four:** Simulation Methodology, to simulate the new model using a MATLAB software program.
- **Phase five:** Examine the performance results for the new proposed model versus the conventional model in terms of spectrum efficiency (SE), average capacity, BER, and outage probability (OP).

1.6 Scope and Limitations

This study is concerned only with DL NOMA PD and CR strategy using energy sensing in the 5G network with limiting factors of (4 to 6) users, BW (60-200) MHz, distances (d) between (50-1000) m, and Rayleigh fading channels.

1.7 Thesis Layout

The thesis is laid forth as follows. The literature review will be presented in chapter two. Algorithms for the proposed methods will be discussed in chapters three through six. A summary and conclusions will be offered in chapter 7.

CHAPTER TWO

Literature Review

This chapter describes the technical knowledge used in this thesis. The background work for OMA and NOMA is set, with subjects like CR, CR-NOMA design, multiple-input multiple-output (MIMO) cooperative DL NOMA, and massive MIMO (M-MIMO) covered. The literature on the subject, focusing on papers that discuss DL NOMA and CR, was reviewed.

2.1 Fundamental concepts

Multiple access is the capability of a wireless communication system to simultaneously serve to route several transmitters and receivers over a single channel utilizing time, frequency, or coding. Creating channels requires first dividing the available resources in an orthogonal or semi-orthogonal way. Although each sender may have its own data-transfer capabilities, users will still be limited to the BW that the receiver makes available to everyone. The idea behind multiple-access technology is to get the most out of scarce resources like energy and BW with as little disruption as possible. Multiple access refers to the practice of allocating distinct channels to individual users. It is commonly used in telephone systems where voice signals are allocated to dedicated channels. The term "random multiple access" refers to a way of sharing BW that depends on burst transmissions but does not ensure access to the channel that has been allotted. Whether a system employs multiple access or random access and what kind of channelization is utilized depends on its specifications and adaptability. Increased channel capacity is achieved by sharing BW [42]. OMA, on the one hand, and NOMA, on the other [43].

2.2 Orthogonal Multiple Access (OMA)

The channels in an OMA system are used to distribute the system's power or BW among its users. Using a variety of basic functions, the receiver in this system can isolate the signal of interest from background noise [43]. Frequency, time, and encoding are only some of the ways that the channel might be divided. The effectiveness of various techniques for dividing traffic into manageable chunks varies widely and is highly context-dependent. OMA's many advantages include its resistance to the near-far effect and its use of higher-order modulation techniques to boost the rate of a single user. It also helps prevent intra-cell

interference by allocating distinct signal sub-spaces to each user. With a straightforward receiver design, OMA systems can provide high throughput for packet-based service delivery [44]. OMA is inefficient in terms of spectral power usage and is sensitive to cross-cell interference and synchronizing frames to preserve orthogonality [45]. OMA is the basis for all of today's wireless networks, even though it was developed more than a decade ago. [46] While 2G networks use TDMA and FDMA, 3G networks use CDMA and 4G networks use OFDMA as their primary mode of operation.

2.2.1 Time Division Multiple Access (TDMA)

Digital transmission systems, whether wireless or wire, frequently use TDMA, a type of multiple access [47]. The channel access method (CAM) is a good option for shared media network situations. To allow for simultaneous use by several users, a single radio frequency is typically partitioned into "time slots" [48]. The users are given time slots that will be used to send and receive data regularly. This is because each user sends out a series of data bursts in quick succession, separated by a guard interval to prevent overlap [49]. The ability to perform the handoff during idle times also allows the user to save battery life by turning off the transmitter when it is not in use.

TDMA is commonly used in conjunction with FDMA because using various carrier frequencies in separate cells results in improved user BW. Reusing these frequencies in more distant cells reduces the likelihood of interference. Additionally, a cell may have a significant number of carrier frequencies, each of which may contain its own TDMA bit stream in addition to a collection of user terminals [47]-[50]. Depending on the BW available, TDMA can be either wideband or narrowband. Technology such as digitally enhanced cordless technology (DECT), wireless networks, and second-generation cellular systems (GSM, IS-54) all utilize this standard.

2.2.2 Code Division Multiple Access (CDMA)

The rising demand for wireless communications may be successfully met by the novel approach known as CDMA. CDMA is an excellent approach for meeting this need since it can be readily adjusted to optimize the user's ability to calculate marginal error performance. While both TDMA and FDMA have limitations on user support, Each access method has a capacity limit for the number of users it can accommodate [51]. Users can have access to both synchronous and

asynchronous channels using this multiplexing technique by changing and deploying their data-carrying signals with predetermined signature sequences. Whether a data signal is intended for an individual user or a collective of users who must collaborate to authenticate its origin, there are two distinct ways in which it can be disseminated [50]. Different types of code division include multicarrier code division multiple access (MC-CDMA), multicarrier direct sequence code division multiple access (DS-CDMA), multitone code division multiple access (MT-CDMA), etc. Increasing the length of symbols helps with transmission synchronisation since the MC-CDMA approach can decrease the rate at which symbols are sent on each subcarrier [52]. Using the specified spreading code, the DS-CDMA transmitter disseminates the original data in the time domain. The ability of a spreading code to reduce interference from several users is dependent on its cross-correlation characteristic.

Superimposing signals with different time delays allow for selective frequency fading in the channel [53]. The autocorrelation property of the spreading codes consequently enables us to isolate a specific part of a received signal among several [52]. By utilizing a predetermined spreading code in the time domain, a transmitter can ensure that the spectra of all the subcarriers are orthogonal and as far apart in frequency as possible [50]. Due to the use of longer spreading codes, MT-CDMA can accommodate a greater number of users than DS-CDMA [52]. The capacity of CDMA technology to treat user signals coming from neighbouring cells as noise has led to its widespread usage in military applications [54].

2.2.3 Orthogonal Frequency Division Multiple Access (OFDMA)

To get around the problems with signalling transmission and boost the transmission rate, the wireless broadband network frequently employs a technology called OFDMA, which is based on OFDM. The whole BW is divided into distinct channels that do not overlap. This converts the channel frequency into numerous parallel streams and modulates them into carriers or sub-carriers to transmit data to many users. The time-domain waveform of these subcarriers is kept at a minimum frequency spacing from them to preserve orthogonality. However, there is still some frequency overlap between the signal spectra of several subcarriers. This ensures efficient utilization of the available BW. If the OFDM transmitter has access to channel knowledge, it can adjust its signalling strategy to work with the channel [55]. The Inverse Fast Fourier Transform

(IFFT) is a technique used to create OFDM with minimal increase in complexity while allowing for a wider spectrum of subcarriers. With sub-channelization, the OFDM system gives higher SNR users less of a priority than lower SNR ones. [56].

This technique is widely used for transmitting data across wireless channels and has been included in several wireless standards, including the IEEE 802.11a local area standard for example. OFDM technology was selected for 4G [59] because of its enhanced processing capacity and simplified receiver design for larger carrier BW.

2.3 Non-Orthogonal Multiple Access (NOMA)

The 5G network may benefit from the use of NOMA [60]-[61]. It solves serious problems like fast data transfer rates, minimal lag time, and extensive network coverage. High SE may be achieved by using superposition coding (SC) at the transmitter and SIC at the receiver to accommodate many users. Decoding and removing the distant user's signal is done by the adjacent user. Due to the local user's faint signal, the distant user experiences minimal challenges in deciphering it [61]-[62]-[63]. CD-NOMA and PD-NOMA are both common kinds of NOMA, with CD-NOMA referring to code domain NOMA and PD-NOMA referring to power domain NOMA. CD-NOMA utilizes sparse code multiple access (SCMA) and low-density signatures (LDS) to divide outgoing signals into a customizable number of SCMA groups. To reduce the effects of symbol-to-symbol interference, the LDS method is used. This LDS is constructed from sparse spreading codes, each of which has some components that are not zero. These sparse codes make it possible to create more differentiated code words for the signal's transmission, which in turn allows for a higher number of users to superimpose in a non-orthogonal form.

Despite having similar power levels, users can be differentiated at the receiver. The usage of multiple access LDS and multicarrier modulation OFDM relies on orthogonal mapping and sparse spreading techniques to facilitate the simultaneous use of frequency diversity and overloading. On the other hand, this can result in exorbitant costs and a complicated receiver. Using LDS and quadrature amplitude modulation (QAM) mapping to produce code words [64], SCMA further optimizes sparse spreading. The complexity of the receiving end is low because the sender and recipient's codebooks are both public [65].

Here, the primary focus of our attention is on PD-NOMA. Sharing the equivalent assets (i.e., time, frequency, and code) efficiently across a wide range of users at variable power levels is made possible by PD-application NOMAs of the superposition principle, in which consumers with lower channel gains are serviced with more power and vice versa. By using the SIC method at receivers to decompose multiple user signals, PD-NOMA dramatically improves spectral efficiency [66]. In a system that uses SIC, the receiver alternates between decoding signals coming from two different users, while disregarding noise signals coming from a third user. When a signal is improved at one receiver, it is no longer usable at a second. See Figure 2.1 for an overview of the core components of this NOMA system.

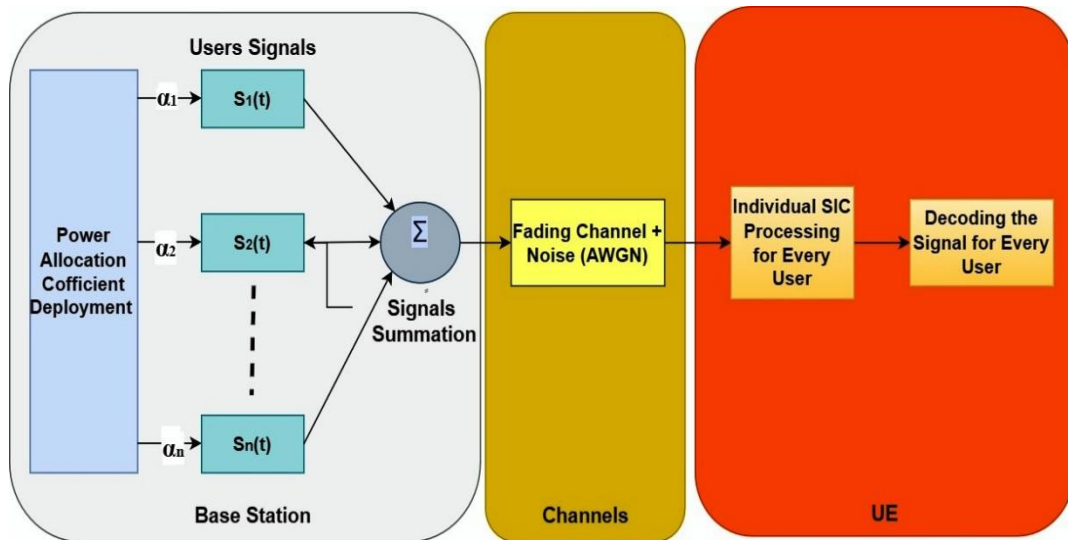


Figure 2.1. Construction of the NOMA System

In comparison to the processes that are now provided by OMA systems, the procedures that are provided by NOMA for resource allocation, user selection, and cauterization are considered to be superior [67]-[68].

Throughout this thesis, the PD-NOMA will be abbreviated to NOMA for the sake of brevity. Furthermore, the name "NOMA" will only apply to the PD-NOMA scheme from now on research.

2.3.1 Power Domain (PD) NOMA

The PD is multiplexed in PD-NOMA so that it may accommodate many users, channel frequencies, code delivery, and access. This is shown in Figure 2.2, PD-NOMA is preferable to OMA since it allows several users inside a single cell to communicate over a single shared frequency channel [69].

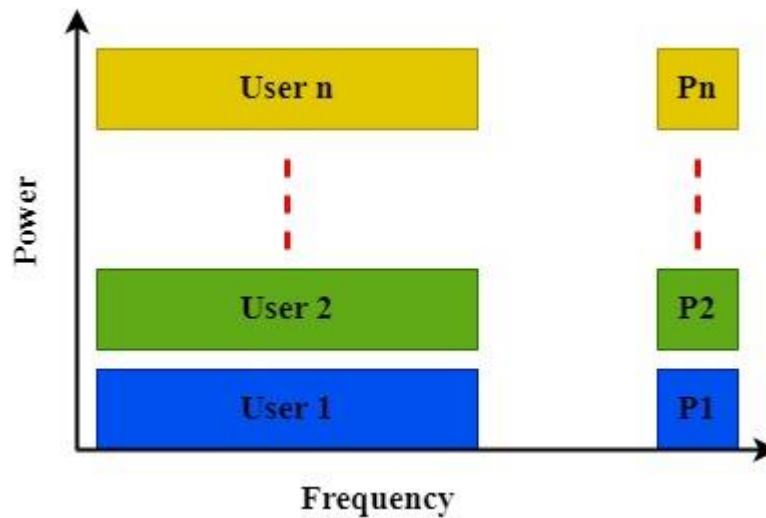


Figure 2.2. The NOMA scheme's TP levels

2.3.2 Transmission Downlink (DL) With NOMA

The BS in a DL NOMA conducts an information wave overlap for its users. Each user (U) employs a process of SIC to pick up its signals. The benefits and number of SIC beneficiaries are displayed in Figure 2.3. The node U_1 will be located near the BS, whereas the node U_n will be positioned at the opposite extremity of the network.

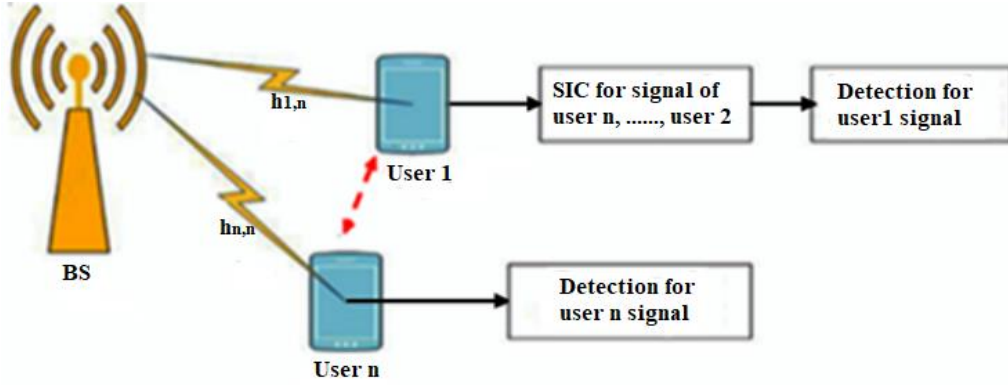


Figure 2.3. NOMA for N-user DL transmissions

Using the NOMA architecture, U users can take advantage of the whole width of the transmission channel (W_T) and the number of subcarriers (NSC).

Additionally, guaranteeing that N users sharing the same subcarrier have no interference, the NOMA system makes use of the SIC. The BS sends out a signal with an intensity of $P_{u,n}$ on the n^{th} sub-carrier ($n = 1, 2, \dots, NSC$) to the u^{th} user ($u = 1, 2, \dots, U$).

$$y_n = \sum_{i=1}^U \sqrt{P_{i,n}} h_{i,n} X_{i,n} + N_i \quad (2.1)$$

where i^{th} user multiplexed on the n th subcarrier is denoted by $h_{i,n}$, and white additive Gaussian noise (AWGN) is denoted by N_i .

2.3.3 NOMA for the Uplink (UL)

The UL NOMA architecture is unique in comparison to the DL NOMA. Figure 2.4 illustrates the UL NOMA network. At the start of UL NOMA transmission, the BS should receive a power allocation control message. This time around, SIC will be utilized by BS to recognize user signals [69].

The optimal detection sequence will involve starting with the stronger signal for decoding before moving on to the weaker one.

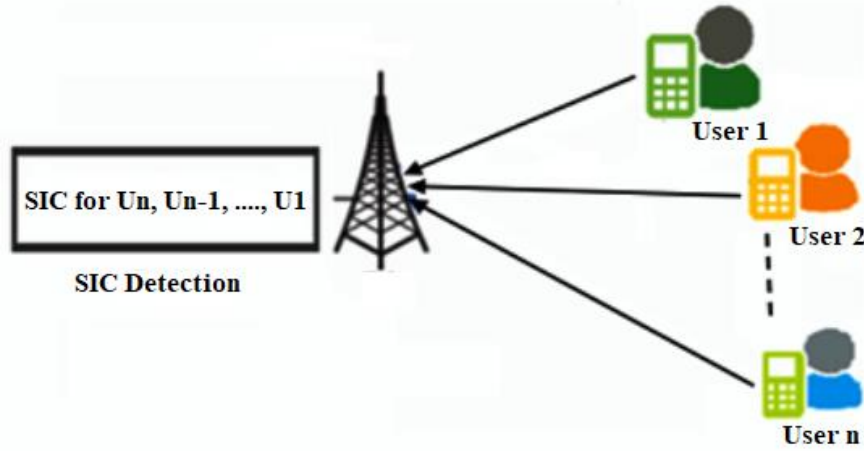


Figure 2.4. NOMA for N-user UL

A complete uplink signal, including all user signals, as received by the BS is represented as:

$$y_k(t) = x(t)g_k + w_k(t) \quad (2.2)$$

AWGN at the U_n with zero mean and density $N_0(W/Hz)$ is denoted by $w_k(t)$, and g_k is the channel attenuation factor between the BS and the U_n .

2.3.4 Superposition Coding (SC)

NOMA transmitters use SC to combine PD user signals. To maximize the capacity of a scalar Gaussian broadcast channel [70], SC takes a non-orthogonal method by fusing the information of several users into a single signal. This paves the way for the simultaneous transmission of data from the number of users through a shared set of radio waves and clock cycles.

Suppose a scenario with N users, complex-valued symbols, x_k , is formed by mapping the data bits for the k^{th} user into the constellation of m-array modulation. Here, N users are considered while discussing quadrature phase-shift keying (QPSK). This occurs when U_1 's (higher-power) constellation is superimposed on U_n 's, and a superposed constellation is formed (with lower transmit power (TP)). The superimposed symbol for an N-user scenario is as follows:

$$x_k = \sqrt{P_T}(\sqrt{\alpha_1}x_1 + \sqrt{\alpha_2}x_2 + \sqrt{\alpha_3}x_3 + \dots + \sqrt{\alpha_n}x_n) \quad (2.3)$$

P_T represents total transmitted power, while α_k represents the fraction subject to the constraint $k=1,2,\dots,n$, where $\alpha_1 + \alpha_2 + \dots + \alpha_n = 1$.

2.3.5 Successive Interference Cancellation (SIC)

After superimposition, the time and BW frequency of the signal transmission remains unchanged. Ensuring considerable variances in power distribution across users at the transmitter [71]-[72]-[73] allows the SIC multiuser detection technique to reveal the wanted signals at the receiver. Use the notation to represent the signal that User k sees.

$$y_k = h_k x_k + w_k \quad (2.4)$$

$$y_k = h_k \sqrt{p_T}(\sqrt{\alpha_1}x_1 + \sqrt{\alpha_2}x_2 + \sqrt{\alpha_3}x_3 + \dots + \sqrt{\alpha_n}x_n) + w_k \quad (2.5)$$

The complex channel coefficient for user k is denoted by h_k , while w_k stands for the AWGN.

The receiver belonging to User1 disregards transmissions from other Users as interference or noise, and quickly converts signal x_1 to desired signal y_1 . The reason is that U_1 's signal is stronger than U_2 's when measured at the receiver, greater than that of U_3 's signal, and greater still than that of U_n 's signal (i.e., $\alpha_1 > \alpha_2 > \alpha_3 \dots > \alpha_n$), this is achievable. But user n is an exception to this rule. User n 's receiver initially deciphers User $n-1$'s signal.

U_1 swiftly decodes the signal y_1 they received by disregarding the signals from other Users as interference or noise.

Contrarily, this is not the case with U_2 . U_2 's receiver decodes the transmitted signal from U_1 before the signal from U_2 may be received. A complete decoding of U_1 's signal at U_2 's receiver would result in a decoded signal. When trying to pick up U_2 's signal, any other signals, including U_1 's recovered signal, are considered interference and cancelled by the received signal. At the U_N 's receiver, the signal from U_{N-1} is decoded first. Assuming that U_N 's receiver correctly decodes the signal from U_{N-1} . For the U_N 's signal to be picked up, the signal from U_{N-1} is retrieved and superimposed on the received signal to cancel itself out (as interference).

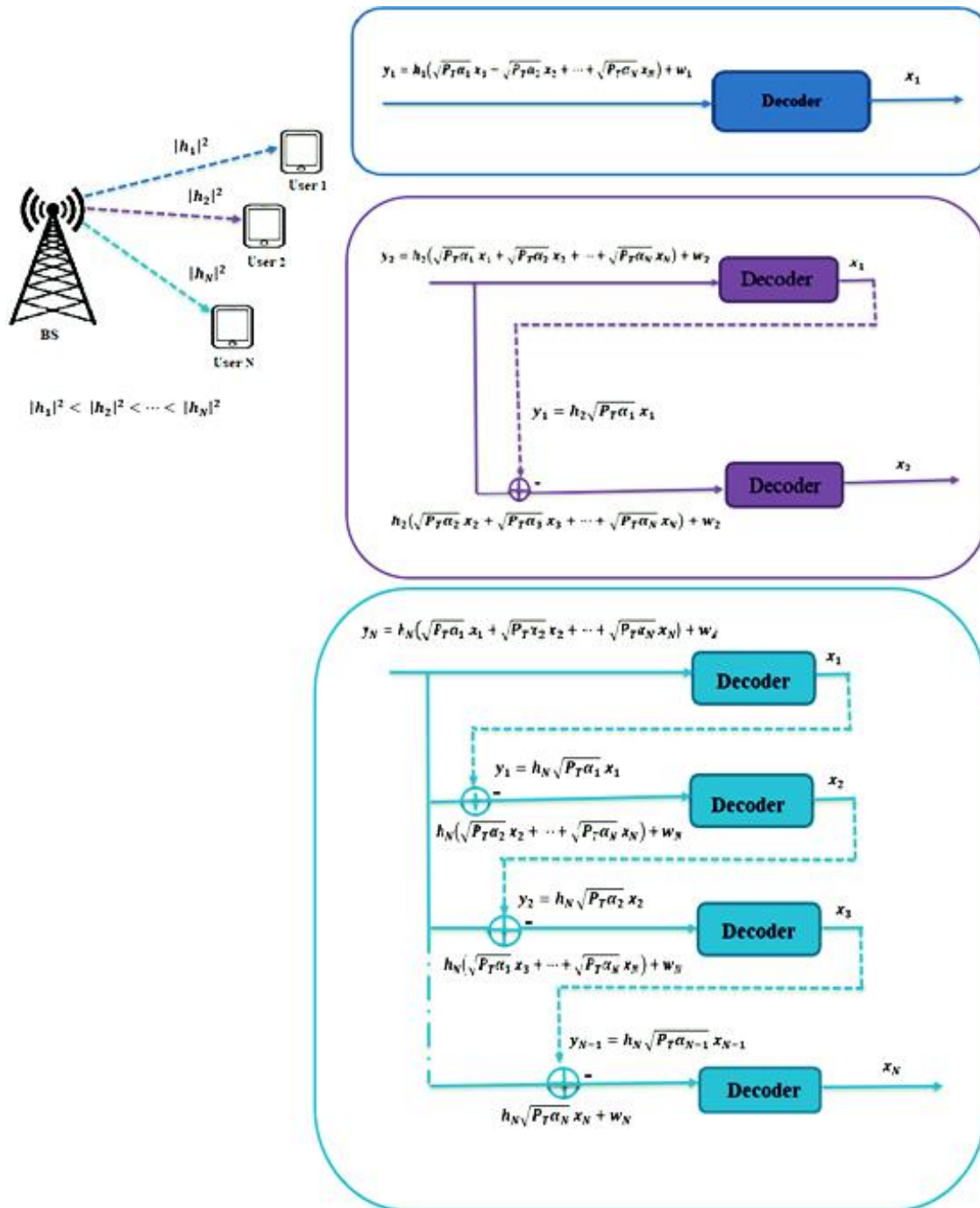


Figure 2.5. Depicts the SIC Procedure and the Techniques in the N-user DL Scenario

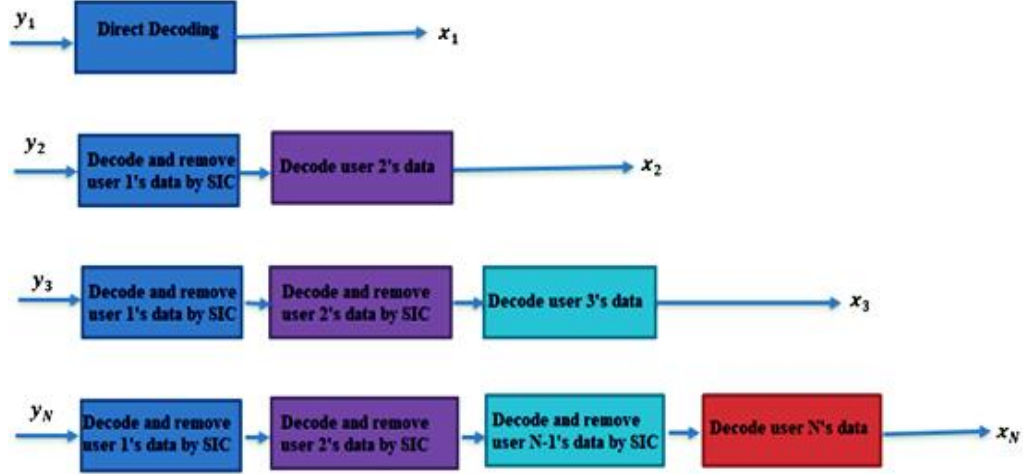


Figure 2.6. Methods of the SIC in the N-user DL Scenario

2.4 NOMA Downlink (DL)

Consider a cellular network with N users, where N is an integer between 1 and N , and a single BS with one antenna. The BS divides system BW into K subbands, or resource blocks (RBs), where each RB uses the same BW to transmit data using an overall transmit power (P_T) over the air. Each RB is predicted to have flat fading since its BW is estimated to be less than the coherent BW. Nonetheless, BW exhibits frequency selective fading. Each RB- n sorts its users in descending order of channel gains, $|h_{1,n}|^2 < |h_{2,n}|^2 < |h_{3,n}|^2 < \dots < |h_{N,n}|^2$. By having the BS and the UE implement the SC and SIC techniques, respectively, NOMA makes it possible for a single RB to support multiple users. However, in OMA schemes like OFDMA, each RB can only support a single user at a time.

The BS uses SC to perform PD multiplexing of user data by assigning a percentage $\alpha_{k,n}$ ($0 < \alpha_{k,n} < 1$) of the P_T to U_N . Since the overall must-TP does not go above the maximum power budget P_T , the power location coefficient (PLC) to each U_N at RB $_n$ is calculated as $\sum_{n=1}^K (\alpha_{1,n} + \alpha_{2,n} + \dots + \alpha_{k,n}) = 1$ requirement that must be met to keep transmission power below the P_T limit.

In SC, the TP is divided so that the user with the poorer signal gets more of it and the user whose signal is stronger receives a lower, (i.e., $P_{1,n} > P_{2,n} > P_{3,n} > \dots > P_{K,n} > 0$) provide QoS or user fairness [74]-[75]-[76]. Nevertheless, this is not always the case from an information theory perspective. Power sharing between paired users is determined by a set of predetermined points within the capacity region. To add insult to injury, if the QoS standards for all users are met, the weaker user may receive less power.

Each user N at RB n receives a superposed signal, which may be represented as,

$$y_{N,n} = h_{N,n}x_s + w_{N,n} \quad (2.6)$$

When the $x_s = \sum_{n=1}^N \sqrt{P_T \alpha_{N,n}} x_{N,n}$ the signal is superimposed on the $w_{N,n}$ AWGN and the AWGN have a power spectral density (PSD) of N_0 . The weakest user will interpret signals from other users (with a higher user index, $N > 1$) to be interference, forcing that user to decode the intended signal. Intracellular interference or intra-cluster interference is the name given to this phenomenon [77]. Initially, the user with greater authority (U_1) decrypts the signal transmitted by the user with lesser authority (U_2). Decoding the U_1 signal involves subtracting the decoded signal from the received signal and discarding the signal for users with a user index greater than 2, denoted as $k > 2$, due to its interference.

To retrieve the required signal, all N users must decode the weaker user's signal, where $j < N$, and after which they subtract the stronger user's signal from the decoded incoming signal, U_l , where $l > N$, as interference. Finally, the strongest user's receiver (U_N) is able to decode the signal with no interference because of the perfect cancellation of all previous interference. The maximum data rate that user N may achieve at each of the N RBs will be calculated assuming optimal SC and SIC values for BS and UE.

$$R_{N,n} = \log_2 \left(1 + \frac{\alpha_N P_{N,n} |h_{N,n}|^2}{\sum_{i=N+1}^N \alpha_i |h_{N,n}|^2 P_{i,n} + \sigma^2} \right) \quad (2.7)$$

The formula that follows determines the maximum throughput that may be accomplished by the N th most powerful user for each of the N RBs.

$$R_{N,n} = \log_2 \left(1 + \frac{\alpha_N P_{N,n} |h_{N,n}|^2}{\sigma^2} \right) \quad (2.8)$$

It is evident that (2.8) can significantly affect individual user rates since there is a one-to-one link between the amount of users and their noise. The weakest user is the most affected. Due to its interference-limited nature, NOMA might not be the best option for all users, particularly in situations with a high user base. As SC and SIC are introduced to serve a greater number of users, it is also possible that the receiver and transmitter may become more complicated [74]. One solution that has been applied to NOMA to deal with these issues is user pairing or clustering, where the participants are divided into smaller groups into various pairs or clusters, wherein the RBs, or each has its own sub-bands.

The success of this method is highly sensitive to the users chosen for each pair or cluster, as users' channel conditions vary widely. According to [78], which investigates the effect of user pairing, pairing users with more dissimilar channel conditions can further boost NOMA with fixed power allocation and outperform OMA in terms of performance.

NOMA's resource allocation takes into account both PLC and user pairing, a sophisticated scheme is needed to provide the best possible performance. Many works, including [79]- [80]- [81], use mathematical optimization theories to apply to the NOMA resource allocation problem.

2.5 Cooperative NOMA

The notion behind cooperative NOMA is that more proficient NOMA users can serve as decode-and-forward (DF) relays for other, less capable NOMA users. There has been no change in our acceptance of the DL transmission for two users. Cooperative NOMA calls for two transmission intervals. The first period corresponds to the direct transmission phase in non-cooperative NOMA. The second interval, commonly referred to as the cooperative stage, is when U_N will use the DF relaying protocol to send U_M the decoded message. Chapter 3 of this thesis is based on a cooperative NOMA design.

The primary advantages of cooperative NOMA over standard NOMA are:
A strong user in NOMA can now decode transmissions from a weak user thanks to SIC technology. A strong user in NOMA can now decode transmissions from a weak user thanks to SIC technology. As a result, the DF relay protocol needs to be considered. Benefits all users more equally as the weak user's dependability is not as heavily relied upon, which is greatly enhanced by the usage of cooperative NOMA. Therefore, NOMA transmission fairness is ensured, and 3)

the large diversity benefit is achieved even for the weak NOMA user, making cooperative NOMA a powerful tool in the fight against multi-path fading [82].

2.6 5G Concept

Seeing as how Information and communication technologies (ICT) have brought about previously unheard-of benefits and conveniences, it has come to be seen as a crucial component of societal and economic growth. Users are now able to access broadband services from their mobile devices, such as smartphones and tablet computers, with an end-user experience that is practically on par with that of wired connections, thanks to the emergence of 4G wireless network services. Mobile services that necessitate fast speeds, rapid reaction times, high dependability, and energy efficiency are challenging to supply, even with the advent of 4G wireless network technologies. As a result, in the 5G era, these capabilities are now prerequisites for any new services to be considered.

The need for existing 4G/Long Term Evolution (LTE) networks to meet the requirements of Internet-related services is growing as technology connected to these services advances. This makes it impossible to provide a service to all customers at a consistently high standard. Additionally, the number of concurrent mobile users who can enjoy a high-quality video experience on LTE networks is restricted.

Future 5G services would enable limitless data transmission, an enormous number of simultaneous connections, and the introduction of novel mobile gadgets, in particular sensors powered by renewable energy sources, making possible new forms of media like 360-degree films and holograms. 5G services can be used in many different contexts, not just for making phone calls or surfing the web.

Given this context, 5G networks are a critical component of the infrastructure that drives growth across the whole ICT sector and beyond. International Mobile Telecommunications-2020 (IMT-2020) is a standardization initiative led by the ITU-R Working Party (WP) 5D that contains a vision statement outlining the many uses for 5G. You can read this declaration here: [83]. Some examples of potential uses include ultra-reliable and low-latency communications (URLLC), enhanced mobile broadband (eMBB), and communications for massive machine-type communications (mMTC).

Important factors in most of the service scenarios examined by ITU-R eMBB include peak data rate, user-perceived data rate, spectrum efficiency, mobility, network energy efficiency, and area traffic efficiency. Additionally, a number of URLLC service use cases emphasize mobility and low latency as two of their top priorities. Reliably and transparently managing the massive swarm of intermittently transmitting devices in mMTC service scenarios is a prerequisite for 5G networks [84]. The data rate as perceived by users and SE are the most important performance parameters. Figure 2.6 displays their importance in essential key performance.

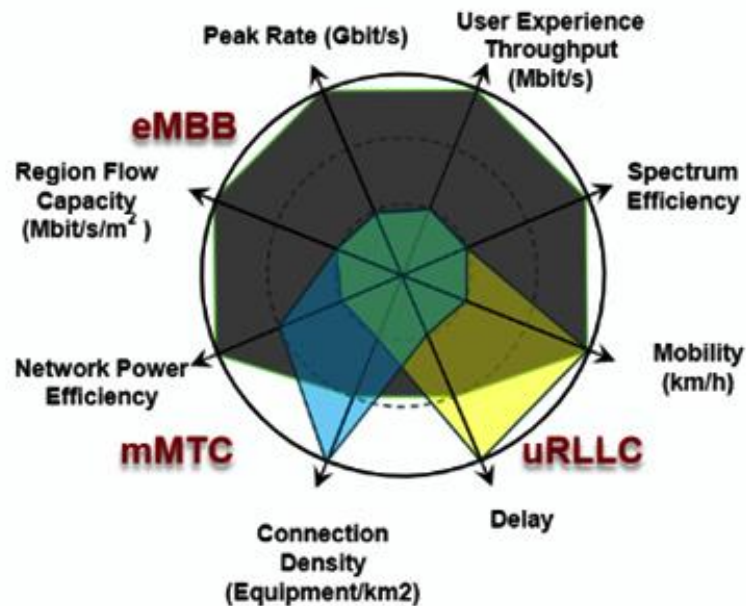


Figure 2.7. Displays the Various application KPIs Requirements [84]

2.6.1 5G Mobile Network Spectrum

According to the recommendations of the Global System for Mobile Communications (GSMA), Figure 2.7 depicts a scenario in which 80-100 MHz of contiguous spectrum is made available to each operator in the core 5G bands, and approximately 1 GHz of the spectrum is made available to each operator in

the millimetre wave bands. According to Table 1, the frequency was split into two classifications [84].

However, spectrum is a finite resource, therefore wireless operators throughout the world will likely need to use a combination of the low, mid, and high bands to deliver the kind of 5G experience their customers need and boost spectrum efficiency by employing novel spectrum sharing technologies.

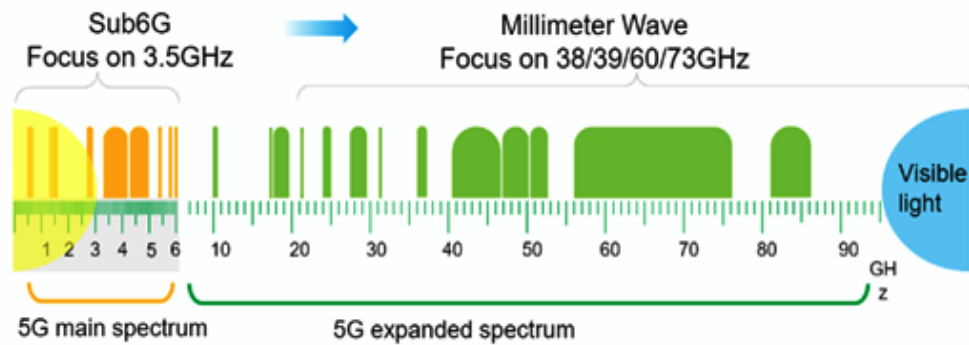


Figure 2.8. 5G Network Spectrum [84]

Table 2.1. The 5G Frequency Classification [84]

Frequency Classification	Frequency Range
FR1	410MHz-7125MHz
FR2	24250MHz-52600MHz

2.7 Spectrum Efficiency (SE) Technique

The definition of "Cognitive Radio" (CR) was developed further in [85] and [86], with a particular emphasis on "Dynamic Spectrum Access" (DSA). The outcome was a revised description of CR as an "environmentally aware, self-learning wireless communication system" that adapts its transmission characteristics in response to statistical fluctuations in the RF signals it receives. This is done to achieve two main objectives.

The IEEE 802.22 [87], the IEEE 1900 [88], and the IEEE 802.11af are just a few of the current CR standardization projects that are underway.

2.8 The Principles of Cognitive Radios (CRs)

The technologies that make opportunistic spectrum sharing possible are crucial to CR's success. One concise definition of CR is provided in [89]: In response to changes in its operating environment, the CR radio adapts the settings of its transmitter. To avoid interfering with the transmission of preexisting networks, the problem is to share the spectrum with them. So-called "Spectrum Hole" (SH) or "white space" is what the CR makes available for such purposes. According to [85], SH is defined as follows: The SH is a piece of the radio spectrum that is ordinarily used by the PU but is being made available to another user at this time and location. If another SU begins to use the same SH where the CR is operating, the CR may relocate to a different SH or remain in the same SH while adjusting the strength of its transmissions or the modulation scheme it employs to mitigate interference.

2.8.1 Critical roles of CR

The critical roles of CR include:

- Learn which spectrums are currently unoccupied.
- Choose the most appropriate channel.
- Assist other users in gaining access to this channel.
- Leave the channel as soon as the authorized user returns.

The CR model necessitates the use of dynamic network protocols within a pre-existing network topology. Cross-layer adaptation to the Open Systems Interconnection (OSI) network architecture is proposed in [89]-[90] to ease CR model implementation. This is done to accommodate the CR model. Spectrum sensing and sharing both contribute to the overall effectiveness of the network in this configuration. Spectrum adaptation requires the coordination of features at the application, transport, routing, medium access, and physical layers, which is accomplished through spectrum decision and spectrum mobility.

2.8.2 Benefits of Cognitive Radio (CR)

Helping networks make the most efficient use of available spectrum bands in order to satisfy customer demands for service quality is the main objective of CR. To accomplish this objective, new activities for managing the spectrum will need to be devised to account for the dynamic character of the spectrum. It is

illustrated visually in Figure 2.11 [85]-[91] how spectral sensing (SS), spectral analysis (SA), and spectrum decision (SD) are interdependent. The SS function is able to detect SH through the use of permitted as well as unlicensed frequency bands. This indicates that their properties are susceptible to change, not only as a result of the ever-shifting radio environment but also as a result of the operating frequency and the BW of the signal.

Because the spectrum is constantly changing, communication protocols must adjust wireless channel parameters. Choosing the best spectrum band requires considering QoS requirements such as transport, routing, scheduling, and sensing data. Realizing SA and SD functions requires a method that crosses many layers and makes use of the interdependence of the characteristics of a stack for communication as well as closeness between them with the physical layer. Therefore, SA and SD are issues that occur at a higher layer, but the core of SS is comprised of the Physical Layer.

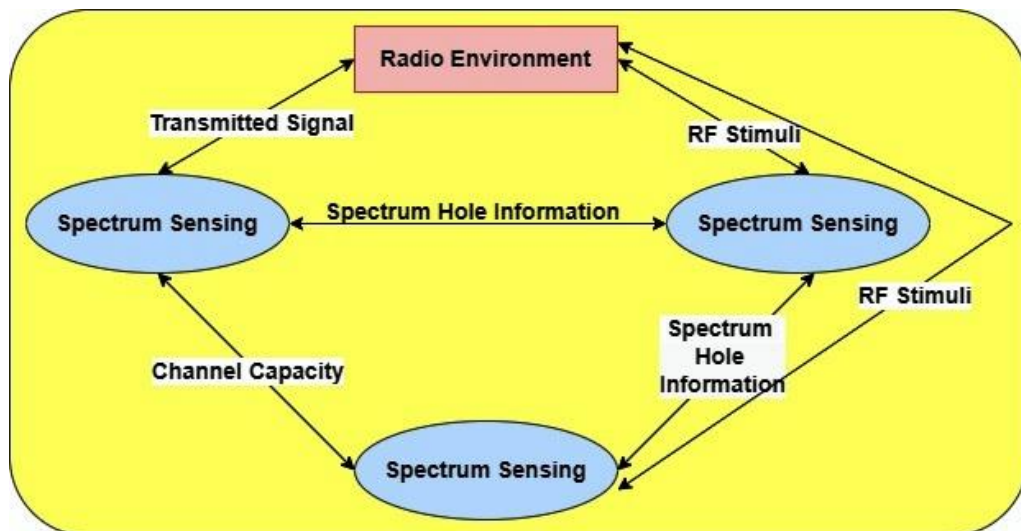


Figure 2.9. The Cognitive Radio Process [85]

2.8.3 Sensing of the Spectrum (SS)

The SS function's job is to keep an eye on things from the vantage point of a network node to identify stale frequencies. By monitoring the electromagnetic spectrum, the CR can detect and react to environmental changes. SS, which is implemented as a physical layer and media access control mechanism [92]-[93], is firmly within the purview of detection theory, as has been discussed at length

in the works [89]-[94]-[95]. Even though the identification of signals is the responsibility of the Physical Layer SS, there are in fact two distinct sorts of detection methods: those that need prior information (like pilot detection), and those that don't (like energy detectors (ED)) [92]-[96]. In terms of when and what spectrum to detect, the MAC portion of the SS (in frequency) is the most important. To put it another way, multipath, shadowing, and local interference all influence how well the SS performs in each area. Interactions between these elements can reduce the SNR, thereby causing detections to be missed or false alarms to be generated by local detectors.

2.8.4 The Spectrum Analyzer (SA)

It is possible to pick the spectrum band that is most appropriate for each node thanks to the SA function of cognitive radio networks (CRNs), which classifies the spectrum bands that are available for availability. Because of the inherently dynamic nature of networks, each SH is required to take into consideration the ever-evolving radio environment, as well as interference and information regarding the frequency band. There are examples of this that may be observed in the bandwidth and frequency of the operating system. Because of this, it is of the utmost importance to develop certain criteria for determining the relevance of a particular range of frequencies that are contained within the electromagnetic spectrum. It is made clear in reference [89] that the following are mentioned explicitly:

Interference: Traits are dependent on the spectrum band being used. There is a negative correlation between operation frequency and path loss. If a node maintains the same level of TP across all frequencies, its range will decrease as the frequency increases.

Error rates in the link can vary based on the type of modulation that is being utilized as well as the quantity of background noise that is present within the channel's working frequency range.

There will be a delay at the connection layer since path loss, wireless link error, and interference will vary by spectrum band. The time required for a packet to go across the link layer will vary substantially because of these differences.

The interference of other users can reduce the network's channel quality during the holding time. The holding time is the average amount of time a node can remain in a band before being evicted. The frequency of spectrum handoffs increases as the holding time decreases. System throughput and connectivity are

compromised during spectrum handoff operations due to the time spent returning transmission to a new channel. Thus, more time spent on hold by a channel is preferable. Time spent waiting during a spectrum handoff can be minimized by thinking back on previous handoff data. The channel capacity, which is determined by the variables, determines the spectrum band. The SNR is commonly used to estimate channel capacity; however, due to its one-sided focus on the receiver's observations, it fails to consider any of the channel's other salient features.

2.8.5 The Spectrum Decision (SD)

As a consequence of this, the anticipated channel capacity of the numerous spectrum bands that have been characterized can be utilized to choose the spectrum band that is best applicable to the situation for operational purposes. The standards for the level of service provided by each node in the CRN can be broken down into a number of discrete metrics, such as the amount of transferable data, allowable error rate, latency bound, communication method, and BW. The results of applying the best decision rule can be used to select the bands of the electromagnetic spectrum that are the most appropriate for a certain application. Numerous best practices are published in the literature that can be included in the SD function. With the assumption that all channels have the same throughput capacity, [97] presents SD ideas that prioritise fairness and communication cost. The SNR of a channel is taken into account while deciding which channels to skip to discover the best ones. This method is presented in [98]. As discussed in [99], a central, adaptable decision-making structure is developed with spectrum sharing in mind. The method of adaption considers not only the number of users but also the available infrastructure at the hub.

2.8.6 Mobility of the Spectrum

The Spectrum Mobility feature allows a network to dynamically use the spectrum by allowing CR nodes to switch to the most optimal frequency band. Spectrum handoffs, also called spectrum mobility functions, are the means by which the CRN node changes its operational frequency. Spectrum mobility occurs in a CRN whenever a node's current channel conditions deteriorate due to relocation or the introduction of an interferer. Spectrum Mobility has resulted in the creation of a brand-new kind of handoff that has been given the name "spectrum handoff" [100]. The effectiveness of the CR can either increase as it is used or decrease as it is used. So, the network protocols will change modes

whenever the CR node's activity frequency changes. The protocols that are used at each network layer need to be able to modify one's behaviour based on the specifics of the working frequency's transmission channel, in addition to being able to remain transparent when a spectrum handoff is occurring and during the related latency. Spectrum mobility management in CRNs ensures that the performance of programs operating on a CRN node is unaffected by the movement of traffic between nodes. Therefore, accurate estimations of the time it will take to switch the spectrum are necessary for mobility management techniques. SS and SA algorithms can collect this information, which provides an estimate of the channel holding time. After a CRN node learns of the delay, it is up to mobility management protocols to lessen the impact on the node's ability to keep communications flowing uninterrupted. Additional delays introduced by spectrum handoffs reduce the efficiency of the underlying communication protocols. Therefore, the most difficult component of establishing spectrum mobility is to work toward a reduction in the SS latency associated with spectrum handoff. Spectrum handoff has an impact on various characteristics of the channel, including link-layer delay, interference, the percentage of dropped wireless connections, and path loss. However, the spectrum handoff could result from modifications to the physical layer or the MAC channel parameters. In addition, the user application can ask for a spectrum handoff to switch to a more desirable frequency band.

2.8.7 Sharing of the Spectrum

Considering that all nodes in the CRN must use the same wireless channel, coordinating their transmission attempts is essential. When compared to typical MAC problems in classical systems, sharing spectrum is easier to grasp. Contrarily, spectrum sharing in CR networks raises a separate set of concerns. These one-of-a-kind problems arise from the necessity of integrating with other systems and the incredible diversity of the observable electromagnetic spectrum. The procedures for sharing radio frequencies in the CRN are summarized in [101]. There are five stages to the spectrum-sharing process:

- Spectrum sensing (SS): Before being able to transfer packets, the various types of CRN nodes first need to have an understanding of how the local spectrum is being utilized.

- Spectrum allocation: Once the node knows how much spectrum is accessible, it can assign a channel. Both spectrum availability and current spectrum access policies contribute to this distribution.
- Spectrum Access (SA): Given the possibility of concurrent spectrum access by different nodes in a CRN, these attempts must be coordinated to reduce the likelihood of interference between users.
- After a piece of the radio spectrum has been chosen for transmission, a "handshake" between the sender and recipient indicates receipt that this portion of the radio spectrum has been chosen for transmission.
- Spectrum Mobility: The nodes in a CRN must employ the spectrum mobility function to move to a different open area of the spectrum if the conditions of the allotted spectrum deteriorate.
- Current literature on spectrum sharing focuses on architecture, allocation behaviour, and access methods. Following are several spectrum-sharing methods that are technically conceivable, given the presence of distinct architectural elements.
- Spectrum access and allocation procedures are managed by a governing body. An innovative distributed sensing method is presented to help with these processes; in this method, various network nodes report their spectrum allocation measurements to a central location. This data is then used to generate a map of the spectrum's usage. You may see some examples of this style of building in [92]-[102]-[103].
- In situations where building new infrastructure is not a desirable option, distributed solutions are often advocated. Spectrum access and allocation are delegated to individual nodes according to either regional or worldwide policies. The vendor or a third party, like the Federal Communications Commission, may establish these guidelines (FCC). An example of this is found in [104].
- Spectrum Sharing methods can be broken down into several categories according to how they handle user access:
- Cooperative approaches consider how a node's communications will affect other nodes. Spectrum allocation techniques consider the interference measurements taken by each node and transmit this information among the nodes. Though there are also distributed cooperative solutions, all

centralized approaches are treated as cooperative by default. The references [105]-[106]-[107]-[108] provide some good examples.

- The present node is the only one taken into account by the non-cooperative method. Individualistic strategies are also known as "selfish" solutions. Less effective spectrum utilization may emerge from non-cooperative techniques, but they don't require nodes to coordinate their actions or share their command data. Some illustrations of this can be seen in [97]-[109]-[110].
- According to reports in the literature, cooperative systems perform better than non-cooperative ones when comparing the architecture and access behaviour of these approaches, and distributed solutions closely follow centralized solutions. This research's findings are supported by the literature (see [111]-[112] for examples).
- Spectrum-sharing methods are categorized following the access technology in use.

A node can join an existing network by making use of unlicensed radio frequencies through the implementation of an overlay spectrum-sharing protocol. As a result, the primary system encounters less interference [108]-[111]-[112].

The Underlay-Underlay paradigm ensures that all participants are cognizant of the interference they may be contributing. If interference from the SU at the PU is below a specific limit, simply simultaneous transmission from the primary and secondary systems is required. The BW requirements and complexity of this technology are higher than those of overlay approaches.

Theoretical research into spectrum access in CRN has shown crucial trade-offs that must be considered while designing spectrum access protocols. Spectrum is used more equally and efficiently, according to studies, when people work together to do so. However, the cost of collaboration owing to signalling overhead may make this advantage less appealing in the long term. Spectrum access techniques always influence the performance of legacy systems, as stated in [113]. Overlay techniques concentrate on the voids in the spectrum, while underlay requires dynamic spreading methods to guarantee interference-free operation across coexisting systems.

2.9 Cognitive Radio NOMA (CR-NOMA)

Recently, CR systems have also begun implementing a revised NOMA strategy. These emerging technologies, when used together, may considerably streamline

the power allocation design and consistently satisfy consumers' requests for high-quality service [114]-[115]. To improve secondary network (SN) connectivity, for instance, the authors of [116] implemented NOMA strategies on huge underlay CR networks. In CR-NOMA systems, the overlapping signals' power must be kept below the interference threshold at the primary network (PN), which is a requirement that isn't present in traditional NOMA wireless networks. Similar work may be found in [117], where secondary NOMA transmitters relay information from PN receivers to SN receivers. Also, in [116], the CR-NOMA networks with an overlay were investigated, wherein NOMA messages are broadcast to the SUs from a secondary source. An examination of the data reveals that NOMA users do better than OMA users when the target data rates and PA parameters are chosen with more attention. In addition, CR-NOMA networks have used cooperative communications to their advantage [118]-[119]. One example may be found in [118], where the authors conducted research on the feasibility of using NOMA to enable superposition transmission between a unicast PU and multicast SUs. In this scenario, the SN cooperates among PUs to compensate for their unequal allocation of the primary spectrum.

2.10 Multiple Input Multiple Output (MIMO)

Problems might arise in signal propagation due to the wireless channel's complexity and temporal variability. Multiple channels allow the wirelessly sent signal to reach the destination node (multipath). Objects, such as trees, hills, buildings, etc., cause the multipath by scattering and reflecting transmitted energy. The path's signal strength, the direction of arrival, and the delay time are all distinct from the others. Weakening of the received signal's amplitude can be caused by multipath propagation, which can lead to destructive interference and poor-quality wireless channel connectivity. Data delivery in digital communication networks like the wireless Internet can be slowed down and error rates can rise. The basic publications [120]-[121] show that multiple antennas and multiple signals from the transmitter and receiver can reduce multipath propagation's detrimental effects. Thus, increasing a wireless network's antenna count for MIMO transmission can linearly enhance its spectral efficiency. MIMO has been hailed as a technological breakthrough that has the potential to completely change the game in light of the looming catastrophe that will be caused by the demand to satisfy the massive data rate requirements of future wireless communications.

Performance advantages are given by MIMO systems' spatial diversity and spatial multiplexing [122]. Space diversity, which broadcasts and/or receives duplicated data symbols across many antennas, can reduce transmission failure owing to deep fades in certain symbol copies but not others. MIMO is in the design specs for the next generation of wireless networks, which include Wi-Fi, WiMAX, 4G, and 5G. This was done because of the potential benefits that MIMO offers [121].

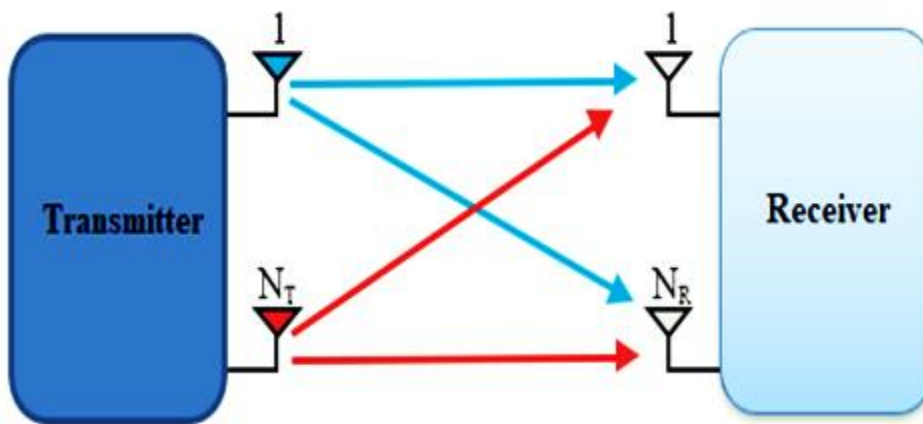


Figure 2.10. The MIMO System Utilizing N_T Transmitters and N_R Receivers

In wireless communications, numerous antennas have various real-world uses; for example, increasing capacity by a factor of two without increasing BW [121]-[122]-[123], increasing transmission reliability dramatically with space-time coding [122] and suppressing co-channel interference effectively in multi-user transmissions [124]. Incorporating MIMO strategies into the design of CR networks has many benefits, one of which is enhanced performance in PNs and SNs [125]. By employing several antennas, the secondary transmitter in a CR network is better able to strike a balance between these two competing, yet interdependent, specifically, it aims to increase its transmission speed while simultaneously decreasing interference levels at its primary receivers.

2.11 Massive MIMO

M-MIMO is a key method in 5G networks since it improves SNR and SE. There is evidence that M-MIMO can boost capacity by more than a factor of 10 and reduce energy consumption by a factor of 100. Greater multiplexing gains, larger

data speeds, more durable connection stability, and a better balance between spectrum and energy economy are just a few of the possible advantages of M-MIMO over classical MIMO, which is limited by the number of antennas.

$$P_r = G_M P_t L / N \quad (2.9)$$

where $G_M = M - N + 1$ is the array gain at users [127]- [128], P_t is the BS's TP, and L is the overall path loss.

Researchers were motivated to try integrating M-MIMO transmission into NOMA because of the promising results that may be achieved. Ding and Poor used the clustering MIMO-NOMA architecture to break down M-MIMO channels NOMA into smaller, more manageable numbers of single-input, single-output (SISO) channels [129]. It was suggested that a one-bit feedback approach could be used to streamline the installation process of the planned M-MIMO NOMA devices.

2.12 Obstructive Parameters of the Surrounding Environment for Wireless Communications

Many factors and parameters affect the work and performance of wired and wireless communication systems, the most important of which are:

2.12.1 Noise

Unwanted signals can be injected into a communication system at any point in time, whether it's during transmission or reception. Noise is the term for any such intrusion. Noise is an unwelcome signal that distorts the message signal's properties through interference with the original signal. The message itself is modified because of this change in the transmission mechanism. Most likely, it will be inputted at the channel or the receiver.

Various factors, such as the nature of the noise's origin, the effects it produces, and the nature of the source's and target's connections, are taken into consideration when categorizing noise. There are primarily two sources of noise. The first is generated by an external source, whereas the second is generated within the receiver itself. Ultraviolet AWGN from sources like heat and gunfire is the most critical factor.

2.12.2 Fading

In transmission systems, fading manifests as a fluctuation in the received signal strength. Instances of fading that can occur include:

- 1) Large-scale fading.
 - Path loss.
 - Shadowing.
- 2) Small-scale fading.
 - Fast fading.
 - Slow fading.
 - Multipath fading.
 - I. Flat fading.
 - II. Selective fading.

Rayleigh fading, caused by a signal's reflection, and described by the Rayleigh distribution, and Rician fading, caused by a signal's reflection and the addition of a line of sight and described by the Rician distribution, are the two most crucial fading parameters.

2.12.3 Inter Symbol Interference (ISI)

ISI is one sort of communication distortion that leads to significant information loss. The square waveform expressing the 1s and 0s is the standard form for transmitting digital information. Data in the adjacent symbol sequence becomes unintelligible when the square waveform spreads and combines with the noise and non-linearities of the channel.

The receiver misinterprets this data because it cannot anticipate the proper level of the square waveform, and hence some of the data is lost.

ISI is typically caused by the multipath signal propagation and non-linear frequency response of a band-limited channel. Errors in the receiver's judgement device are introduced when ISI is present. Therefore, it is important to consider ISI while designing transmitting and receiving filters so that digital data is transmitted with as few mistakes as possible.

2.13 Quality of Service (QoS)

Speaking of "communication" The basic properties of a network that are essential to its capacity to deliver the promised service or function to users are

called "quality of service" for short. Some examples of these characteristics include being able to keep high-priority applications and traffic running smoothly even when BW is limited. Each service model has its own unique set of QoS characteristics that determine how the network responds to user requests for specific outputs, such as packet delay or loss. Spectral efficiency must be improved with each new generation of mobile communications networks to satisfy QoS requirements.

2.13.1 Spectral Efficiency (SE)

Given the limited amount of spectrum available, it must be used effectively. Maximum data transmission across a given BW indicates efficient utilization of that resource. The rate at which data is transported over a certain BW in particular communication systems is referred to as its spectral efficiency. You can also refer to spectral efficiency as BW efficiency. The speed at which information is carried over a given BW is typically described in terms of the underlying communication system.

2.13.1.1 Spectral Efficiency (SE) of 5G NR

The SE of the 5G network can be measured by the formulation that can be used to measure roughly the specimens of 5G new radio (NR) (bit/sec / Hz):

$$\text{Spectral efficiency } 5G = \frac{5G \text{ NR Throughput, bps}}{\text{Channel (Band) Bandwidth, Hz}} \quad (2.10)$$

It expands upon the guidance provided by the 3GPP.

2.13.2 Throughput

Simply explained, throughput is the quantity of information that can be sent and received in each length of time over a certain communication link. Technical variables such as latency, packet loss, jitter, and Others have the ability to impact the rate at which data is transmitted (measured in kilobits per second, or multiples thereof). not to be equal to BW. Evaluation of 5G New NR throughput (which varies with MIMO layer count, BW, frequency range, modulation type, etc.). Based on the 3GPP standard TS 38.306: Radio connectivity capability of DL and UL 5 G to receive NR User Equipment, the maximum performance is determined (UE).

$$\text{data rate (in Mbps)} = \sum_{j=1}^J \left(v_{Layers}^{(j)} \cdot Q_m^{(j)} \cdot f^{(j)} \cdot R_{max} \cdot BW^{(j)} \cdot S_u^{(j)} \cdot (1 - OH^{(j)}) \right) \quad (2.11)$$

CC Index(the j-th CC)
 Overhead
 • [0.14], for frequency range FR1 for DL
 • [0.2], for frequency range FR2 for DL
 • [0.14], for frequency range FR1 for UL
 • [0.2], for frequency range FR2 for UL
 Spectral utilization
 Bandwidth in MHz
 $R_{max} = 948/1024 = 0.926$
 Scaling Factor
 The scaling factor can at least take the values 1 and 0.75, signalled per band and per band per band combination
 Max Modulation Order
 Max Number of Layers

2.13.3 Bandwidth (BW)

BW measures information transmission and reception speed. More information can be transferred over a network if its BW is increased. Instead of referring to a measurement of velocity, the term BW is more commonly associated with a measurement of power. There is a wide range of frequencies available, but only those below a few hundred GHz may be used for practical communication. They make cautious use of the limited number of accessible frequencies to meet our massive demands. Government bodies are established to establish policies about the use of available BW.

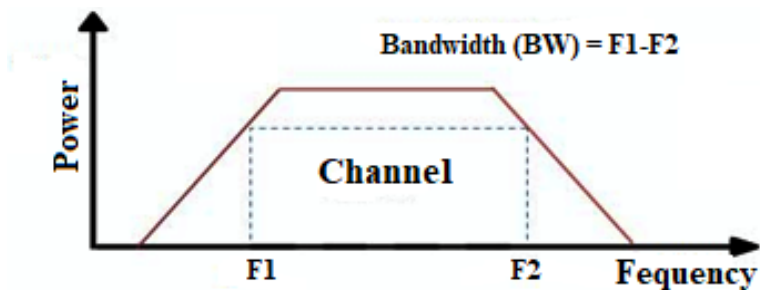


Figure 2.11. The BW of the Channel

2.13.4 Channel Capacity

The maximum number of users on a frequency band is called radio communications "channel capacity". The maximum information that can be successfully conveyed over that frequency range determines this value. This parameter is crucial since radio capacity determines a cellular network's maximum data transfer speed. The carrier-to-interference ratio (CIR) and radio spectrum availability (B) determine the maximum data rate that may be broadcast on a radio channel. For any wireless system, this phrase can measure radio capacity.

$$C=B \log_2 (1 + CIR) \quad (2.12)$$

Estimating the CIR in dB is as simple as

$$CIR_{dB} = 10 \log_{10}(CIR) = 10 \log_{10} \left(\frac{P_{rec}(Serving\ BS)}{\sum P_{rec}(Interfering\ BSs)} \right) \quad (2.13)$$

Where P_{rec} is the signal power from the serving or interfering BSs. Calculate $P_{rec}(d)$, the received signal intensity at varying distances (d) from the BS.

$$P_{rec}(d) [dB] = P_t [dB] - P_L(d) [dB] \quad (2.14)$$

P_t [dB] is TX power and $P_L(d)$ [dB] is path loss at distance d. Per $P_L(d)$, UL and DL device capacity must be estimated separately.

2.13.5 Signal-to-noise ratio (SNR)

SNR quantifies signal strength compared to ambient noise. In wireless signal transmission systems, the SNR and BW are two essential components.

2.13.6 Bit Error Rate (BER)

A transmission's BER is the ratio of damaged data bits to the total number of data bits received. You can see this figure expressed as a percentage.

2.13.7 Outage Probability (OP)

The possibility that a receiver is beyond the BS's coverage area when its power value falls below a threshold (the cell's minimum SNR) is the OP.

2.14 Related Works

Towards 5G wireless networks, two emerging technologies NOMA and CR could improve spectrum efficiency. The future of wireless spectrum use would be improved by the implementation of two new technologies [130]-[131]. However, this method of combining NOMA and CR into a single, complete system, known as a cognitive NOMA network [131], does not often attain the greatest achievable data rate for a given spectrum efficiency.

Increased SNR at the PU and SU receivers, made possible by a temporal mismatch between the two user groups, is used to boost the CRNs' overall performance. Although asynchronous transmission can boost the efficiency of CRN, it is counterproductive for heavy traffic and large amounts of data [132].

Due to its benefits, wireless full-duplex (FD) may be used in 5G wireless networks and beyond. BW doubling and spectrum efficiency improvements are among these benefits. FD can sense and transmit data simultaneously, send and receive data simultaneously, boost sense efficiency, provide a secondary output, and address the disguised terminal problem. Sending and receiving data simultaneously is another benefit. Despite this, FD technology's biggest challenge is reducing severe self-interference (SI) [133], [134].

Potential wireless communications systems are in jeopardy due to a lack of available spectrum. Spectrum sharing is one solution to the problem of an insufficient official spectrum that cannot meet current and future traffic demands. Both unlicensed and licensed radio frequencies exist in the electromagnetic spectrum. The 5G cognitive radio-based spectrum sharing technique employs a spectrum sensing function, unlicensed users can be more effectively allocated spectrum. Instead of focusing solely on the unauthorized user, a comprehensive system for all of them should be developed [135].

In the future of wireless networking, effective SS will be necessary for emerging multi-access technologies like NOMA and SS. To ensure that a NOMA-based cooperative relaying system (CRS) can manage its data flow requirements, the PLC must be fine-tuned. A combination of SS and CRS-NOMA outperforms SC and MRC systems when the peak interference power is higher. Secondary network disruption may result from PU transmitter and receiver interference [136].

Spectrum sensing is among the most essential components of CR communications. NOMA demonstrates tremendous potential in two areas, namely spectral efficiency and the capacity to enable extensive connectivity, both of which are essential to the development of next-generation wireless communication. Utilizing a system based on the Directed Acyclic Graph-Support Vector Machine makes it possible to do spectrum sensing that is both highly effective and extremely precise (DAG-SVM). On the other hand, a prediction time of less than 1 millisecond and several hundred points of training data might be required [137].

E-CRNs, or enhanced cognitive radio networks, rely on the cooperative use of available radio channels. Unlicensed spectrum includes industrial, research, and medical bands, whereas unlicensed spectrum is shared with PU networks. The E-CRNs framework demonstrates one potential way in which 5G wireless networks will make use of the available spectrum. Unused television white space (TVWS) might be a source of spectrum for CRNs. The TVWS can be located by listening to the PU's emissions with the help of some complicated spectrum sensing methods. Even yet, the concealed terminal problem makes it so that sensing systems, in particular passive PU receivers, cannot totally prevent CRNs' detrimental PU network interference [138].

The most promising of the modern technologies being employed to improve spectral performance are cognitive radios and multi-access. The success of perceptual radio communication relies heavily on accurate spectrum detection. As a result of the complexities of the radiation environment, multi-user cooperative spectrum sensing (CSS) is an elegant method for maximizing spectral efficiency. CSS methods are precise and very efficient, but they are time- and resource-intensive [139].

Nakagami-m fading networks linked to a low-power cooperative network using NOMA technology to link a larger number of users across a greater area will increase spectrum performance and establish service life guarantees for relay nodes by fitting power collectors. However, a NOMA network with several users that distributes power collectors in the relay node can improve network availability [140].

An investigation on a cooperative MIMO NOMA system incorporating half-duplex operation, SIC, and partial channel state information is conducted in

[141] for Nakagami-m fading channels. However, the data showed that the participants' distance from BS was not a factor in any bias.

BPSK modulation at both the ideal and imperfect SIC stages was used to test the possibility of creating a closed-form representation of the DL NOMA network's BER rate using AWGN and Rayleigh fading channels. Nonetheless, the study did not account for transmission distance and PLCs, two crucial elements that impact BER [142].

Three power assignment methodologies [143] increase NOMA SE by optimizing NOMA power. However, little research has examined how interference affects energy allocation.

Researching the upper bounds of synchronised UP NOMA data rates, the authors show that the measured bottom bound is close to the standard synchronised NOMA systems' rate [144]. But each user can only send a certain amount of symbols, so drawing too many inferences might be a problem.

Decoding in the two separate channels that are utilized for DL and UL broadcasts can be made easier by monitoring and validating the ergodic rate that has been achieved, as described in [145]. Due to the lack of enough users to verify the validity of the perfect case and because the impact of this strategy on OP or BER, for example, is unable to reach any conclusions at this time.

Although many strategies for obtaining CRN are thoroughly examined in [146], certain elements remain unknown. The results won't hold up on a bigger network since the sample size is too tiny. Nothing is said about how the PLC may have a role either.

The spectrum access methods explored in [147] can be classified by purpose. The integration of active CSS in CRN is accomplished by the usage of MIMO NOMA technology, serving both PUs and SUs Using AWGN and Rayleigh Fading channels increases CRN capacity. However, the methods for accessing CRN have not been clearly explained, and only a small number of people use it.

Through cooperative communication, the author integrates an underlay CRN, therefore increasing the data transmission rate of an already-established multi-carrier NOMA network. Simulations demonstrate the proposed network boosts throughput. The Programmable Logic Controller's (PLC's) effects are unknown, and the results cannot be extended to a broad network [148].

The CRN may enable active CSS for main and secondary users using MIMO NOMA. Real CRN capacity has risen. Unfortunately, neither CRN's user base nor access mechanisms are clear. Nevertheless, the results cannot be applied to a broad network since the PLC's influence is not considered [149].

The study examines the CR-NOMA-based MIMO communication system the author has developed, specifically in the UL and DL situations. Fascinating results emerge from the inquiry. Additionally, the total throughput of the interferometer and the calculation of several frames were also considered. The PLC for each user and the particular type and way of accessing the CR scheme are not yet specified.

A multitude of researchers have advanced the wireless spectrum through the use of NOMA and CR, resulting in significant enhancements [130]–[131]. Among them, S. Sodagari et al. [133] CRN performance is improved by increasing PU and SU receiver SNR. The 5G CR-based spectrum-sharing solution employed the spectrum sensing function to allocate spectrum more efficiently to unlicensed users, as proposed by P. K. Sangdeh [135]. The study conducted by V. Kumar et al. [136] demonstrates that the implementation of spectrum sharing using CRS-NOMA outperforms selected SC and MRC combining systems when faced with greater interference peak power levels. Consequently, P. Kansal [137], utilized the DAG-SVM technology to enable the achievement of both high efficiency and high accuracy in spectrum sensing. S. Singh et al. presented [141] analyses of the cooperative MIMO NOMA system with half-duplex operation, SIC, and partial CSI for Nakagami-m fading channels. The method presented in [143] improved NOMA SE and proposed three power allocation approaches to optimize the power distribution among each NOMA. J. Zeng et al. presented a method in [144] that the minimum value reported is similar to the achievable rate of conventional synchronized NOMA systems for UP NOMA under synchronized transmission circumstances. Recently, T. Perarasi et al. integrated an underlay CRN utilizing cooperative communication to increase the data transfer rate in a multi-carrier NOMA network [148]. Enabling active CSS in the CRN is achieved by implementing MIMO NOMA technology for PUs and SUs. The current capacity of the CRN has increased proposed by A. S. Parihar [149]. For more research and study on NOMA with spectrum-sharing techniques to enhance performance and QoS, the reader may consult references 132, 134, 138, 139, 140, 142, 145, 146, 147, and 150.

The following table presents a comparative analysis of our work with previous literature, providing a concise explanation of our contributions.

Table2.2. Author's Contribution Table

Author's Name	NOMA	CR	Cooperative CR	UL	DL	OP	BER	SE	Average Capacity	MIMO	M-MIMO	5G
L. Lv (2018)	Yes	Yes	Yes	Yes	Yes	Yes	No	No	No	No	No	No
P. K. Sangdeh (2020)	No	Yes	No	No	No	No	No	No	No	Yes	No	No
V. Kumar (2019)	Yes	Yes	No	No	No	Yes	No	No	No	No	No	No
P. Kansal (2020)	No	Yes	No	No	No	No	No	No	No	No	No	Yes
W. Zhang (2018)	No	Yes	No	No	No	No	No	Yes	Yes	No	No	Yes
S. Arzykulov (2019)	Yes	Yes	No	No	No	Yes	No	No	No	No	No	No
S. Singh (2022)	Yes	Yes	No	No	Yes	Yes	No	No	No	No	No	No
K. Srinivasarao (2022)	Yes	Yes	No	No	Yes	Yes	No	No	No	No	No	Yes
A. Celik (2017)	Yes	No	No	No	Yes	No	No	No	Yes	No	No	No
J. Zeng (2018)	Yes	No	No	Yes	Yes	Yes	Yes	No	No	No	No	Yes
T. Balachander (2022)	Yes	Yes	No	No	Yes	No	No	Yes	No	Yes	No	Yes
A. S. Parihar (2021)	Yes	Yes	No	No	No	Yes	No	No	No	No	No	No
This research	Yes	Yes	Yes	Yes	Yes	Yes	Yes	Yes	Yes	Yes	Yes	Yes

CHAPTER THREE

Modeling of NOMA-MIMO Based Power Domain for 5G Network Under Selective Rayleigh Fading Channels

3.1 Introduction

This chapter introduces the modeling and design of PD-NOMA technologies. It also includes a reevaluation of the BER, SE of the DL, average capacity, and OP of the UL in the 5G network. The main objective of this investigation is to assess the influence of modifying the BWs and antenna count of a 5G network, which operates in an environment with AWGN and Rayleigh fading, on the BER, SE, average capacity, and OP performance of the network. In MATLAB, the model is used to validate all possible configurations of the system. This study examines the NOMA system by employing two different proposed BWs. All four NOMA users experienced a significant increase in performance, particularly following the combination with MIMO technology.

3.2 DL PD-NOMA Model

Let's examine a wireless network with MIMO technology. The network has a size of 64x64 and is designed to serve four users using the PD DL-NOMA technique. This configuration is depicted in Figure 3.1. The four users possess BWs that vary between 80 and 200 MHz. Let d denote their BS distances, with d_1 being more than d_2 , d_2 being greater than d_3 , and d_3 being greater than d_4 , in the desired sequence. User U_1 is distant from the BS, whereas U_4 is the BS-close user. Let h_{T1} , h_{T2} , h_{T3} , and h_{T4} represent the selective Rayleigh fading coefficients. The magnitudes of these coefficients satisfy the inequality $|h_{T1}|^2 < |h_{T2}|^2 < |h_{T3}|^2 < |h_{T4}|^2$ [151].

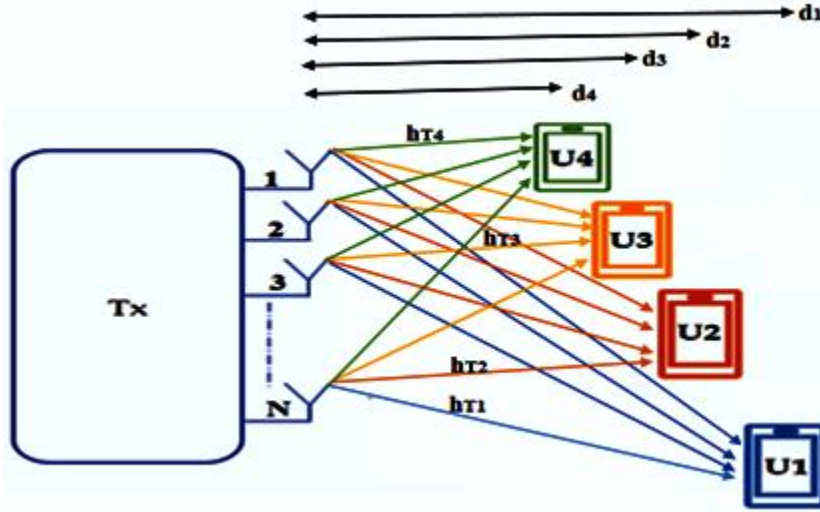


Figure 3.1. The wireless network has four users with 64x64 MIMO PD DL-NOMA

Each user's whole Rayleigh fading channel is divided up in accordance with the parameters given in the reference [152]:

$$h_{Ti} = \sum_{i=1}^M h_{Ti} \quad (3.1)$$

Users are $i = 1, 2, 3, 4$ and channels are 64. Power coefficients $\alpha_1, \alpha_2, \alpha_3,$ and α_4 represent them. PD-NOMA advocates giving weaker users more power and powerful users less.

Therefore, the power location coefficients should be arranged in the following sequence of magnitudes: $\alpha_1 > \alpha_2 > \alpha_3 > \alpha_4$. Let's examine the QPSK-encoded transmissions $x_1, x_2, x_3,$ and x_4 that are intended for BS $U_1, U_2, U_3,$ and U_4 . As stated in reference [153], the encrypted overlay signal of the BS is subsequently defined.

$$x = \sqrt{p}(\sqrt{\alpha_1}x_1 + \sqrt{\alpha_2}x_2 + \sqrt{\alpha_3}x_3 + \sqrt{\alpha_4}x_4) \quad (3.2)$$

When user 1 is at full power, it decodes y_1 directly, causing interference to the signals of users 2, 3, and 4. Thus, the initial user rate candidate is.

$$R_1 = \log_2 \left(1 + \frac{\alpha_1 P |h_{T1}|^2}{\alpha_2 P |h_{T1}|^2 + \alpha_3 P |h_{T1}|^2 + \alpha_4 P |h_{T1}|^2 + \sigma^2} \right) \quad (3.3)$$

Since SIC already removed user1 data, the obtained rate applies to user2.

$$R_2 = \log_2 \left(1 + \frac{\alpha_2 P |h_{T2}|^2}{\alpha_3 P |h_{T2}|^2 + \alpha_4 P |h_{T2}|^2 + \sigma^2} \right) \quad (3.4)$$

After SIC scrubbed data from user1 and user2, the success rate is for user3.

$$R_3 = \log_2 \left(1 + \frac{\alpha_3 P |h_{T3}|^2}{\alpha_4 P |h_{T3}|^2 + \sigma^2} \right) \quad (3.5)$$

After SIC scrubbed the data from user1 through user3, the acquired rate was calculated for user4.

$$R_4 = \log_2 \left(1 + \frac{\alpha_4 P |h_{T4}|^2}{\sigma^2} \right) \quad (3.6)$$

To determine the spectrum efficiency performance rate.

$$SE = \frac{Th}{BW} \quad (3.7)$$

SE, Th, and BW indicate spectrum efficiency, throughput, and bandwidth.

3.3. UL PD-NOMA Model

There is little association between DL variety and UL PD-NOMA multiplexing. The BS provides PD multiplexing in the DL via superposition coding. In the UL, only battery capacity limits users. This optimizes signal strength for all users. Changes in users' channel gains affect BS receiver power allocation.

UL PD-NOMA four users send messages x_1 , x_2 , x_3 , and x_4 . Given comparable wireless signals from both users, the 64x64 MIMO system has BWs of 80 and 200 MHz, as shown in Figure 2. Please call the distances d_1 , d_2 , d_3 , and d_4 . U_1 has a weak or far BS signal, whereas U_4 has a strong or close signal. Connected selective Rayleigh fading coefficients are arranged as $|h_{T1}|^2 < |h_{T2}|^2 < |h_{T3}|^2 < |h_{T4}|^2$ [151].

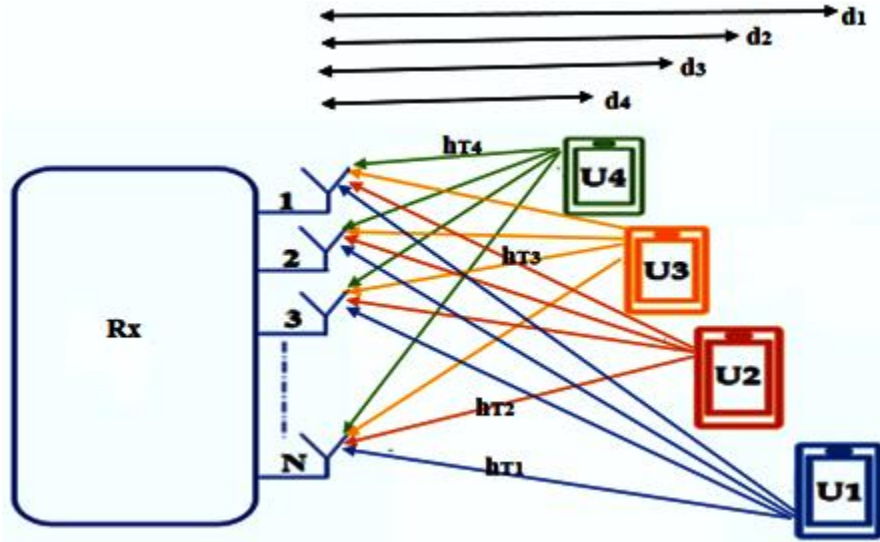


Figure 3.2. Shows the four-user 64x64 MIMO UL PD-NOMA wireless network

Each user's total Rayleigh fading channel can be calculated as follows:

$$h_{Tj} = \sum_{j=1}^N h_{Tj} \quad (3.8)$$

N is the total number of channels, 64, and j is the total number of users, 1, 2, 3, or 4.

The BS was successful in picking up the signal.

$$y = \sqrt{P_{x1}}h_{1T} + \sqrt{P_{x2}}h_{2T} + \sqrt{P_{x3}}h_{3T} + \sqrt{P_{x4}}h_{4T} + w \quad (3.9)$$

where w stands for the intensity of the noise.

3.3.1. Capacity Rates Achieved by Four Users According to UL NOMA

Decoding begins with the signal from the nearest user, disregarding further signals as interference. Thus, a nearby user's BS decoding speed is [154]-[155].

$$R_{U4} = \log_2 \left(1 + \frac{P|h_{4T}|^2}{P|h_{1T}|^2 + P|h_{2T}|^2 + P|h_{3T}|^2 + \sigma^2} \right) \quad (3.10)$$

The maximum rate U_3 can be determined once the SIC has been computed.

$$R_{U3} = \log_2 \left(1 + \frac{P|h_{3T}|^2}{P|h_{1T}|^2 + P|h_{2T}|^2 + \sigma^2} \right) \quad (3.11)$$

Following the determination of the SIC, the highest achievable rate is U_2 .

$$R_{U_2} = \log_2 \left(1 + \frac{P|h_2T|^2}{P|h_1T|^2 + \sigma^2} \right) \quad (3.12)$$

After the SIC is determined, the highest possible U_1 rate can be attained.

$$R_{U_1} = \log_2 \left(1 + \frac{P|h_1T|^2}{\sigma^2} \right) \quad (3.13)$$

3.3.2. UL's NOMA OP for Four Users

Consider that the four users have different rate targets that they want to achieve.

$$r_1 = 1, r_2 = 2, r_3 = 3, r_4 = 4$$

The following expression describes the capability of U_4 :

$$C_4 = \sum_{i=1}^N \log_2 \left(1 + \frac{P|h_4|^2}{P|h_1|^2 + P|h_2|^2 + P|h_3|^2 + N_4} \right) \quad (3.14)$$

For the purpose of determining the capacity of U_3 , the following equation is utilized.:

$$C_3 = \sum_{i=1}^N \log_2 \left(1 + \frac{P|h_3|^2}{P|h_1|^2 + P|h_2|^2 + N_3} \right) \quad (3.15)$$

The following equation is used to determine U_2 Carrying capacity:

$$C_2 = \sum_{i=1}^N \log_2 \left(1 + \frac{P|h_2|^2}{P|h_1|^2 + N_2} \right) \quad (3.16)$$

The capacity of U_1 is estimated as follows:

$$C_1 = \sum_{i=1}^N \log_2 \left(1 + \frac{P|h_1|^2}{N_1} \right) \quad (3.17)$$

U_1 has the OP condition of:

$$P_r (C_1(k) < r_1) \parallel P_r (C_2(k) < r_2) \parallel P_r (C_3(k) < r_3) \parallel P_r (C_4(k) < r_4) < r$$

The U_1 OP:

$$P_r(U_1) = (\sum_{i=1}^N P_r (C_1(K) < r_1) \parallel P_r(C_2(K) < r_2) \parallel P_r(C_3(K) < r_3)) \parallel P_r (C_4(K) < r_4)) / N \quad (3.18)$$

U_2 has the OP condition of:

$$P_r (C_2(k) < r_2) \parallel P_r (C_3(k) < r_3 \parallel P_r (C_4(k) < r_4)) < r$$

U_2 's OP:

$$P_r(U_2) = (\sum_{i=1}^N P_r (C_2(K) < r_2) \parallel P_r(C_2(K) < r_2) \parallel P_r (C_4(K) < r_4))/N \quad (3.19)$$

Has the OP condition of:

$$P_r (C_3(k) < r_3 \parallel P_r (C_4(k) < r_4)) < r$$

U_3 's OP:

$$P_r(U_3) = (\sum_{i=1}^N P_r (C_3(K) < r_3) \parallel P_r (C_4(K) < r_4))/N \quad (3.20)$$

U_4 has the OP condition of:

$$P_r (C_4(k) < r_4) < r$$

U_4 's OP:

$$P_r(U_4) = (\sum_{i=1}^N P_r (C_4(K) < r_4))/N \quad (3.21)$$

where N indicates the total samples exchanged.

3.4. Parameters for simulation

In 5G networks, PD DL and UL NOMA are designed to work with and without MIMO, and this functionality is modelled in MATLAB. The settings used to simulate the model are displayed in Tables 3.1 and 3.2.

Table 3.1. DL Scenario Simulator Parameters.

No.	Parameters	Values	
1.	Modulation	QPSK	
2.	Path loss	4	
3.	BW	BW 1	80 MHz
		BW 2	200 MHz
4.	Distances	U_1	800 m
		U_2	600 m
		U_3	300 m
		U_4	100 m
5.	PLCs	U_1	0.75
		U_2	0.188
		U_3	0.047

		U_4	0.011
6.	TP	0 to 40 dBm	
7.	MIMO	64 x 64	
8.	Number of users	4 users	

Table 3.2. UL Scenario Simulator Parameters

No.	Parameters	Values	
1.	Path loss	4	
2.	TP	-30 to 30 dBm	
3.	BW	BW1	80 MHz
		BW2	200 MHz
4.	Distances	U_1	800 m
		U_2	600 m
		U_3	300 m
		U_4	100 m
6.	Number of users	4 users	
7.	MIMO	64 x 64	

3.5. Computer Model

The flowcharts below depict the process of implementing the code in two scenarios: DL and UL NOMA.

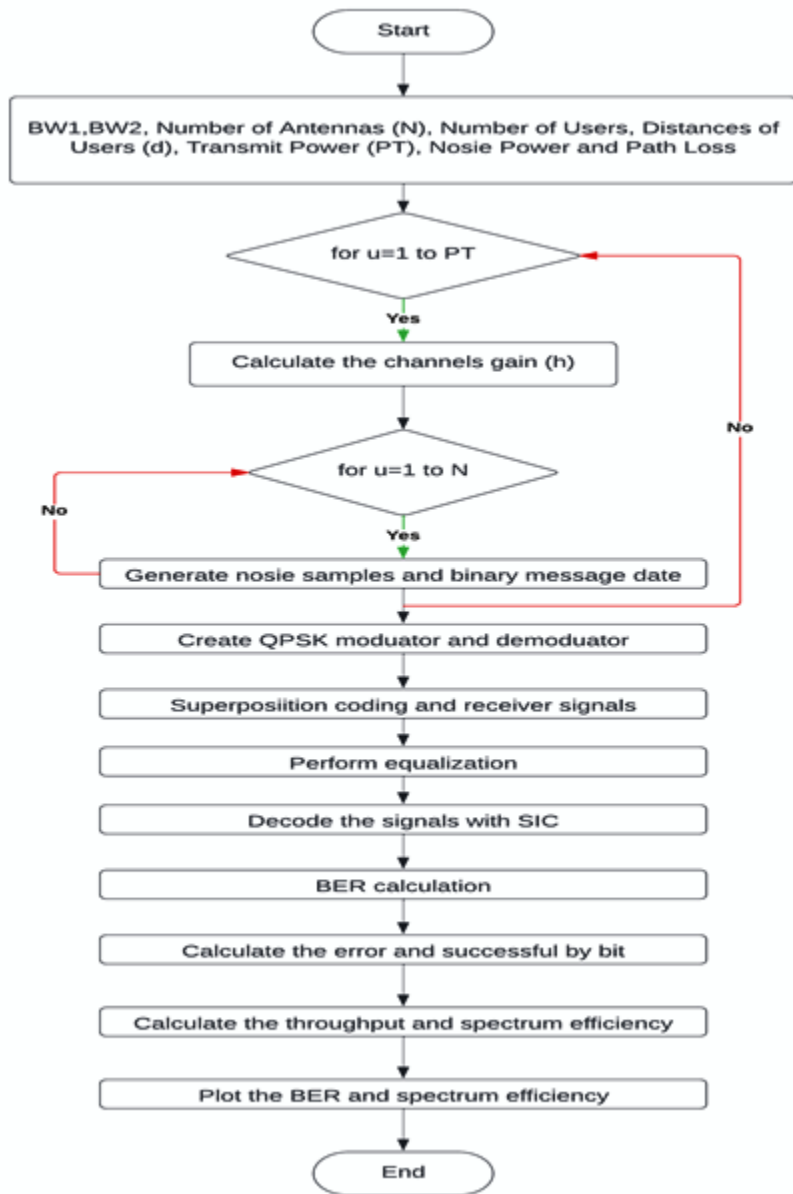


Figure 3.3. DL-NOMA Flowchart Scenario

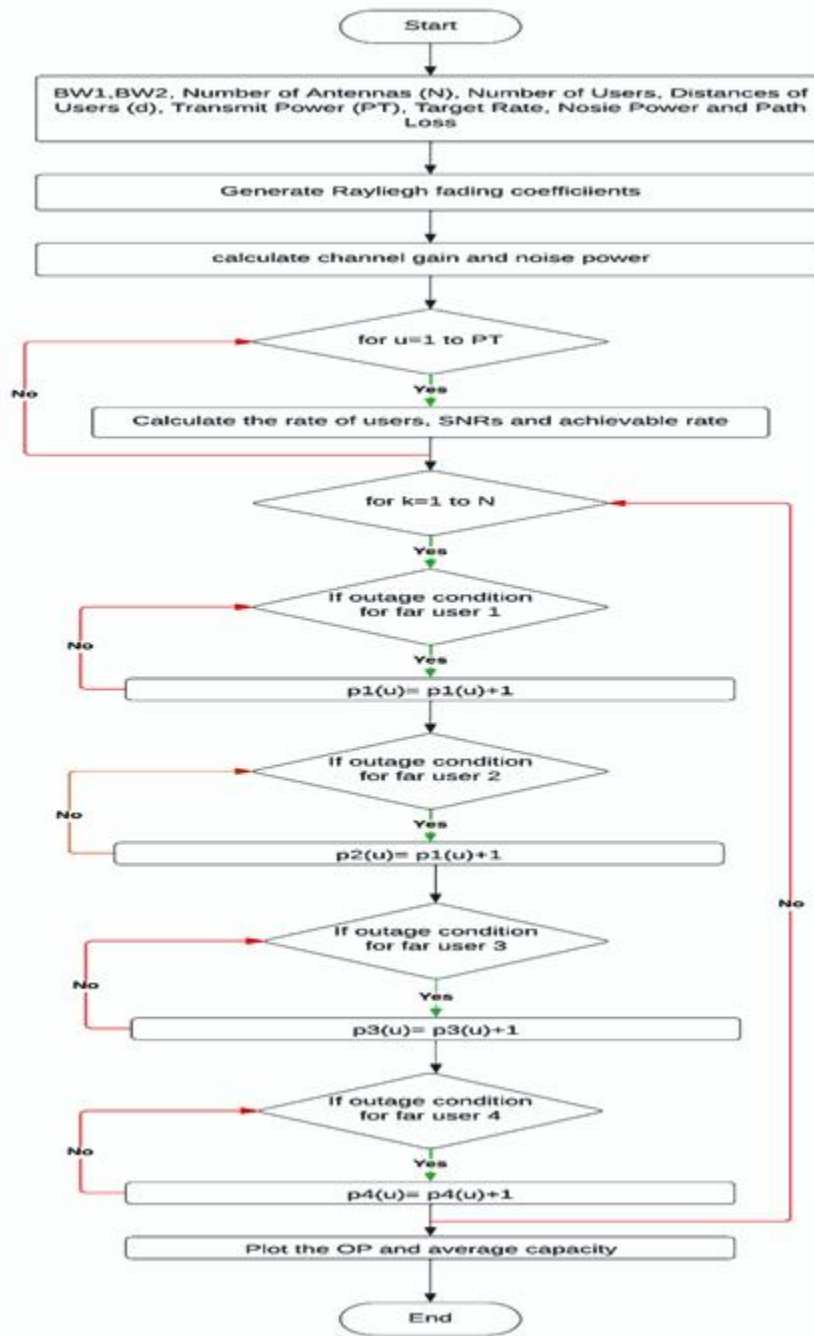


Figure 3.4. UL-NOMA Flowchart Scenario

3.6. Results and Discussion

Results from running the software in the DL scenario are displayed in the accompanying figures, which compare BER and SE versus TP for DL NOMA with and without MIMO. For the UL case, plot the average capacity and OP vs. SNR from the program with and without MIMO.

3.6.1. The DL NOMA Model's Outcomes

Figure 3.5 depicts the performance of 80 MHz BW DL NOMA BER versus TP. The U_4 provides the best BER performance for all users since it's nearest to the BS and has the minimum interference. As the TP approaches 10 dBm, the performance of the other three users begins to converge. Because their power location coefficient values and distances are close together, making them more interfering with one another, the second user is the worst.

Figure 3.6 shows that when the TP increases, at 200 MHz BW, DL NOMA BER diminishes. The U_4 gives the best BER performance for all users since it is closest to the BS and has the least interference. When the TP gets close to 13 dBm, the other three users' performance starts to converge. Similar considerations apply to the second user's poor performance. Regardless, the BER was larger than the previous result because of the increased BW.

Note that many elements, including power location coefficients, technology, channel conditions, SIC, BW and distance, affect the BER performance of DL-NOMA either positively or negatively. These elements can exhibit complex interactions, and their effects on DL-NOMA's BER performance are varied. The parameter determines the power distribution between individual users, and its size affects the BER performance.

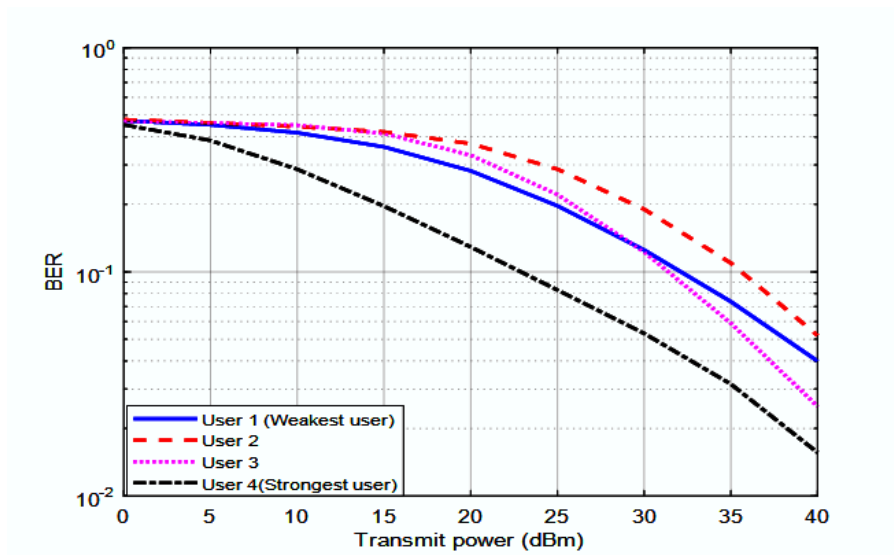


Figure 3.5. DL NOMA at 80 MHz BW: BER against TP for four 4 users located at different distances

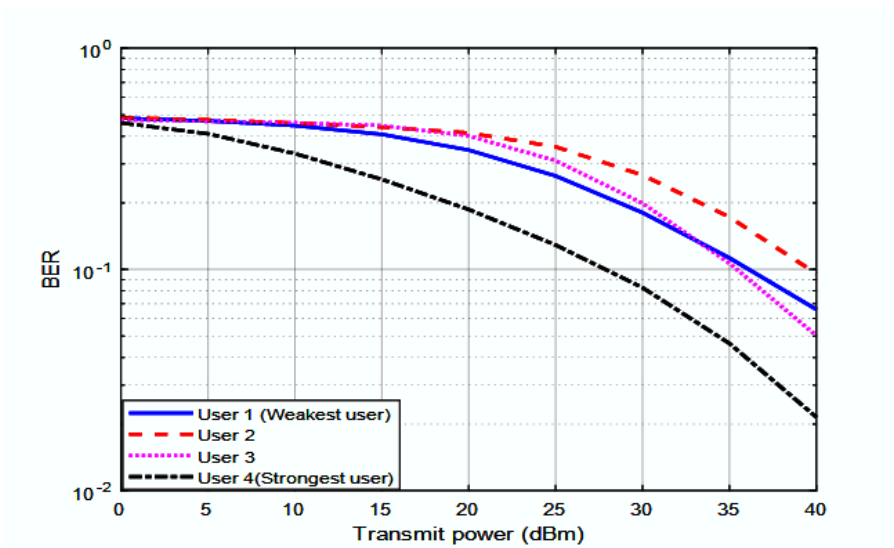


Figure 3.6. DL NOMA at 200 MHz BW: BER versus TP for four users at varying distances

Figure 3.7 illustrates that when TP increases at 80 MHz BW, the DL 64x64 MIMO NOMA BER drops. U₄ has the best BER performance for all users since it is nearest to the BS and has the least amount of interference, while the first user has the poorest performance due to its distance. The first and second users' performances were identical due to the convergence of the value power coefficient and distance settings. The resulting values of BER performance were 8.1e-04, 8.0e-05, 3.0e-05, and 2.5e-05, respectively.

Figure 3.8 demonstrates that when the TP grows with a bandwidth of 200 MHz, the DL 64x64 MIMO NOMA BER decreases. U₄ has superior BER performance compared to all other users because of its proximity to the BS and less interference. Conversely, the first user experiences the lowest performance as a result of its distance from the BS. The performances of the first and second users were indistinguishable as a result of the convergence of the value power coefficient and distance settings. The obtained values of BER performance were 9.1e-04, 9.0e-04, 1.5e-04, and 3.0e-05, respectively.

The use of the MIMO technology resulted in a significant reduction and became more comparable in the BER. MIMO technology has the potential to enhance the performance of wireless communication in terms of data throughput, signal strength range, and BER.

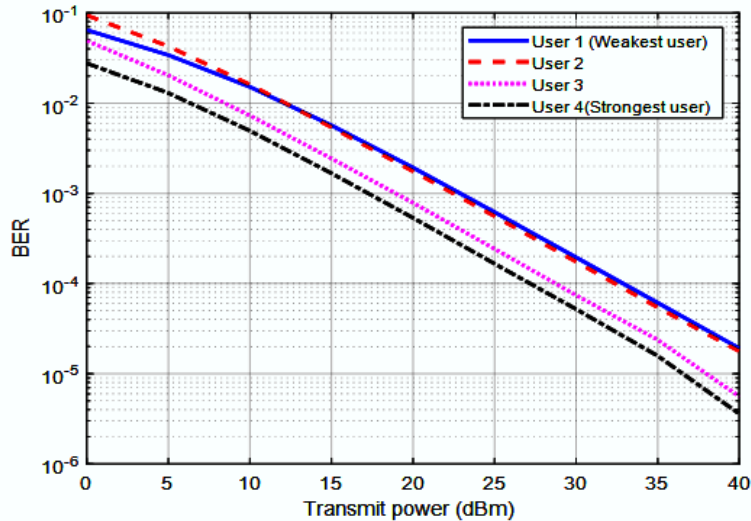


Figure 3.7. BER for four users in DL-NOMA against TP for 64x64 MIMO at 80 MHz BW

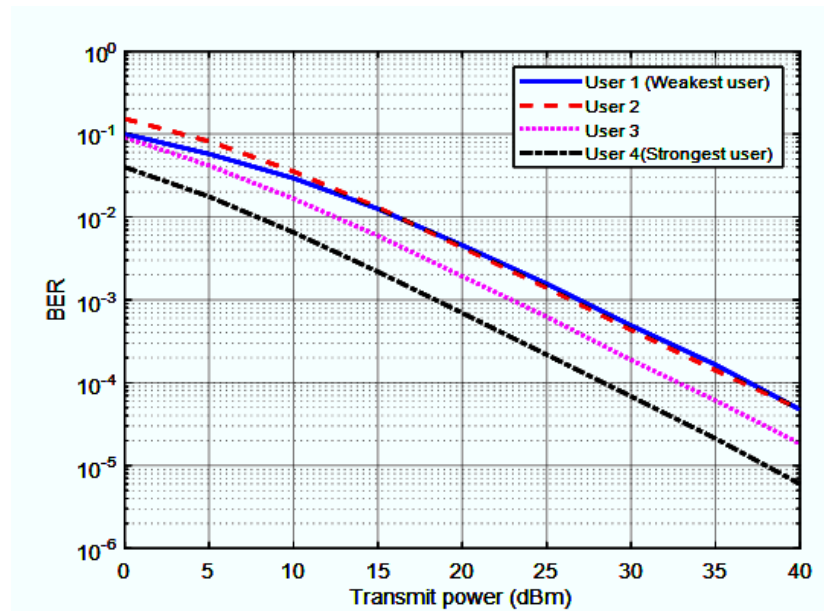


Figure 3.8. BER versus TP in DL NOMA with 4 Users and 200 MHz BW using 64x64 MIMO

The results of the experiment showing the SE performance versus TP for 80 MHz BW DL NOMA are shown in Figure 3.9. The SE performance improves with higher TP. Due to its convenient location, U_4 offers the highest SE performance to other users. The second user is by far the worst. The power coefficients and the close distances of the four users lead to similar performance between them, and this is evident in the SE performance between the three users until the TP reaches 5 dBm.

Increasing the TP improves the DL NOMA SE performance, as seen in Figure 3.10, even at a BW of 200 MHz. All other users are surpassed by U_4 SE. The second user is the most inferior. The power factor and the proximity between them and the four users result in a closely correlated performance. The SE performance of the three users reaches a point of convergence when the TP reaches 7dBm.

The investigation and assessment revealed that the parameters affecting SE in DL-NOMA are the distribution of users on the network might affect the SE and uneven user distribution might reduce resource allocation and system efficiency. The achieved results were better than the best user U_2 's in [156]-[157].

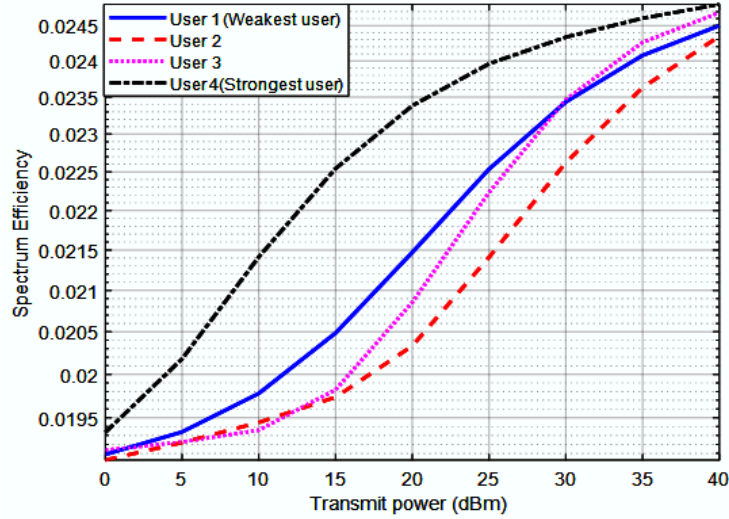


Figure 3.9. Four users at various distances, SE versus TP, 80 MHz BW for DL NOMA

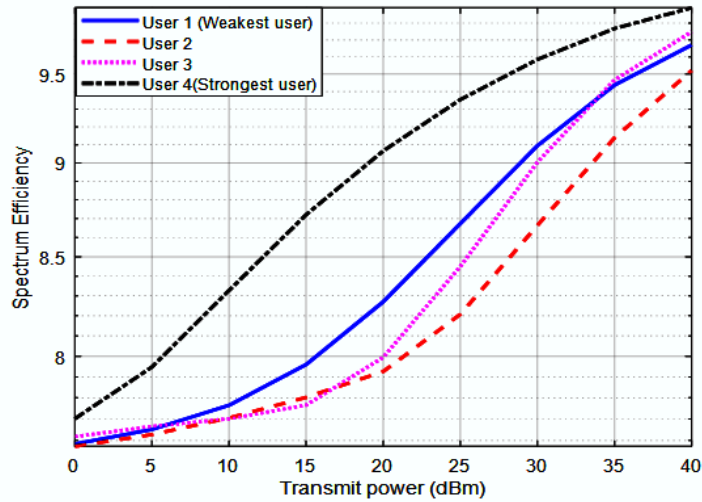


Figure 3.10. DL NOMA SE compared to TP for four users located at different distances with the BW of 200 MHz

The results of the experiment showing the SE performance versus TP for 80 MHz BW DL 64x64 NOMA are shown in Figure 3.11. The SE performance improves with higher TP. Initially, there was a distinct disparity in the

performance of the users until the TP reached a level of 22dBm. At this point, all users exhibited similar levels of performance.

Enhancing the TP enhances the DL 64x64 MIMO NOMA SE performance, as seen in Figure 3.12, even when the BW is 200 MHz. At first, there was a clear difference in the performance of the users until the TP reached a level of 25dBm. Currently, all users showed comparable levels of performance.

In MIMO, many data streams are generated by the transceiver's antennas. According to the research, Wireless data speed, signal strength, range, and SE performance are all improved using MIMO technology. Enhancing SE performance is one area where MIMO has a direct influence. By making better use of the available resources, MIMO systems are able to achieve larger SE by maximizing the BW of the wireless channel.

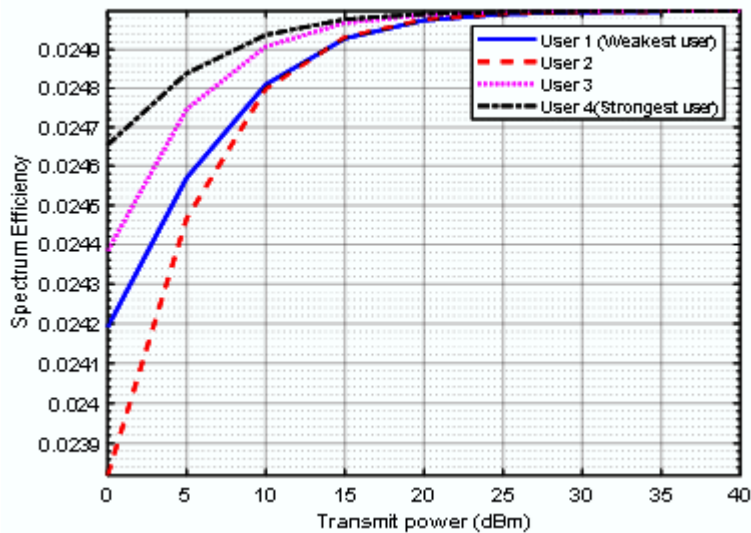


Figure 3.11. SE versus TP for four users at varying distances, using 64x64 MIMO and the BW of 80 MHz in DL NOMA

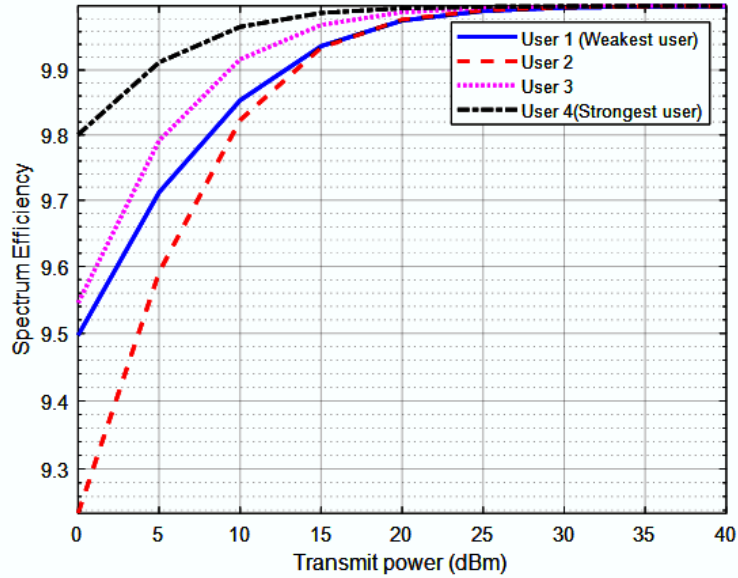


Figure 3.12. SE versus TP for four users at varying distances, with 64x64 MIMO and BW 200 MHz for DL NOMA

3.6.2. The UL NOMA Model's Outcomes

Figure 3.13 depicts the results of the experiment that compares average capacity performance to SNR for 80 MHz BW DL NOMA. The average capacity performance improves as SNR increases. Initially, there was a convergence between the second and first users until the SNR reached 0.1 dB, after which there was a noticeable difference in the performance of all users. Due to the user's distance and closeness to the BS, the fourth user performs best and the first user performs the worst. The average capacities for four users were (1.6873, 2.8718, 6.4962, and 12.7814) bps/Hz, respectively, at the SNR of 1 dB.

Using 200 MHz BW DL NOMA, Figure 3.14 shows the experimental findings comparing average capacity performance to SNR. Raising the SNR enhances the overall capacity performance. Initially, the second and first users converged until the SNR hit 0.08 dB, at which point all users' performance started to diverge. Because of the user's proximity to the BS, the fourth user has the highest performance, while the first user has the poorest. Under conditions of channels and SNR equal 1 dB, the four users' average capabilities were (2.6015, 3.9841, 7.7910, and 14.1068) bps/Hz, respectively.

Understanding the elements that affect UL-NOMA's average capacity is crucial to improving system performance. The study found that the following factors affect UL-NOMA's average capacity: As the user population expands, UL-NOMA's average capacity increases, but the fairness factor, which measures resource allocation, decreases. BW affects UL-NOMA performance, with smaller BW reducing average capacities. Additionally, the results demonstrate that performance in terms of average capacity is enhanced when the SNR is increased.

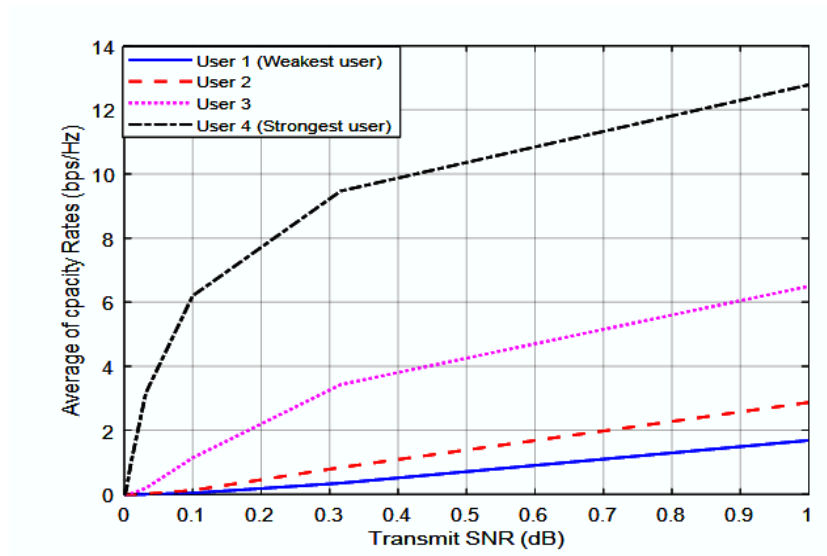


Figure 3.13. Average capacity against SNR for four UL NOMA users at varied distances and BW 80 MHz

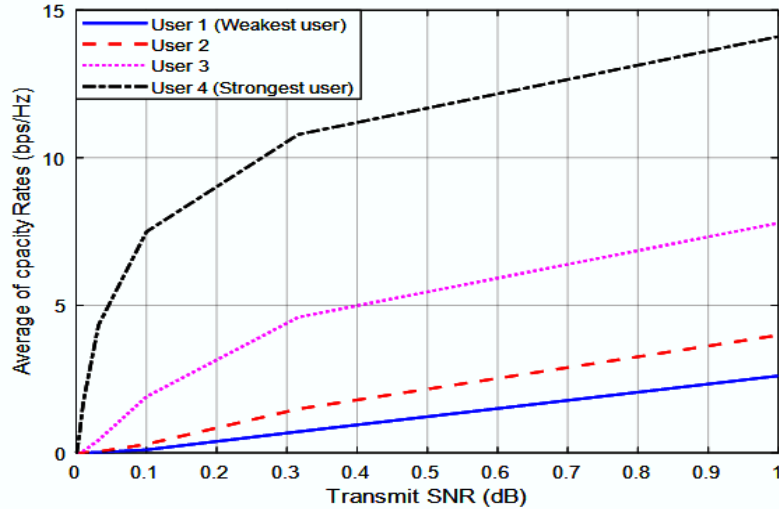


Figure 3.14. The relationship between average capacity and SNR for four users at various distances and BW 200 MHz in UL NOMA

Figure 3.15 shows the typical average capacity versus SNR performance of UL NOMA for 80 MHz BW with 64x64 MIMO. Right from the start, there was a disparity in the performance of the four users. The preference was for the user closest to BS, which is the fourth user, and quite the opposite was the performance of the first user. With four users, the average capacity was (12.7881, 14.4423, 18.4489, and 24.7815) bps/Hz at the SNR of 1 dB.

In Figure 3.16, the average capacity vs. SNR performance of UL NOMA with a 200 MHz BW and 64x64 MIMO were seen. When the SNR is raised, the average capacity also rises, leading to better overall performance. There was little difference in performance between the four users from the start. The fourth user, who was closest to BS, was preferred, but the first user performed poorly. U_4 has the best average capacity performance of 26.1040 bps/Hz, U_3 of 19.7693 bps/Hz, U_2 of 15.7659 bps/Hz, and U_1 of 14.1110 bps/Hz according to the four users' data at SNR of 1 dB. Users will notice a significant performance improvement. A higher BW is associated with a higher average capacity and vice versa.

The research found that the average capacity of UL-NOMA systems is affected by several parameters, including the number of users and BS antennas. These features strongly impact the average capacity of UL-NOMA systems with MIMO; system throughput improves, while system complexity increases.

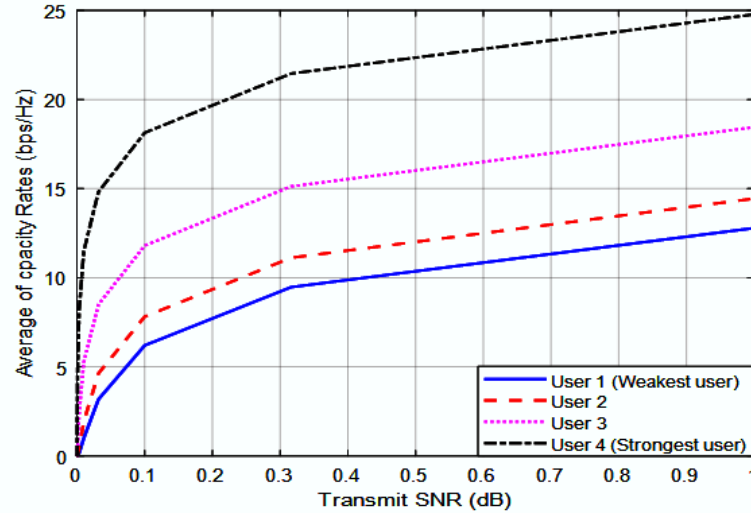


Figure 3.15. The average capacity vs SNR for UL NOMA with 64x64 MIMO and 80 MHz BW for four users at different distances.

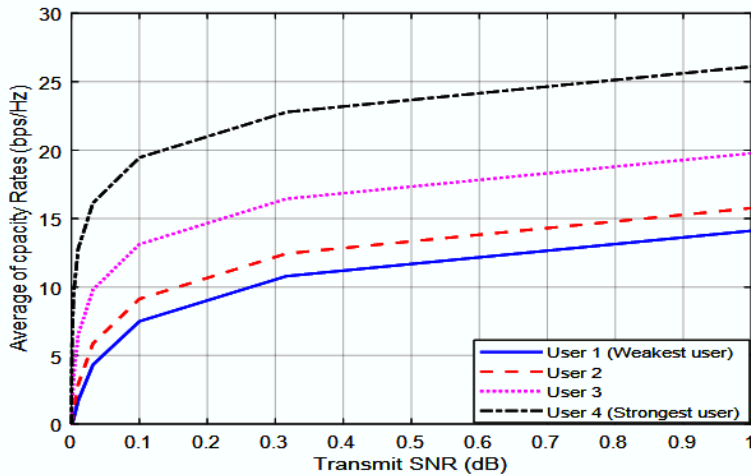


Figure 3.16. The average capacity against SNR for UL NOMA with 64x64 MIMO and 200 MHz BW for four users at varied distances.

Figure 3.17 depicts the typical OP vs SNR performance of the UL NOMA at 80 MHz BW. The four users' performance varied from the outset. The first and second users perform similarly until the SNR reaches 0.05, at which point the

performance of all users diverges. The fourth user, who was closest to BS, was preferred, but the first user performed poorly. The OP for four users was 0.9, 0.8, 0.44, and 0.014 at an SNR of 0.5 dB, respectively.

Figure 3.18 depicts the OP performance versus typical SNR for UL NOMA at 200 MHz BW. Note that the performance of the four users differed from the beginning and that there was a noticeable difference and improvement in the performance of the four users when comparing the results obtained in the previous figure, due to an increase in the BW. The fourth user, closest to the BS, was preferred, but the performance of the first user was substantially different. At 0.5 dB SNR, the OP for four users was 0.099, 0.097, 0.0037, and 0.00012.

The basic performance parameter UL-NOMA OP depends on various parameters. To understand and enhance UL-NOMA systems, notably OP, the research indicated that transmission SNR, power allocation coefficients, channel characteristics, and increasing BW effect OP. As SNR grows, OP performance declines. Output exceeds the top user [158].

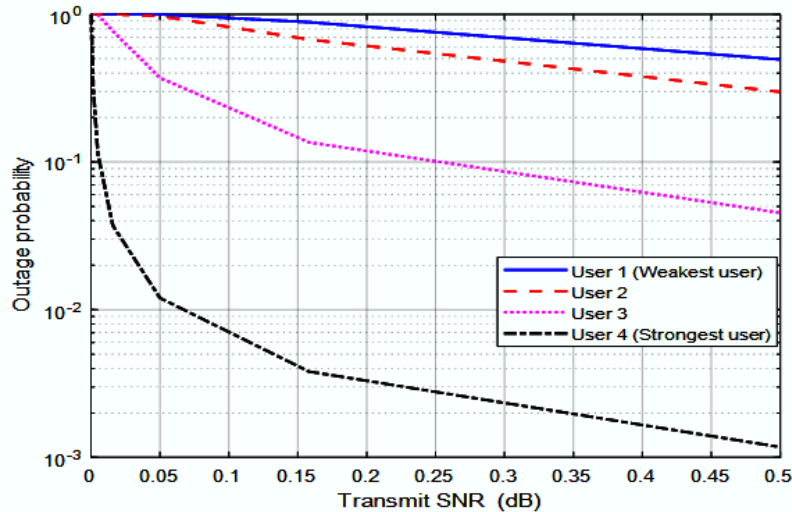


Figure 3.17. Four users at varying distances and a bandwidth of 80 MHz are considered for UL NOMA's OP versus SNR

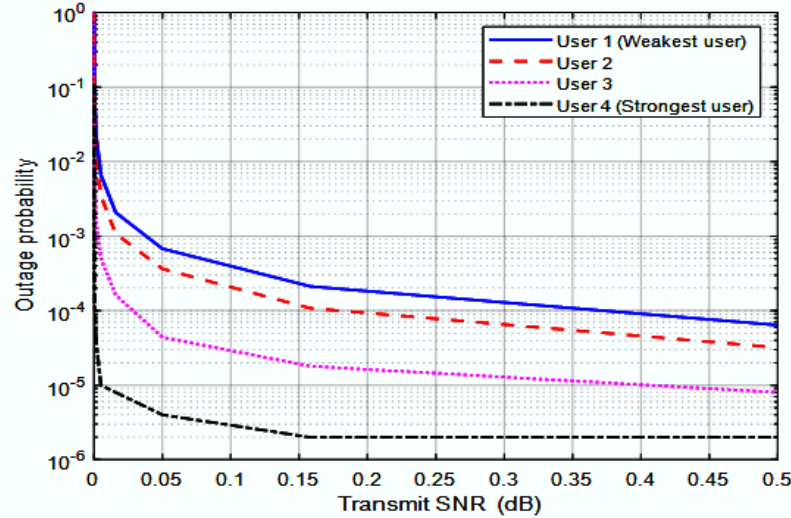


Figure 3.18. The UL NOMA's OP vs. SNR takes into account four users at different distances and the 200 MHz BW

Figure 3.19 illustrates the relationship between OP and SNR of UL 64x64 MIMO NOMA at 80 MHz BW. It should be noted that the performance of the four users varied from the start and there is variability in the performance of all users. The fourth user, who was nearest to the BS, was the favoured choice. The OP for four users at the SNR of 0.17 dB was measured to be 0.005, 0.0027, 0.0003, and 0.00009, respectively.

Figure 3.20 depicts the correlation between the OP and the SNR of UL 64x64 MIMO NOMA at BW of 200 MHz. The performance of the four users differed from the beginning and all users exhibit performance fluctuation. The fourth user, which was closest to the BS, was the preferred option. The OP was determined for four users at the SNR of 0.17 dB. The measured OP values were 0.0021, 0.0009, 0.0001, and 0.00001, respectively.

MIMO system OP is affected by many variables, including transmitting antenna count. The research shows that more transmitting antennas lower OP. Multiple antennas minimize fading and interference by creating spatial contrast. As SNR rises, OP falls. A high SNR makes the signal more resilient to fading and interference. As BW grows, OP decreases, and vice versa. MIMO optimization considerably reduces OP. The findings are proven to be $10^{-1.9}$ times more efficient in OP than the best U_2 , users, as reported in [155].

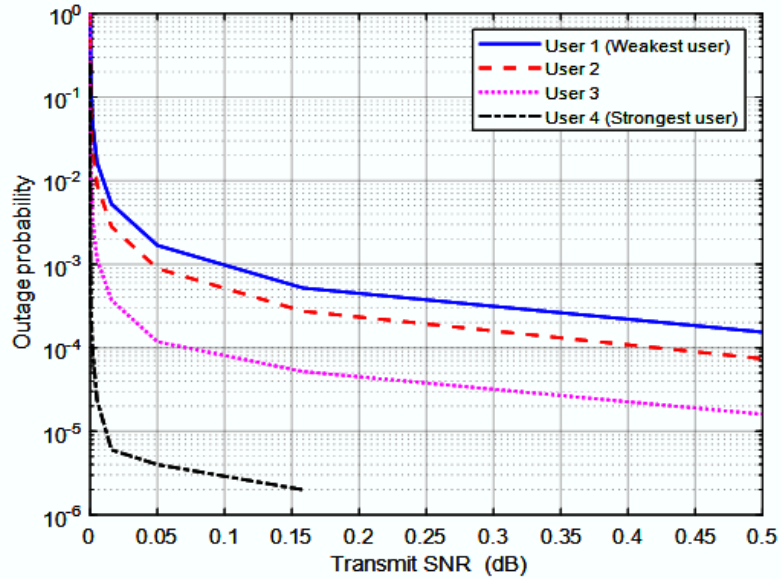


Figure 3.19. UL NOMA with 64x64 MIMO and the 80 MHz BW pits OP vs SNR for four users at varying distances

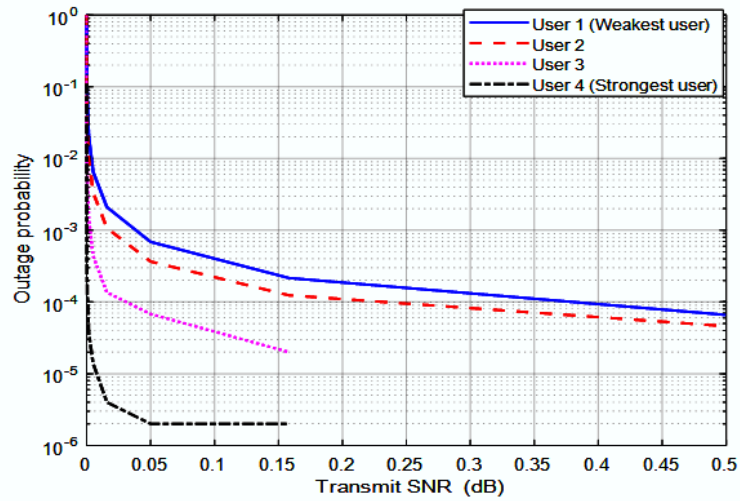


Figure 3.20. For four users at different distances, UL NOMA with 64x64 MIMO and the 200 MHz BW compares OP and SNR

3.7 Summary

This chapter showed DL and UL NOMA PD on the 5G network with and without 64x64 MIMO. The DL NOMA system's findings indicate that 64x64 MIMO fixes the near-far user's conundrum by bringing all users' performance to par regardless of TP, distance, or power location coefficient factors, and it also enhances SE and BER performance. The evaluation of DL NOMA's BER and SE performance was done using different distances, PLCs, TPs, and BWs, while the OP and average capacity of UL NOMA were probed using different SNRs and BWs.

The best user U_4 's BER improved with MIMO DL NOMA at 80 MHz BW and 78% at 200 MHz BW and 40 dBm TP. At 40 dBm TP, the MIMO system enhances SE performance for the best user U_4 by 20% bps/Hz for 80 MHz BW and 18% for 200 MHz BW.

For the optimal user U_4 , the results of the MIMO study on UL NOMA systems showed a 29% improvement in average capacity performance, a 95% drop in OP at 80 MHz BW, and a 31% improvement at 200 MHz BW, a 97% decrease in OP.

Typically, BER and average capacity go up as BW goes up, whereas SE and OP go down when BW goes down. Using MIMO greatly enhances performance for every user.

CHAPTER FOUR

Average Rate Performance for Pairing Downlink NOMA Networks Schemes

4.1 Introduction

Wireless communication systems use three different multiple-access methodologies: NOMA, TDMA, and SC-NOMA. The above methods are compared below:: NOMA lets several users share frequency and temporal resources at varying power levels. To preserve fairness and employ time and frequency diversity, users with better channel conditions are given less power. Enhance connection and increase data transfer rate within resource constraints. Has a lower outage probability (OP) compared to TDMA. Can be utilized in 5G networks to optimize time-critical, data-intensive services.

TDMA multiple users use the same carrier frequency, with each user utilizing distinct time intervals that do not overlap. Not as intricate and not as effective as NOMA.

SC-NOMA holds great potential for 5G and further wireless communication technologies. It provides a large amount of connection, low latency, and a powerful system, according to the research. SC-NOMA is a modification of NOMA that uses a solitary carrier to accommodate numerous users, whereas MC-NOMA utilizes multiple carriers to service multiple users. An obstacle faced by SC-NOMA is the requirement to distribute power and resources effectively among several users. Many power allocation strategies aim to enhance SC-NOMA performance. However, these systems may be difficult.

In an effort to reduce the computing complexity, less-than-ideal user matching procedures have been proposed. To improve the performance of wireless communication networks, the paired approach in NOMA with TDMA is an essential component. Future wireless networks will rely on NOMA. The system's capacity is enhanced since several users are able to share a single physical channel. To make the most of the disparity in channel gains, NOMA pairs users according to their channel circumstances.

When it comes to NOMA, the use of this pairing procedure is necessary since it enables the effective distribution of resources and the management of interference. Following this, the paired users are each given a distinct power level, which enables the receiver to differentiate between the signals by the use of SIC.

This chapter explains the basics of NOMA networks and proposes two coupling strategies for downlink NOMA networks: near-far (NF) coupling and close-and-close (C-C) or far-and-far (F-F) coupling. Subsequently, six users were analysed using the MATLAB simulation tool to ascertain the average rate vs SNR at various intervals and distances utilizing the suggested methods of single carrier NOMA (SC-NOMA) [160] and TDMA.

4.2 System Model

NOMA enables simultaneous service of a significant quantity of users on a singular frequency. Network performance decreases as the number of users capable of sharing a certain frequency carrier hits a given limit. There must therefore be a cap on the total number of subscribers served by any network operator. Mixed NOMA refers to a network architecture in which NOMA is used in conjunction with another OMA technology. Figure 4.1 shows that by combining TDMA with NOMA, as is done in this study, a total of 4 ms is required to support 6 users. The fact that NOMA gives all six users four milliseconds instead of one reveals how SIC complexity and processing time have increased. TDMA now only gives one slot per user. Conversely, in the NOMA mixed, three NOMA users are allocated to each of the two 2-millisecond slots that make up the 4-millisecond period [161].

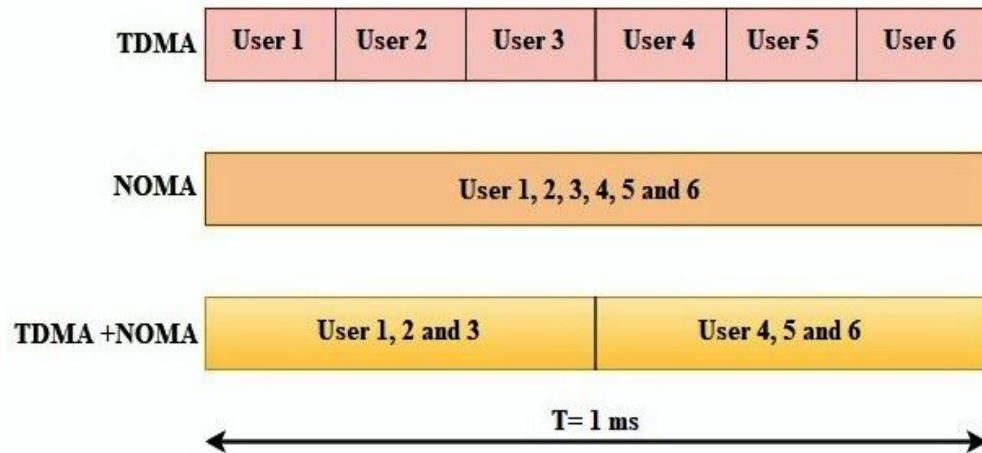


Figure 4.1. Displays how users are assigned to various multiple access methods

Let's have a look at the six-user model of a DL communication system shown in Figure 4.2. Let's pretend the distances from U_1 , U_2 , U_3 , U_4 , U_5 , and U_6 to the home base are d_1 , d_2 , d_3 , d_4 , d_5 , and d_6 , respectively. User 1 is physically located closest to BS, while User 6 is the furthest one. Thus, the following are the parameters for their channel (h_i): $|h_1|^2 > |h_2|^2 > |h_3|^2 > |h_4|^2 > |h_5|^2 > |h_6|^2$.

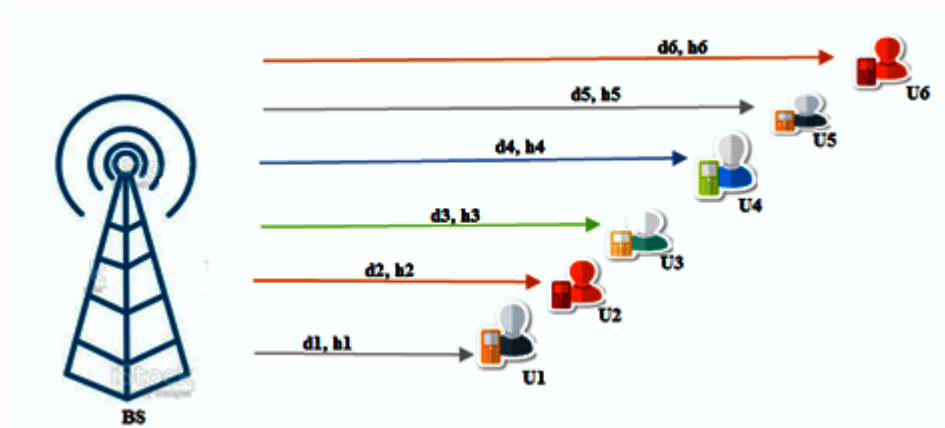


Figure 4.2. Shows a model of the downlink transmission system with six users at varying distances

It can be accomplished using one of two primary strategies:

4.2.1 NOMA, the First Strategy to Match Nearby and Far Users (N-F)

Pairing up users who are geographically distant from the BS with those who are physically closer to it is how this method is put into action. This continues until the next closest user is connected to the farthest user. The nearest user is U_1 and the farthest is U_6 from the BS. U_1 and U_6 combined their resource blocks because of the N-F pairing. In the subsequent pool of materials, U_2 is joined with U_5 . U_3 and U_4 are connected in the last data block.

The initial user pair consists of one nearby user (U_1) and one distant user (U_6). Therefore, the coefficients for the distribution of power should be selected as $\alpha_1 < \alpha_6$. Therefore, U_1 should do cascading de-interlacing (SIC) and U_6 should handle straight decoding. The second user pair consists of U_2 , the local user, and

U_5 , the remote user. Therefore, $\alpha_2 < \alpha_5$ is the best option. U_2 is responsible for SIC management, whereas U_5 oversees direct decoding. In a similar vein, U_3 represents the user closest to the BS, while U_4 denotes the user farthest. Therefore, since $\alpha_3 < \alpha_4$ and the SIC is best handled by U_3 , direct decoding is best left to U_4 . These are the maximum achievable rates for the first pair of users:

$$R_{1,nf} = \frac{1}{2} \log_2 \left(1 + \frac{P\alpha_1|h_1|^2}{\sigma^2} \right) \quad (\text{After SIC}) \quad (4.1)$$

$$R_{4,nf} = \frac{1}{2} \log_2 \left(1 + \frac{P\alpha_4|h_4|^2}{\alpha_1 P|h_4|^2 + \sigma^2} \right) \quad (4.2)$$

Similarly, with the second set,

$$R_{2,nf} = \frac{1}{2} \log_2 \left(1 + \frac{P\alpha_2|h_2|^2}{\sigma^2} \right) \quad (\text{After SIC}) \quad (4.3)$$

$$R_{5,nf} = \frac{1}{2} \log_2 \left(1 + \frac{P\alpha_5|h_5|^2}{\alpha_2 P|h_5|^2 + \sigma^2} \right) \quad (4.4)$$

To the same extent, about the third set,

$$R_{3,nf} = \frac{1}{2} \log_2 \left(1 + \frac{P\alpha_3|h_3|^2}{\sigma^2} \right) \quad (4.5)$$

$$R_{4,nf} = \frac{1}{2} \log_2 \left(1 + \frac{P\alpha_4|h_4|^2}{\alpha_3 P|h_4|^2 + \sigma^2} \right) \quad (4.6)$$

The sum average rate in the NF method.

$$R_{nf} = R_{1,nf} + R_{2,nf} + R_{3,nf} + R_{4,nf} + R_{5,nf} + R_{6,nf} \quad (4.7)$$

4.2.2 NOMA Using the Alternate Approach of Close-to-Close or Remote-to-Remote Pairing (C-C, R-R)

Another method involves pairing the user who is physically closest to the BS with the next user. Both U_1 and U_2 are linked to the same pool of resources. U_3 and U_4 are matched in the subsequent resource block. In the last set of materials, U_5 and U_6 are paired. In the initial pair of users, U_1 is now physically closer to the BS than U_2 .

Therefore, pick $\alpha_1 < \alpha_2$. After deciding that U_1 should manage the SIC, U_2 should handle direct decoding, and U_3 is more conveniently located near the BS than U_4 , $\alpha_3 < \alpha_4$ was reached. The SIC is handled by U_3 , while direct decoding is handled by U_4 . As a result of its proximity to the hub, U_5 ranked higher than U_6 's $\alpha_5 < \alpha_6$ in the final selection process. It is recommended that U_5 handle the SIC and U_6 handle straight decoding.

Assuming two users, the feasible rates are:

$$R_{1,cc} = \frac{1}{2} \log_2 \left(1 + \frac{P\alpha_1|h_1|^2}{\sigma^2} \right) \quad (\text{After SIC}) \quad (4.8)$$

$$R_{2,cc} = \frac{1}{2} \log_2 \left(1 + \frac{P\alpha_2|h_2|^2}{\alpha_1 P|h_2|^2 + \sigma^2} \right) \quad (4.9)$$

Similarly, with the second set,

$$R_{3,cc} = \frac{1}{2} \log_2 \left(1 + \frac{P\alpha_3|h_3|^2}{\sigma^2} \right) \quad (\text{After SIC}) \quad (4.10)$$

$$R_{4,cc} = \frac{1}{2} \log_2 \left(1 + \frac{P\alpha_4|h_4|^2}{\alpha_3 P|h_4|^2 + \sigma^2} \right) \quad (4.11)$$

The third pair follows the same pattern,

$$R_{5,cc} = \frac{1}{2} \log_2 \left(1 + \frac{P\alpha_5|h_5|^2}{\sigma^2} \right) \quad (4.12)$$

$$R_{6,cc} = \frac{1}{2} \log_2 \left(1 + \frac{P\alpha_6|h_6|^2}{\alpha_5 P|h_6|^2 + \sigma^2} \right) \quad (4.13)$$

The mean sum in the N-F system.

$$R_{cc} = R_{1,cc} + R_{2,cc} + R_{3,cc} + R_{4,cc} + R_{5,cc} + R_{6,cc} \quad (4.14)$$

4.3 Simulation Parameters

Table 4.1 provides a full breakdown of the simulation settings.

Table 4.1. Details the Simulation Settings.

No.	Parameters	Values		
		1.	Distances	$d_1 = 200m$
		$d_4 = 800m$	$d_5 = 900m$	$d_6 = 1000m$

2.	Path loss exponent	4
3.	The number of bits for each symbol	10^4
4.	SNR	10 to 30 (dB)
5.	Number of users	6

4.4 Computer Model

Channel gain is generated in MATLAB using the simulator's parameters and the model of the system, and the sum average rate versus the SNR is calculated for two approaches. The following flowchart illustrates the procedures needed to put the code into action in four distinct circumstances.

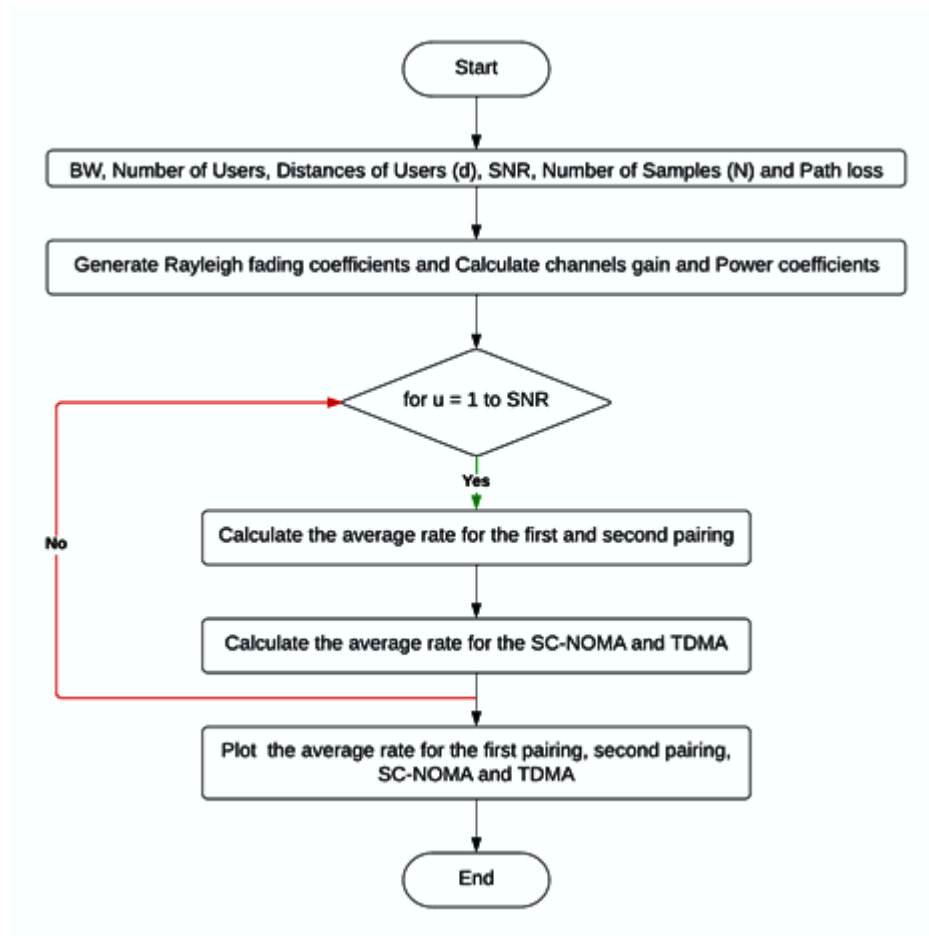


Figure 4.3. Flowchart of PD DL-NOMA for four cases

4.5 Result and Discussions

Figures 4.4 and 4.5 show the average sum rate versus SNR for six users at varying distances, based on simulations done in MATLAB for a variety of access modes (NOMA with first and second schemes of pairing, SC-NOMA, TDMA). The average rate total vs SNR for NOMA using the initial pairing scheme, SC-NOMA, and TDMA at varying ranges is depicted in Figure 4.4. The study's findings indicate that parameters such as noise power, signal power, channel conditions, user interference, and power allocation have an impact on the SNR and average sum rate in NOMA, TDMA, and SC-NOMA systems. Improving these factors makes it possible to increase the overall rate and boost the systems' efficiency.

Increasing the SNR increases the average sum rate. The performance disparity among the three methods was evident from the outset. At an SNR of 30 dB, six users in NOMA with the initial pairing approach have an average total rate of 3.8 bps/Hz, TDMA users average 1.8 bps/Hz, and SC-NOMA users average 0.39 bps/Hz. In this way, NOMA with the initial pairing technique has a higher average sum rate than other multi-access schemes when there are six users involved.

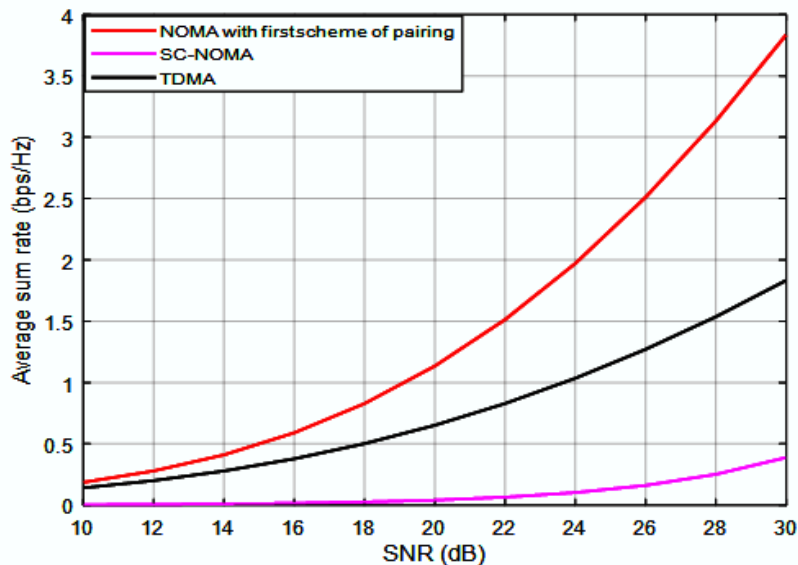


Figure 4.4. Presents six users' average sum rates vs. SNR at varying distances using three distinct multiple-access approaches (NOMA using the initial scheme of pairing, SC-NOMA, and TDMA)

For NOMA using the second pairing method SC-NOMA and TDMA at various separations, the average sum rate as a function of SNR is seen in Figure 4.5. According to what the numbers show, the average total rate goes up as SNR goes up. The performance disparity among the three models was evident right from the start. Six users in NOMA's second pairing approach achieved an average total rate of 3.42 bps/Hz at SNR of 30 dB, compared to an average rate of 1.8 bps/Hz in TDMA and 0.39 bps/Hz in SC-NOMA. This explains why NOMA with the second pairing strategy has a higher average sum rate than comparable multi-access systems with six users.

In NOMA, TDMA, and SC-NOMA systems, increasing SNR improves data speeds and reduces errors. There is a 5% enhancement between the first-pairing strategy when compared with the second-pairing approach. The first pairing technique is designed to decrease interference between users (N-F), but the second pairing approach may increase interference (N-N or F-F).

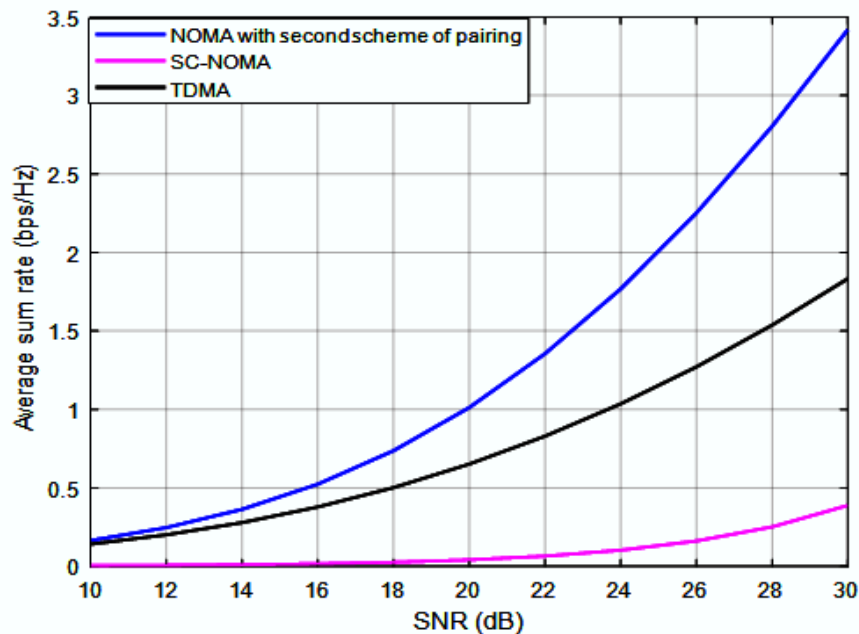


Figure 4.5. The average total vs. SNR for six users at three different distances utilizing three distinct multiple access approaches is depicted (NOMA with the second scheme of pairing, SC-NOMA, TDMA)

4.6 Summary

According to the findings, the average sum rate is greater when a close user is paired with a far user. Even with the second scheme's near-near, far-far pairing in place, NOMA still outperforms TDMA and SC-NOMA on average sum rate, albeit the margin was less in the initial matchup. Because interference problems become greater when several users share a single channel, SC-NOMA performs worse than TDMA. The integration of NOMA with OMA will yield a novel and notably enhanced paradigm by amalgamating the distinctive attributes of both technologies.

When the first-pairing method is compared to the second-pairing technique, there is a 5% improvement in the first-pairing strategy. Combining NOMA with TDMA is a crucial step in making wireless communication networks more efficient and having a higher average capacity. In comparison to TDMA, NOMA improves system average capacity and spectrum efficiency. To harness NOMA's full potential in future wireless networks, however, further challenges and unanswered questions must be addressed.

SC-NOMA is promising for next-generation wireless networks because of its low latency, large system capacity, and enhanced SE. The figures reveal that performance declines as user numbers increase owing to interference.

CHAPTER FIVE

Outage Probability Enhancement for DL Cooperative NOMA in 5G Network

5.1 Introduction

The cooperative NOMA approaches have a great deal of promise in terms of providing unrivalled connection and speed, which will allow them to overcome the challenges that will be presented by 5G and future wireless networks. Several studies have looked at how the power location coefficient (PLC) affects the efficiency of several types of cooperative DL NOMA, including DL NOMA, MIMO cooperative DL NOMA, and M-MIMO cooperative DL NOMA, with the goal of serving users at a distance. Potential difficulties for novel use cases may arise from DL NOMA interruptions in 5G networks. Therefore, the goal of this effort is to reduce their frequency. We analyzed the performance of DL cooperative NOMA PD networks as well as the performance of DL conventional NOMA PD networks in this study, concerning their outage probabilities (OPs) and then compared the findings.

To keep things simple, focus on the scenario with just two users and ignore the potential for interference from additional NOMA users. Listed here are some of our most significant contributions:

- Theoretically, for both the two-user and cooperative NOMA systems, we were able to derive closed-form formulations of the OPs for a range of distances and PLCs.
- The use of simulations demonstrated, that the generated OP expressions have a higher degree of precision in comparison to those found in [141].
- Our previous results and improvement estimates were compared with the outcomes of the OP and effect PLCs from an examination of the cooperative NOMA system with 16x16, 32x23, and 64x64 MIMO, and this was done in order to determine whether or not our estimates were accurate.
- To reduce the impact of the PLC on users located far away, we may employ cooperative NOMA with massive 128x128, 256x256, and 512x512 MIMO to enhance OP performance.

5.2 System Model

The system encompasses four scenarios: the first involves NOMA, the second includes the independent operation of cooperative NOMA networks, the third combines the simultaneous operation of cooperative NOMA networks and MIMO, and the fourth scenario utilizes massive MIMO (M-MIMO) with cooperative NOMA [82].

5.2.1 Models of the DL PD NOMA and DL PD Cooperative NOMA Method

Firstly, the NOMA PD network is shown by a single BS in Figure 5.1. Dual users: one next to the BS with a robust channel, and a second further with a less robust one. Every user possesses a distinct combination of parameters that determine the distances to the BS (d_1 , d_2) and the personal local regions (α_n , α_f).

Two users are seen participating in a DL cooperative NOMA PD network in Figure 5.2. A user close to the base station gets a strong signal, while the other user further has a weak signal. The figure also shows the PLCs of the users, denoted as (α_n , α_f , α_{nf}), together with their corresponding distances (d_1 , d_2 , and d_{12}).

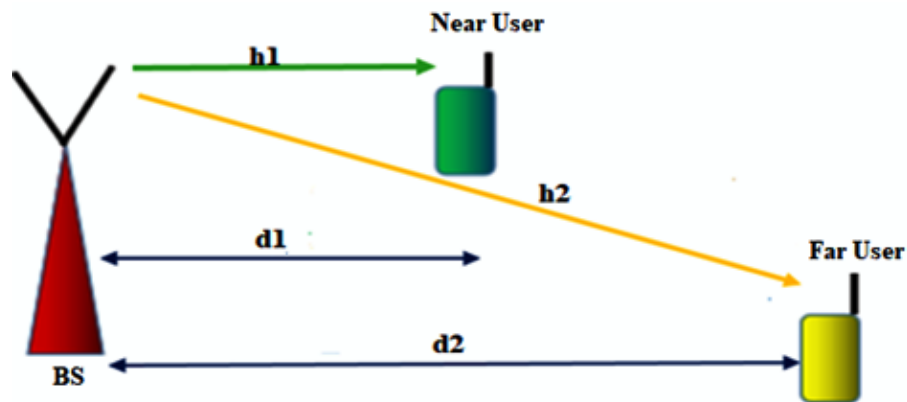


Figure 5.1. Transmitting DL PD NOMA network

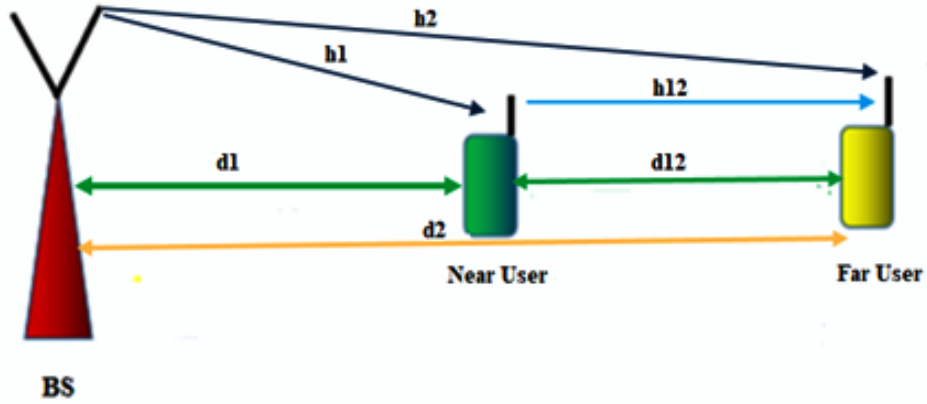


Figure 5.2. Transmission in the DL for the cooperative NOMA

5.2.2 Models of the DL PD Cooperative NOMA with MIMO and Massive-MIMO

Within the third scenario, the cooperative NOMA network allows MIMO setups with dimensions of 16×16 , 32×23 , and 64×64 , as seen in Figure 5.3. These configurations are associated with distinct PLCs of the users, represented as $(\alpha_n, \alpha_f, \alpha_{nf})$, along with their respective distances (d_1, d_2 , and d_{12}).

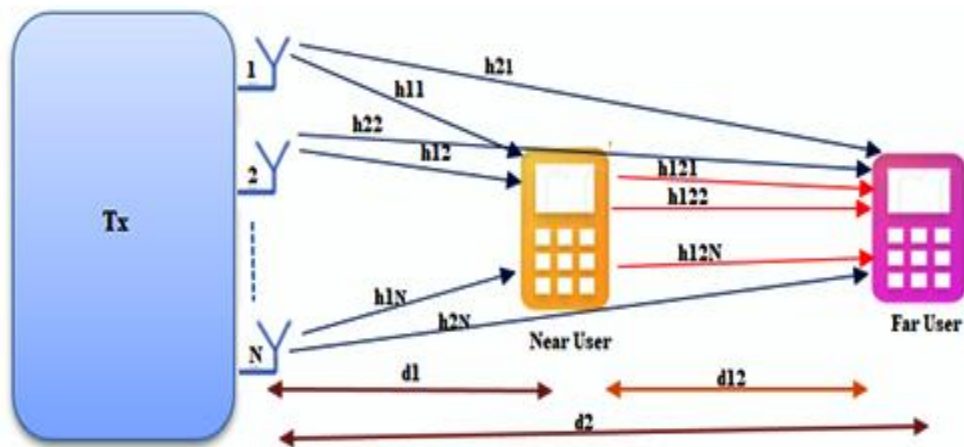


Figure 5.3. Cooperative NOMA network DL transmission using 16×16 , 32×23 , and 64×64 MIMO

The fourth scenario is the integration of NOMA cooperative networks with M-MIMO methods of varying dimensions, specifically 128x128, 256x256, and 512x512. Figure 5.4 provides a vivid demonstration of this. The users are connected with certain PLCs, which are represented by $(\alpha_n, \alpha_f, \alpha_{nf})$, and their corresponding distances are denoted as $(d_1, d_2, \text{and } d_{12})$.

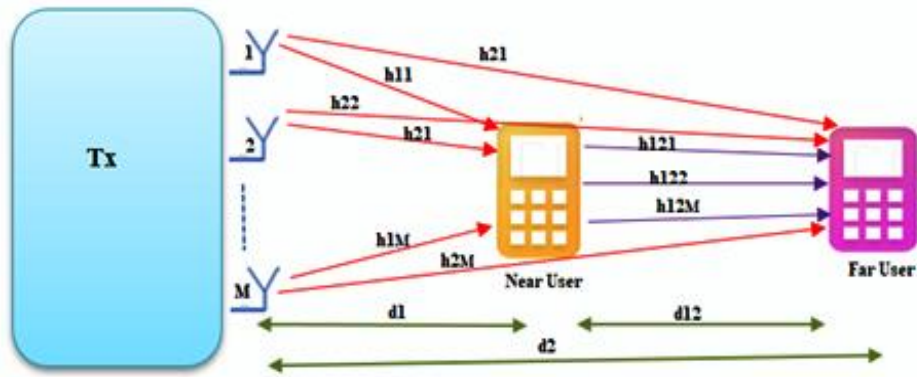


Figure 5.4. DL transmission in a cooperative NOMA network utilizing 128x128, 256x256, and 512x512 M-MIMO

To transmit data, DL cooperative NOMA [162] requires one of two window widths. The first one is called a relay slot, while the second one is called a direct transmission slot. Finding out each user's combined Rayleigh fading channel is what this computation is all about. According to [163], in Rayleigh fading, each user has access to a pool of distinct channels.

$$h_{fN} = \sum_{f=1}^N h_{fN} \quad (5.1)$$

$$h_{nN} = \sum_{n=1}^N h_{nN} \quad (5.2)$$

In this instance, f symbolises the afar user, n the local user, and N the total antennas.

The DL cooperative NOMA and DL NOMA protocols both need a single antenna, represented by the letter N . M-MIMO DL cooperative NOMA supports 128x128, 256x256, and 512x512, whereas MIMO supports 16x16, 32x32, and 64x64.

5.2.3. Slot for Direct Transmission

The BS sends data to both the near (xn) and remote (xf) users if the direct transmission slot is open. SIC first decodes remote user data and then closes user data. The remote user's only involvement in the encoding process is the decoding step. According to [160], the data rates at the nearby and distant users after the direct transmission slot are as follows.

$$R_n = \frac{1}{2} \log_2 (1 + \alpha_n \rho |h_{nN}|^2) \quad (5.3)$$

$$R_{f,1} = \frac{1}{2} \log_2 \left(1 + \frac{\alpha_f \rho |h_{fN}|^2}{\alpha_n \rho |h_{fN}|^2 + 1} \right) \quad (5.4)$$

The SNR is calculated by dividing the TP by the noise variance. A PLC for close users is represented by α_n , whereas a PLC for far users is represented by α_f . The BS has two channels that connect to users: h_n , which is close by, and h_f , which is far. That $\alpha_f > \alpha_n$ and $\alpha_n + \alpha_f = 1$ is common knowledge, as is the fact that these two numbers must always be different [164].

5.2.4. The Slot for Relaying

Last time, remote user data was encrypted. The relay user just delivers it to the remote user during the relay. At the relay slot end, distant users can obtain maximum throughput,

$$R_{f,2} = \frac{1}{2} \log_2 \left(1 + \alpha_n \rho |h_{n fN}|^2 \right) \quad (5.5)$$

A near-far channel is denoted by h_{nfN} . For two reasons, $R_{f,2} > R_{f,1}$. The first is that there is no transmission interference and no need for a power ratio. All the energy is sent to the remote user [165].

5.2.5 Combining Diversity

Both sets of data are similar, but the distant user can access them through different channels and periods. People in outlying places might pick a method that mixes things up. A remote user can estimate the pace at which alternatives are blended,

$$R_f = \frac{1}{2} \log_2 \left(1 + \max \left(\frac{\alpha_f \rho |h_{fN}|^2}{\alpha_n \rho |h_{fN}|^2 + 1}, \rho |h_{n fN}|^2 \right) \right) \quad (5.6)$$

Cooperative relaying is unnecessary for the majority of remote users.

$$R_{f,noncoop} = \log_2 \left(1 + \frac{\alpha_f \rho |h_{fN}|^2}{\alpha_n \rho |h_{fN}|^2 + 1} \right) \quad (5.7)$$

5.3 Simulation Parameters

All MATLAB simulation parameters of the model are configured. This allows us to construct the channel gain concerning SNR in four distinct cases: the first is DL NOMA, the second is DL cooperative NOMA, the third is DL cooperative MIMO NOMA and the fourth is DL cooperative M-MIMO NOMA. We also determine the OP for the remote user. Table 5.1 demonstrates how a wide variety of characteristics have been utilized to implement the infinite inherent potential that may pave the way to making significant contributions to the field.

Table 5.1. The list of variables used in the simulation

No.	Parameters	Values
1.	Path loss	4
2.	Bits per symbol.	10^6
3.	Slots	Direct T _x and Relaying slots
4.	PLCs	α_f 0.9, 0.8, 0.7, and 0.6
		α_n 0.1, 0.2, 0.3, and 0.4
5.	Distance	$d_2 = 2d_1$
6.	SNR	0-25dB
7.	MIMO	16x16, 32x32 and 64x64
8.	Massive MIMO	128x128, 256x256 and 512x512

5.4 Results and Discussions

The simulation was conducted to meet the wide study goals of analysing the NOMA OP. The OP's position in relation to SNR is elucidated by the following figures.

Figure 5.5 illustrates how the DL OP for the remote cooperative NOMA user at (0.8, 0.6) PLCs decreases with increasing SNR. A correlation exists between the users' performance until the SNR approaches 21 dB. Beyond this threshold, the user with a power factor of 0.8 outperforms the other. Due to the increased interference between remote and near users when a lower PLC is used. In the

cooperative NOMA system, the PLC is implemented to minimize the influence of power allocation on distant users and coefficient calculations consider users' distance from the BS.

It is utilized to distribute power to users in a manner that minimizes the likelihood of service interruption and maximizes the overall data transfer rate of the system.

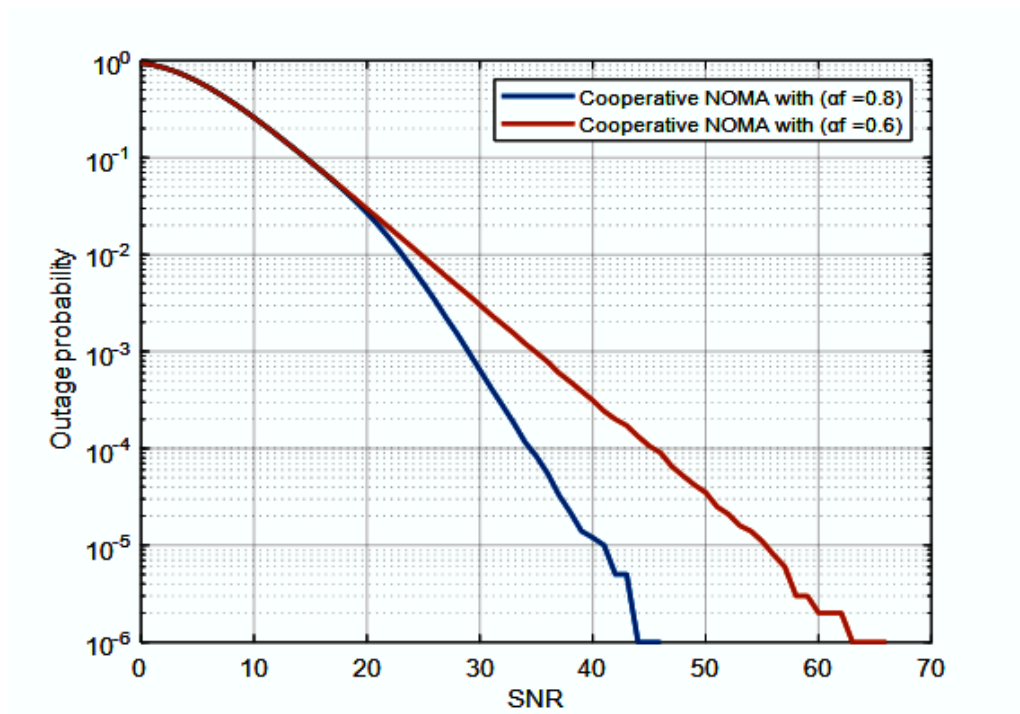


Figure 5.5. DL OP versus SNR for distant cooperative NOMA users with 0.8, 0.6 PLCs

At (0.8, 0.6) PLCs, the DL OP for the distant NOMA user reduces as the SNR increases, as shown in Figure 5.6. As the SNR becomes close to 10 dB, a correlation between user performance begins to emerge. Once we pass this point, the user with the power factor of 0.8 starts to enhance performance than another user. Because a lower PLC causes more interference between nearby and far users.

NOMA systems' power distribution and performance depend on the PLC. This coefficient is utilized to distribute power among users in a manner that maximizes the system's throughput while guaranteeing fairness among users.

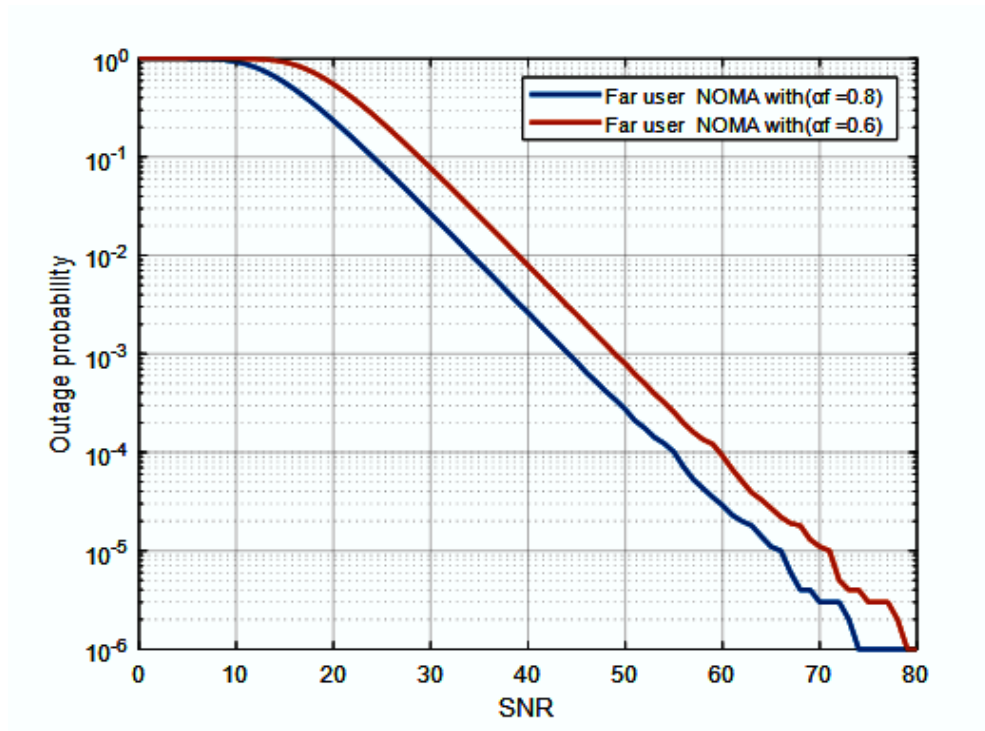


Figure 5.6. DL OP vs. SNR for remote cooperative NOMA users with 0.8, 0.6 PLCs

For the distant user at (0.9, 0.7) PLC for comparison between cooperative NOMA and NOMA, Figures (5.7 –a) and (5.7- b) display the DL OP vs SNR. The DL OP for the PLC performs cooperative NOMA better than the NOMA user in two cases. The results here are 10% better than those in the data sets from [141]–[142].

The PLC plays a crucial role in NOMA and Cooperative NOMA systems, and its optimization is vital for improving system performance. The number of relay nodes, channel conditions, SIC, fixed power allocations, and other factors all have an effect on the PLC system. Understanding the impacts of these parameters is essential for building effective cooperative NOMA systems.

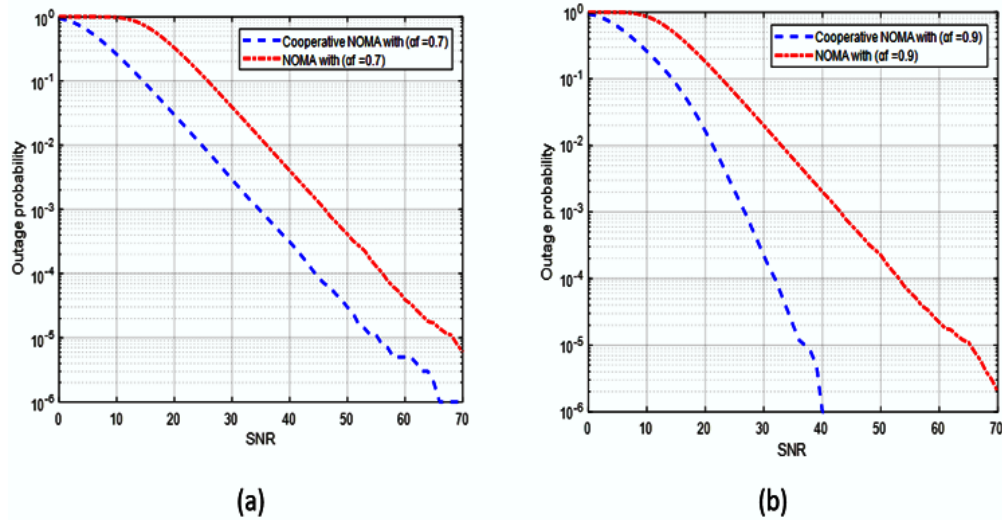


Figure 5.7. DL OP versus SNR for NOMA and cooperative NOMA distant users using various PLCs

For remote users with varied MIMO 16x16, 32x32, and 64x64, the findings show that when the SNR rises, the OP decreases in Figure 5.8 of the cooperative NOMA at 0.8 PLC. $8.0e-05$ is the best OP performance for remote user cooperative NOMA using 64x64 MIMO. The OP for 32x32 MIMO is $4.0e-05$, for 16x16 MIMO is $6.0e-04$, while the OP without MIMO is $5.0e-02$ at SNR of 25 dB. This means that the best performance of MIMO boosts OP by $2.0e-05$.

The use of MIMO methods has a significant effect on PLC. Implementing MIMO technology can enhance the overall OP, and it may be necessary to make appropriate adjustments to the PLC system accordingly. Overall, the MIMO technique enhances OP performance, resulting in values that are 4% higher than those reported in references [166]-[167] and [168].

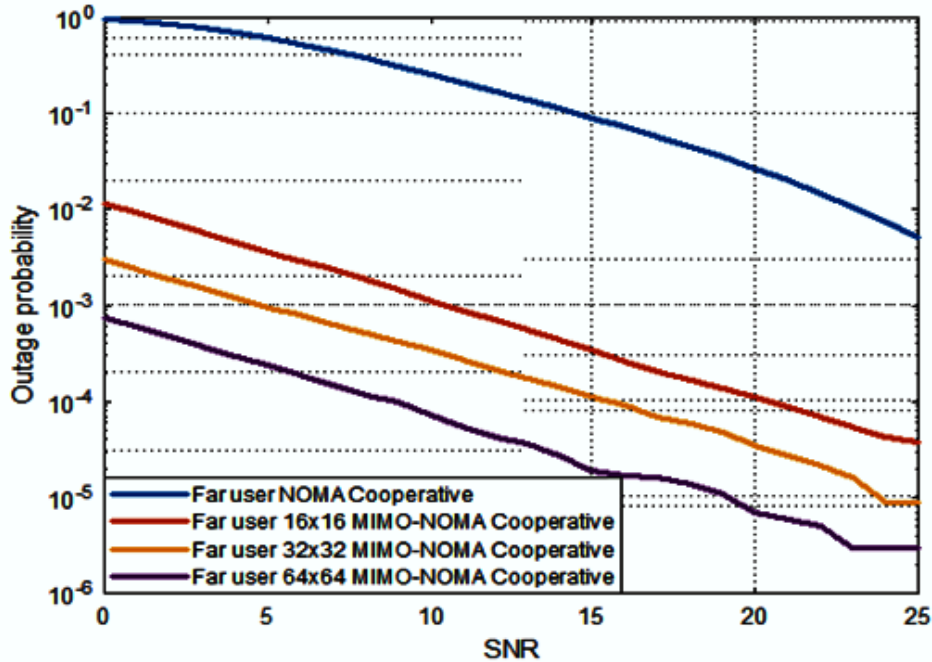


Figure 5.8. A DL OP vs. SNR analysis of cooperative NOMA distant users using various MIMO techniques

For four remote users, Figure 5.9 shows the PLC of 0.8 for 128x128, 256x256, and 512x512 M-MIMO cooperative NOMA against an SNR. Using a 14 dB SNR, the OP for distant user 512x512 M-MIMO cooperative NOMA is 1.0e-06, for user 256x256 M-MIMO cooperative NOMA is 4.3e-06, for user 128x128 M-MIMO cooperative NOMA is 1.0e-05, and for user cooperative NOMA it is 3.0e-01. When using cooperative 512x512 M-MIMO-NOMA, the rate of enhancement of OP between the best user and the worst user is 3.0e-06.

Through the analysis of the results, it was discovered that cooperative interaction enhances user cooperation and fairness by modifying the allocation of power among various user categories. Furthermore, the use of M-MIMO significantly enhances the PLC system, particularly for users located at a far distance. Utilizing M-MIMO technology greatly enhances the OP performance. The OP's performance is substantially improved when M-MIMO technology is used. We found that compared to the results in reference [169], our method performed 15% better.

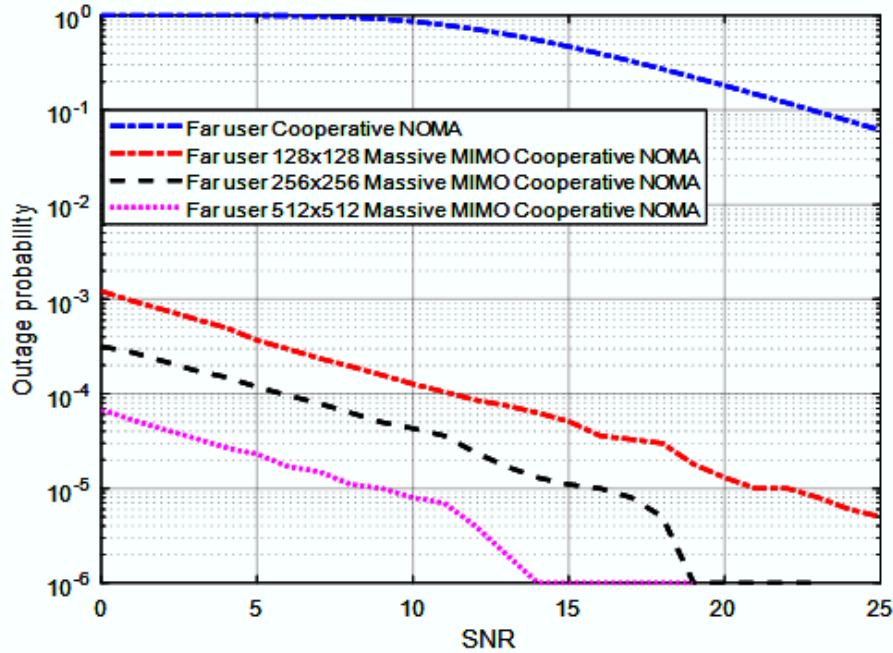


Figure 5.9. Comparing the DL OP vs SNR for cooperative NOMA distant users with and without varying massive MIMO configurations

5.5 Summary

The purpose of comparing cooperative DL NOMA PD with DL NOMA PD in terms of OP and SNR was to examine the effect of PLCs on both nearby and distant users. This allowed us to see how the two types of NOMAs compared to each other, and MIMO 16x16, 32x32, and 64x64 and M-MIMO 128x128, 256x256, and 512x512 were also implemented.

As the remote user's PLC usage grows, the data shows a decrease in the OP rate. Based on the findings, the distant user utilizing cooperative NOMA is capable of attaining the most minimal OP in comparison to the NOMA approach. This is due to the fact that it gets two identical copies of the message one from the BS and another from a nearby user acting as a relay. According to these findings, improving cooperative DL NOMA and DL NOMA's OP may be achieved by decreasing the distant user's PLC by reducing the interference between users. Because the distant user is experiencing a decrease in PLC, the interference between the two users becomes more severe.

The results show that the OP rate for DL 5G Cooperative NOMA is 11% better than that of DL NOMA. With the SNR of 10 dB, the OP is enhanced by 67% with 16x16 MIMO, improved by 74% with 32x32 MIMO, and optimized by 82% with 64x64 MIMO. The OP is enhanced by 91% with 128x128 M-MIMO, optimized by 97% with 256x256 M-MIMO, and improved by 99% with 512x512 M-MIMO when compared with C-NOMA OP performance.

The performance improvement achieved by DL 512x512 M-MIMO cooperative NOMA as a result of OP was 17% more than that of DL 64x64 cooperative NOMA, suggesting a significant disparity in improvement.

CHAPTER SIX

Spectrum Efficiency in 5G Networks Using Cooperative Cognitive Radio NOMA

6.1 Introduction

NOMA is a powerful method to target the SE and capacity of 5G and beyond. By incorporating NOMA into the CRN, a new age of dependable communications is predicted to emerge. SE, average capacity, and BER are all features of wireless communication that are becoming increasingly significant as more mobile services are employed, particularly in real-time applications.

It was necessary to develop and implement new models to improve SE, average capacity, and BER across a wide variety of system configurations.

For various user counts, distances, and antenna numbers, the SE, average capacity, and BER of DL PD NOMA in the 5G network using a novel cooperative cognitive radio network (CCRN) strategy were examined under AWGN and Rayleigh fading.

A dedicated channel (D-CH) or a competitive channel (C-CH) is offered to the principal user (PU) in accordance with the suggested technique when the channel quality degrades, which leads to improved performance for average amplitude SE and BER, and this is the main contribution of this research. Also, important additions to the current study are the following:

- DL NOMA PD is deployed in the CCRN-based 5G network through a shared C-CH or D-CH channel.
- The proposed model achieves better SE, average capacity, and BER results than the conventional PD NOMA model.
- Even after accounting for the impacts of distance, BW, PLCs, and fading, the proposed system's performance in SE, average capacity, and BER was significantly improved by combining 64x64 MIMO with 128x128 Massive MIMO (M-MIMO).

6.2 System Model

There are three main parts to the system model, and they are as follows:

6.2.1 DL-NOMA

As shown in Figure 6.1, let's pretend that a wireless network is available that can support (N) NOMA users. The distances between each BS are represented as d_1, d_2, \dots, d_N . Distances indicate that U_1 is the user who is weak and not in close proximity to the BS, whereas U_N is the user who is powerful and located nearby. Let each of these corresponding Rayleigh fading coefficients, $h_1, h_2, h_3, \dots, h_N$, they correspond to $|h_1|^2 < |h_2|^2 < |h_3|^2 \dots < |h_N|^2$. Within a single cell, their current PLCs are $\alpha_1, \alpha_2, \alpha_3, \dots, \alpha_N$. According to NOMA PD, the more powerful user should have less control, and the weaker user should have more control over the system. For that reason, alter the PLCs. QPSK messages will be delivered to the BSs, therefore let's $x_1, x_2, x_3, \dots, x_N$ go over them. In this case, the BS receives the encoded overlay signal as $x = \sqrt{p}(\sqrt{\alpha_1}x_1 + \sqrt{\alpha_2}x_2 + \sqrt{\alpha_3}x_3 + \dots + \sqrt{\alpha_N}x_N)$. U_i 's receiver AWGN is denoted by n_i , so the user sees the signal via $y_i = h_i x + n_i$.

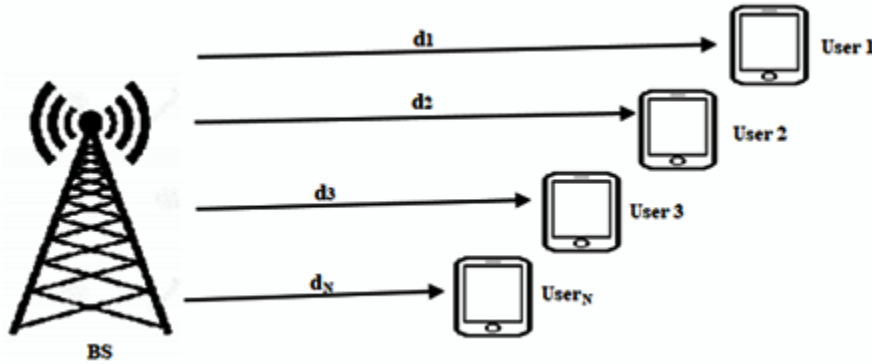


Figure 6.1. Displays the DL-NOMA PD network configured with (N) users

For U_1 , the strongest signal is utilized to decode y_1 , as it has the greatest direct impact on the other N users. In [11]–[170]–[171], the boundaries of what is feasible are outlined.

$$R_1 = \log_2 \left(1 + \frac{\alpha_1 P |h_1|^2}{\alpha_2 P |h_1|^2 + \alpha_3 P |h_1|^2 + \dots + \alpha_N P |h_1|^2 + \sigma^2} \right) \quad (6.1)$$

That can be reduced to:

$$R_1 = \log_2 \left(1 + \frac{\alpha_1 P |h_1|^2}{(\alpha_2 + \alpha_3 + \dots + \alpha_N) P |h_1|^2 + \sigma^2} \right) \quad (6.2)$$

Even though the overlapping term $U_1, U_2, U_3, \dots, U_N$ ($\alpha_3 < \alpha_1, \alpha_3 < \alpha_2, \dots, \alpha_N < \alpha_{N-1}$) is in the denominator, y_3 is still correct. At last, three SIC operations must be performed to remove y_3 from storage. There is a priority on getting rid of α_1 because it is the most powerful. After that, the α_3 phrase needs to be taken out. Achievable rates are:

$$R_2 = \log_2 \left(1 + \frac{\alpha_2 P |h_2|^2}{(\alpha_3 + \alpha_4 + \dots + \alpha_N) P |h_2|^2 + \sigma^2} \right) \quad (6.3)$$

Even though the overlapping term $U_1, U_2, U_3, \dots, U_N$ ($\alpha_3 < \alpha_1, \alpha_3 < \alpha_2, \dots, \alpha_N < \alpha_{N-1}$) is in the denominator, y_3 is still correct. At last, three SIC operations must be performed to remove y_3 from storage. There is a priority on getting rid of α_1 because it is the most powerful. After that, the α_3 phrase needs to be taken out. Achievable rates are:

$$R_3 = \log_2 \left(1 + \frac{\alpha_3 P |h_3|^2}{(\alpha_4 + \dots + \alpha_N) P |h_3|^2 + \sigma^2} \right) \quad (6.4)$$

Success requires y_N since the numerator contains the phrase $U_1, U_2, U_3, \dots, U_N$ ($\alpha_3 < \alpha_1, \alpha_3 < \alpha_2, \dots, \alpha_N < \alpha_{N-1}$). Eventually, two SIC operations will be required to delete y_N information. The α_1 reign must be removed first because it is the most important. Next, let's look at the α_{N-1} term in that sequence.

$$R_N = \log_2 \left(1 + \frac{\alpha_N P |h_N|^2}{\sigma^2} \right) \quad (6.5)$$

Using the formula [19]-[169], determine the SE.

6.2.1.1 Competitive Channel (C-CH) CCRN-NOMA

In a wireless network with N users, $U_1, U_2, U_3, \dots, U_N$ ($\alpha_3 < \alpha_1, \alpha_3 < \alpha_2, \dots, \alpha_N < \alpha_{N-1}$) NOMA, the anticipated behaviour of a CCRN is shown in Figure 6.2. Their BS distances will be denoted by the notation $d_1, d_2, d_3, \dots, d_N$. U_1 is the less powerful, farther user of BS, while U_N is the more powerful, closer user. The formula $|h_1|^2 |h_2|^2 |h_3|^2 \dots |h_N|^2$ in a single cell is used to describe the Rayleigh fading values.

The CCR spectrum is a valuable instrument employed by academics to get insights into the condition of a channel and its capacity for communication. There are two potential responses to a communication channel that is either unstable or weak, and both of them depend on the presence of the CCR channel. Provided that the CCR channel is accessible, NOMA will utilise it.

NOMA lets several users share time and frequency resources, improving SE and system capacity. CRN allows SUs to operate in the same frequency range as PUs without disrupting or interfering. Due to its ability to let many SUs access the spectrum simultaneously, NOMA improves CRN system throughput. However, successful NOMA communication inside CRN requires advanced signal processing and interference management.

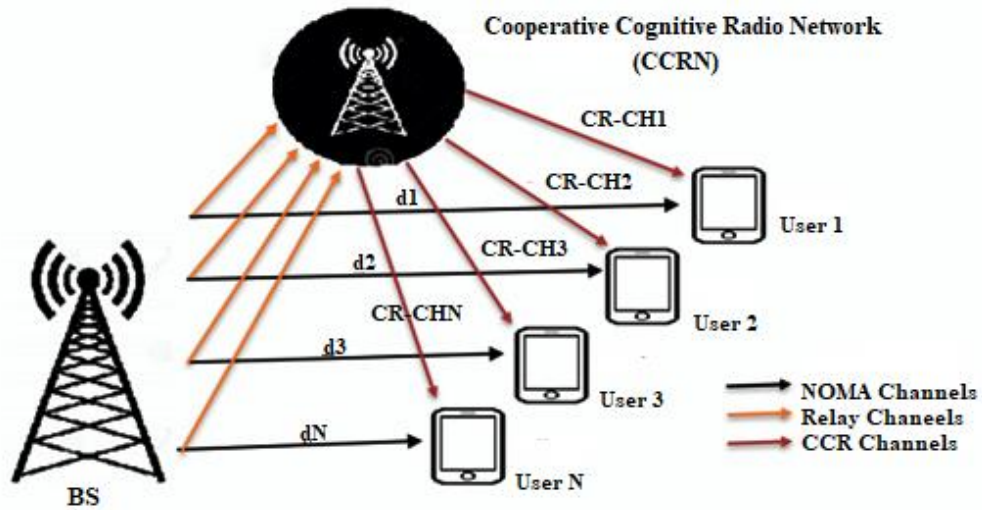


Figure 6.2. Model of the system with DL- PD NOMA and CCRN for N users

For successful packet transmission, CR must take advantage of the entire available spectrum (s). For the sake of argument, let's say that the period T_{window} describes a window in the spectrum. Incontestably, [172].

$$T_{\text{window}} \geq T_{\text{sense}} + T_{\text{CR-Transmission}} + T_{\text{ramp-up}} + T_{\text{ramp-down}} \quad (6.6)$$

where T_{sense} is the minimum sensing to assure CR transmission opportunity and acquisition of associated communication characteristics, $T_{\text{CR-Transmission}}$ is the CR packet transmission time, and $T_{\text{ramp-up}}$ and $T_{\text{ramp-down}}$ are the transmission ramping period.

While the distance between the beacon signals is constant, the window of opportunity for CR transmission opens up, as shown in Figure 6.3, [173].

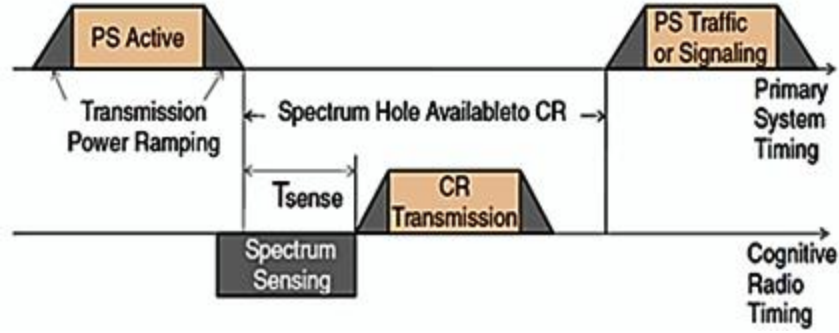


Figure 6.3. Transmission of CR is possible during a brief window

$$PD = \frac{\text{Number of acquisitions}}{\text{Total number of opportunities}} = \frac{\text{Over_Num}}{NOP} \quad (6.7)$$

One primary system used spectrum sensing at link-level targets to select one over the other.

$$y[n] = \begin{cases} w[n] & H_0 \\ h s[n] + w[n] & H_1 \end{cases} \quad (6.8)$$

Let's define the following variables: $y[n]$ as the received complex signal of the cognitive radio, $s[n]$ as the broadcast complex signal of the primary user, $w[n]$ as the complex signal of the AWGN, and h as the complex gain of the ideal channel. N represents the number of observations.

Convolution, not multiplication, occurs due to channel issues. From 1 to N , integers exist. The chief user signal is H_1 , whereas H_0 indicates no primary user. Spectrum sensing methods are energy- or feature-based [173].

The incoming signal is squared and integrated constantly throughout the observation. Next, if there is a primary user, the integrator's output is compared to a standard. So it's either/or dependent on:

$$\begin{cases} H_0, & \text{if } \sum_{n=1}^N |y[n]|^2 \leq \lambda \\ H_1, & \text{otherwise} \end{cases} \quad (6.9)$$

where λ is the receiver noise-affected sensitivity threshold.

$$PF = P\left(\frac{H_1}{H_0}\right) = P\left(\frac{PU}{H_0}\right) = P\left(\frac{yn}{H_0}\right) = 1 - F_{H_0}(Th) \quad (6.10)$$

The cumulative distribution function and the false alarm probability F_{H_0} .

$$PD = \frac{\text{Number of acquisitions}}{\text{Total number of opportunities}} = \frac{\text{Over_Num}}{\text{NOP}} \quad (6.11)$$

$$PD = 1 - P_M = 1 - P\left(\frac{H_0}{H_1}\right) \quad (6.12)$$

$$PD = \left[e^{-\frac{Th}{z}} * \frac{1}{n!} \left(\frac{Th}{z}\right)^n \right] + \left[e^{-\frac{Th}{2(1+L)}} * \left(\frac{1+L}{L}\right) \right] - \left[e^{-\frac{Th}{z}} * \frac{1}{n!} * \frac{Th * L}{z(1+L)} \right] \quad (6.13)$$

$$Pm = 1 - PD \quad (6.14)$$

PD is the probability of signal detection, Th is the threshold, L is the SNR, and PM is the probability of non-detection. Reference [173] defines P_{FA} as the chance of a false alarm.

To calculate the probability of error:

$$P_e = P_F * P_{(H_0)} + P_M * P_{(H_1)} \quad (6.15)$$

6.2.1.2 Dedicated Channel (D-CH) CCRN-NOMA

Here, the CCR checks the channel's health to see whether it's possible to communicate using the spectrum even when the primary means of communication are operational, the channel may be unreliable or have a weak signal. The sole requirement in this case is that the CCR channel be available at all times and given first priority. Once the channel is available, NOMA users utilize it without any delay, as shown in Figure 6.2.

6.2.2 MIMO DL PD NOMA

Consider 64x64 MIMO DL NOMA PD, 64x64 MIMO DL NOMA PD with CCRN C-CH, and 64x64 MIMO DL NOMA PD with CCRN D-CH under the assumption that there are N users, $U_1, U_2, U_3, \dots, U_N$ ($\alpha_2 < \alpha_1, \alpha_3 < \alpha_2, \dots, \alpha_N < \alpha_{N-1}$) in a single cell in the 5G network.

$$x = \sqrt{P}(\sqrt{\alpha_1}x_1 + \sqrt{\alpha_2}x_2 + \dots + \sqrt{\alpha_N}x_N) \quad (6.16)$$

where α are the NOMA PLCs.

The transmit antennas all broadcast x simultaneously. what U_1 is picking up as a signal is known:

$$y_1 = xh_{11} + xh_{12} + \dots + xh_{1N} + n_1 \quad (6.17)$$

In addition to U_2 , which is also used to represent the signal,

$$y_2 = xh_{21} + xh_{22} + \dots + xh_{2N} + n_2 \quad (6.18)$$

The signal's U_N , is also a representation of it.

$$y_N = xh_{N1} + xh_{N2} + \dots + xh_{NN} + n_N \quad (6.19)$$

where N is the total number of samples from the AWGN with a zero-mean and σ^2 variation.

For each user, their Rayleigh fading channel can calculate:

$$h_{iN} = \sum_{i=1}^N h_{iN} \quad (6.20)$$

Considering that there are a total of 64 channels and $i=1,2,3,\dots, N$ users.

Here is the signal that the BS received:

$$y = \sqrt{P_{x1}}h_{1N} + \sqrt{P_{x2}}h_{2N} + \sqrt{P_{x3}}h_{3N} + \dots + \sqrt{P_{xN}}h_{NN} \quad (6.21)$$

We evaluated the channel's state and communication potential using the same CCR spectrum-based methodology. In unstable and poorly articulated conditions, the CCR channel might move C-CH or D-CH. MIMO NOMA allows several users to share a frequency band and time slot without affecting signal integrity by using different beamforming patterns. Optimal secondary-link beamforming patterns in MIMO CRNs aim to balance SU data transmission rate with PU interference.

6.2.3 Massive MIMO DL PD NOMA

One option is the 128x128 M-MIMO DL NOMA PD, while another is the 128x128 M-MIMO DL NOMA PD with CCRN C-CH. Based on the previous part, let's pretend that the wireless network includes N users, denoted as $U_1, U_2, U_3, \dots, U_N$ ($\alpha_2 < \alpha_1, \alpha_3 < \alpha_2, \dots, \alpha_N < \alpha_{N-1}$), distributed over varying distances, all operating under identical conditions and utilizing the 128x128 M-MIMO DL NOMA PD. Once again, the method was employed to evaluate the

channel's current precision and viability as a means of communication. Once the CR channel is up and running, users with NOMA will be able to utilise it. Continuing with the same fundamental concept, NOMA users can prioritise tuning into the CCR frequency.

M-MIMO reduces CRN inter-user interference (IUI) by connecting Pus and SUs simultaneously. Transmitting main and secondary data simultaneously improves system performance.

For each user, their Rayleigh fading channel can be calculated as:

$$h_{jM} = \sum_{j=1}^M h_{jM} \quad (6.22)$$

where M=128 is the number of channels and j=1,2,3, and 4 are users.

6.3 Simulation Parameters

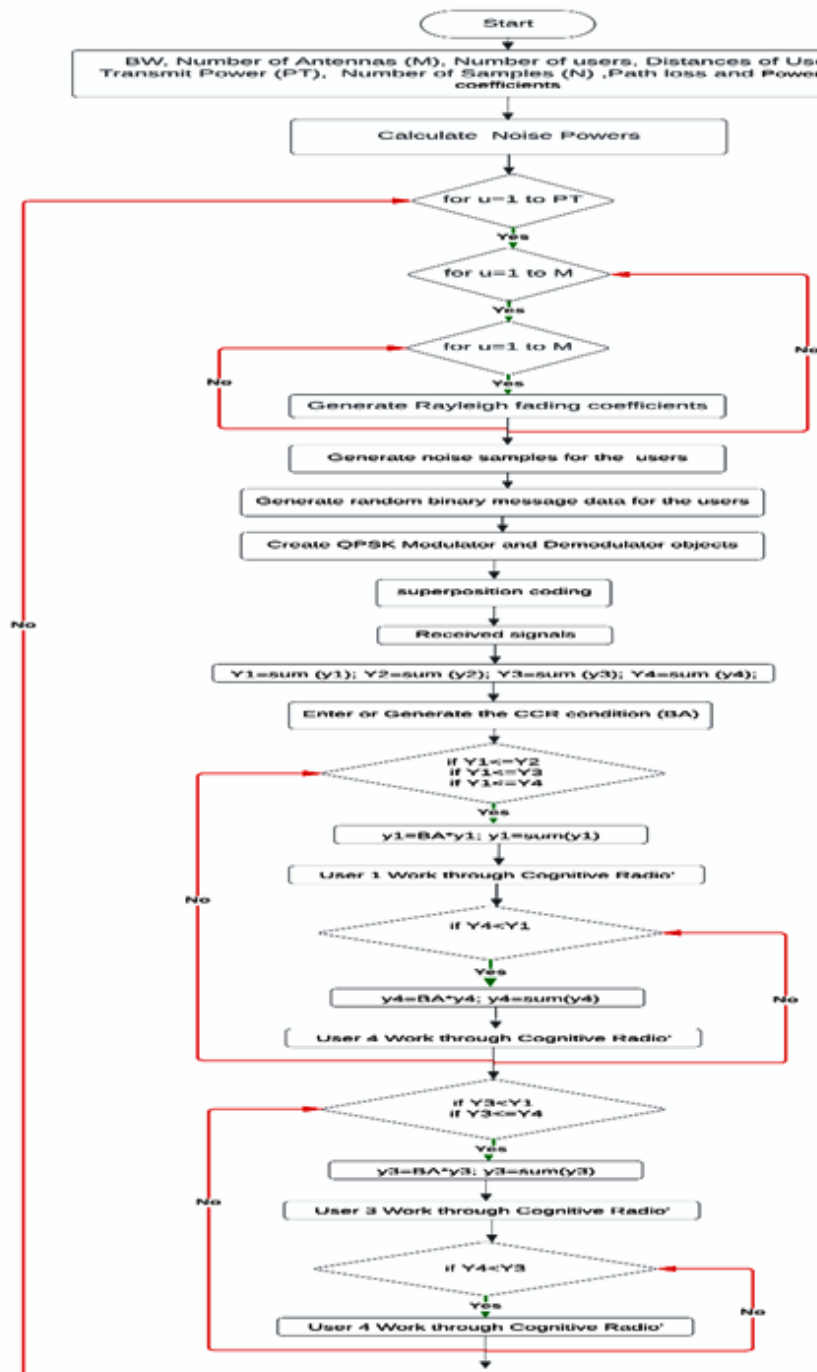
The simulated parameters that were used in the first, second, and third cases are listed in Table 6.1. These parameters were determined based on the program that was executed in each of the three cases.

Table 6.1. Simulation settings for scenarios 1, 2, and 3

No.	Parameters	Values
1.	Number of users (N)	4
2.	TP	0 to 40 dBm
3.	BW	60 MHz
4.	Distances	800 m, 600 m, 300 m, 100 m
5.	PLCs	0.6, 0.3, 0.075, 0.01875
6.	Path loss	4
7.	MIMO	64x64
8.	M-MIMO	128x128
9.	Modulation	QPSK
10.	Number of cells	1

6.4 Computer Model

The flowchart below depicts the steps involved in putting the code into action in three different scenarios.



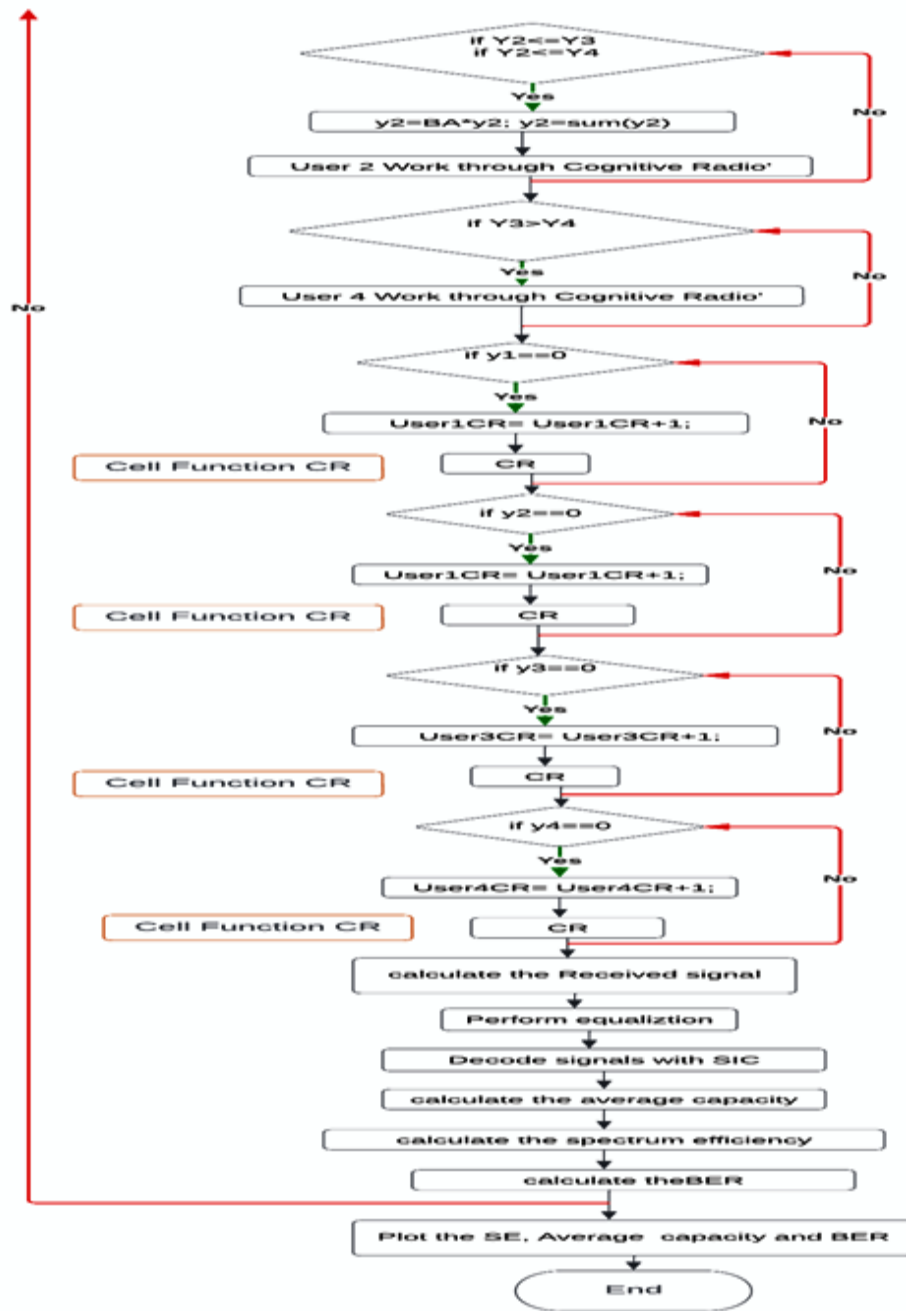


Figure 6.4. Flowchart of PD DL-NOMA for three scenarios

6.5 Results and Discussions

The following figures demonstrate the SE, average capacity, and BER rating against TP for DL NOMA PD and CCRN C-CH or D-CH with 64x64 MIMO and 128x128 M-MIMO in three separate models, based on the programme implementation in those situations.

6.5.1 DL-NOMA Scenario Results

For DL NOMA PD with an unstable channel state, Figure 6.5 displays the SE vs. TP for four users (U_1 , U_2 , U_3 , and U_4) at various distances (800 m, 600 m, 300 m, and 100 m) and PLCs (0.6, 0.3, 0.075, and 0.01875). The SE performance of all NOMA users varies, as observed. In terms of SE performance, the fourth user occupies an advantage in SE performance, opposite to the first user. The results demonstrated that the SE rose in tandem with the TP. With the SE of 3.9 bps/Hz/cell at 40 dBm, U_4 , which is physically nearest to the BS, outperforms U_3 , U_2 , and U_1 in that order.

The SE is shown versus the TP in Figure 6.6. The DL NOMA PD and the CCRN with C-CH. After using the first proposal to integrate with the NOMA network, they found that there is a divergence between the SE performance of all NOMA users. The closest U_4 still has the best performance, while the farthest U_1 has the worst performance. Compared to the previous model, there is a noticeable improvement in all users' SE performance. The optimal SE result for U_4 at 40 dBm TP is 5.09 bps/Hz/cell.

For the DL NOMA PD combined with the CCRN D-CH, Figure 6.7 shows the SE versus the TP for four users situated at various distances and PLCs. They discovered that all NOMA users' SE performance differs after implementing the second proposal to connect with the NOMA network. Even now, U_4 , which is the closest, performs better than U_1 , which is the furthest. The SE performance of all users is generally better than it was with the two previous models. The U_4 algorithm gets the best SE value of 7.2 bps/Hz/cell at a TP of 40 dBm. Comparatively, our findings outperform those of other studies on SE [151].

The NOMA system's user allocation has an impact on spectrum utilization efficiency. The SE of NOMA systems depends on communication channel quality. Inadequate fading, interference, and noise reduction reduce SE. By distributing power across users, the power allocation coefficient helps NOMA systems achieve high SE. Coding and modulation methods have an impact on NOMA spectrum utilization efficiency. Cooperative spectrum sharing is when

many networks or systems share a frequency band. This also enhances NOMA SE. In NOMA systems, especially CRNs, optimal SE requires spectrum perception and energy identification. To address the growing demand for wireless data services, NOMA systems may optimize these factors to achieve high SE.

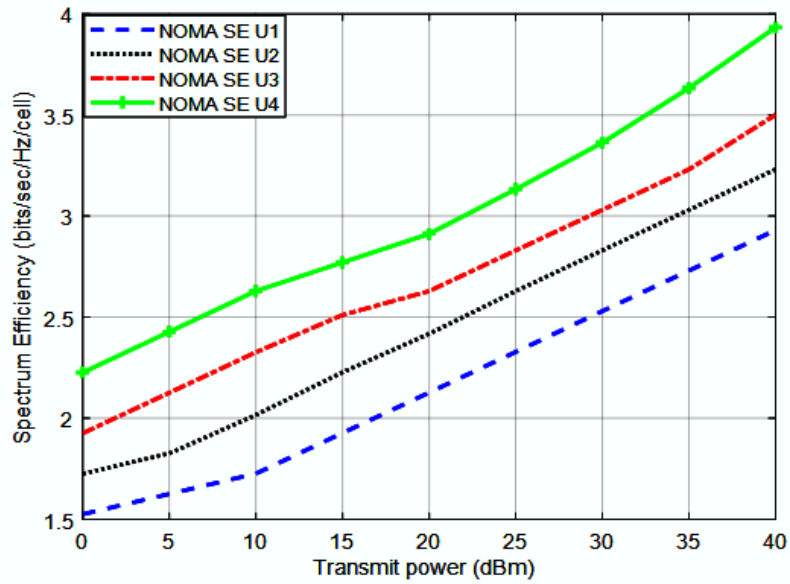


Figure 6.5. SE against TP for four DL PD NOMA users

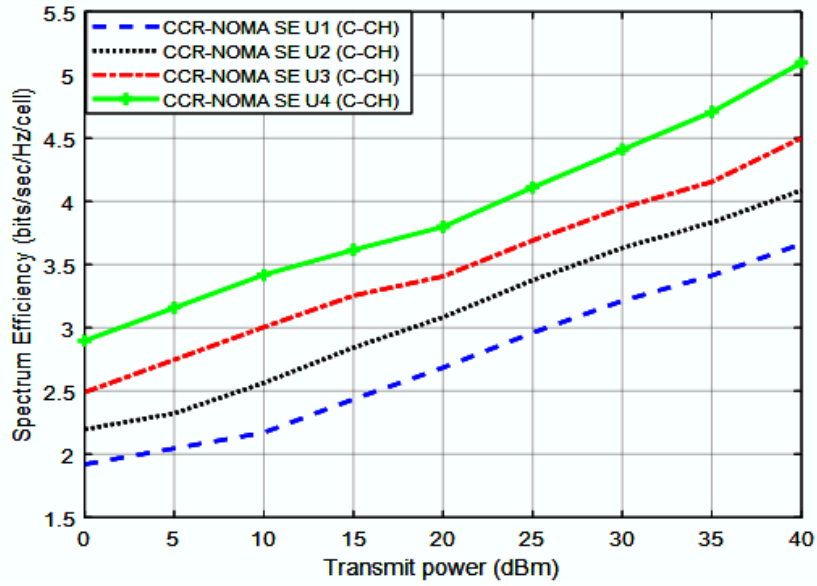


Figure 6.6. SE versus TP for four DL CCR- PD NOMA users with C-CH

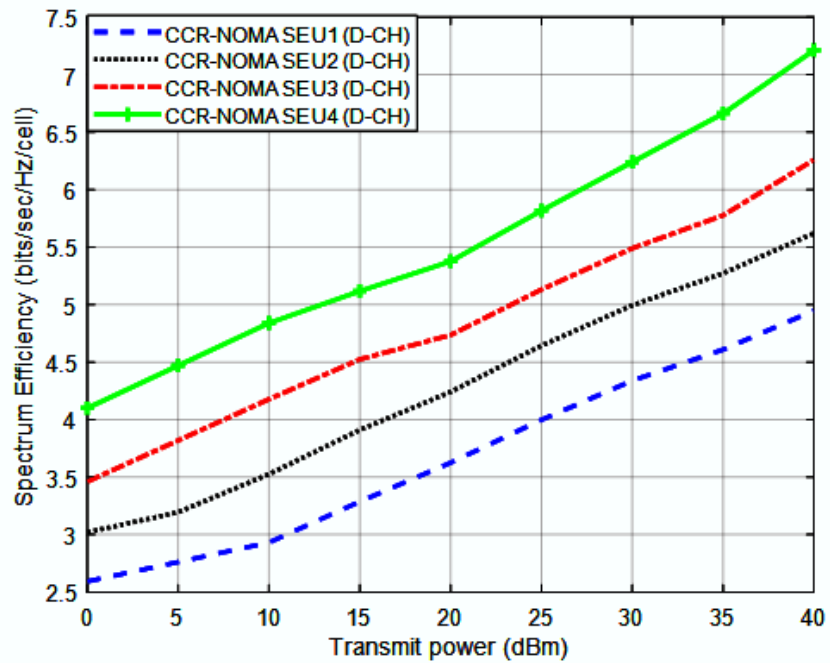


Figure 6.7. SE vs. TP for four DL CCR- PD NOMA users using D-CH

Figure 6.8 shows the average capacity performance of DL NOMA PD in an unstable channel state as a TP approach for four users at different distances (800 m, 600 m, 300 m, and 100 m), respectively, with PLCs of (0.6, 0.3, 0.075, and 0.01875). As we can see, there is an average capacity divergence in performance for all NOMA users. The fourth user has the best performance overall, but the first user has the worst performance in terms of average capacity. Additionally, shows an inconsistency in the acquired results caused by interference among users, which was evident in the channel's quality. Average capacity performance also improved, on average, as TP rose. U_4 achieves the greatest average capacity performance with 40 dBm of TP and the shortest distance to the BS, with a rate of 14.49 bps/Hz/cell. On average, U_4 's capacity performance is 3.03 bps/Hz/cell better than U_1 . The results are better than the cutoff at [174].

The graph in Figure 6.9 displays the average capacity of the TP for the integration of DL NOMA PD with the CCRN and C-CH. There is a noticeable difference in average capacity performance among all NOMA users. Once the initial proposal to establish communication with the NOMA network is executed, the closest U_4 is thriving, whereas the farthest U_1 is underperforming. Compared to the previous model, the average capacity performance of all users has significantly improved. Furthermore, we see a discrepancy in the obtained outcomes due to interference between users, which was noticeable in the quality of the channel. In terms of average capacity performance, the U_4 came out on top with 16.1 bps/Hz/cell. U_4 has an average capacity that is 3.8 bps/Hz/cell higher than U_1 . This result is an improvement over [40].

Figure 6.10 displays the average capacity vs. TP for four users with various PLCs using DL NOMA PD over the CCRN with D-CH. There is a clear disparity in average capacity performance across all NOMA users, except for the 5 dBm TP, where the second and third users perform equally. When the second proposal to create a link with the NOMA network is implemented, the nearest U_4 experiences significant growth, while the most distant U_1 exhibits subpar performance. On average, the capacity performance for all users has usually increased compared to the previous models. Furthermore, we observed variability in the outcomes achieved as a result of user interference, which was evident in the channel's quality. U_4 has the highest average capacity performance at 17.2 bps/Hz/cell. Compared to U_1 , U_4 's average capacity performance is 5.3 bps/Hz/cell higher, thanks to its TP of 40 dBm. The results obtained are better than the average capacity performance of the reference [175].

The users of the system faced several obstacles, such as channel fluctuations, multipath fading, and synchronisation difficulties, as a result of which the

system's steady-state responsiveness is affected and fluctuates. The utilizing modern techniques such as SIC and optimal power allocation, in addition to integrating with other technologies such as CCRN, the findings showed that the average capacity of the NOMA improved.

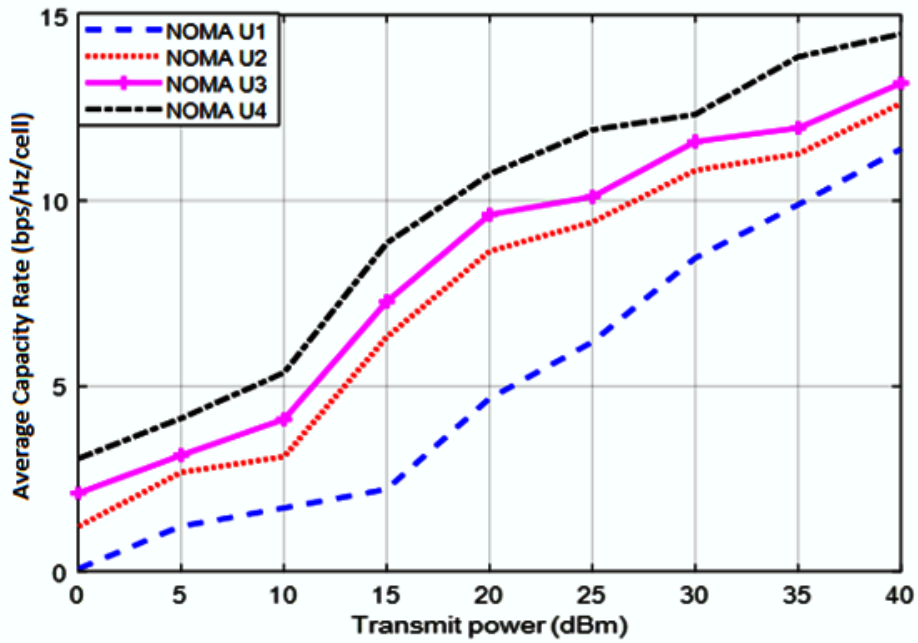


Figure 6.8. Four DL PD NOMA user's average capacity against TP

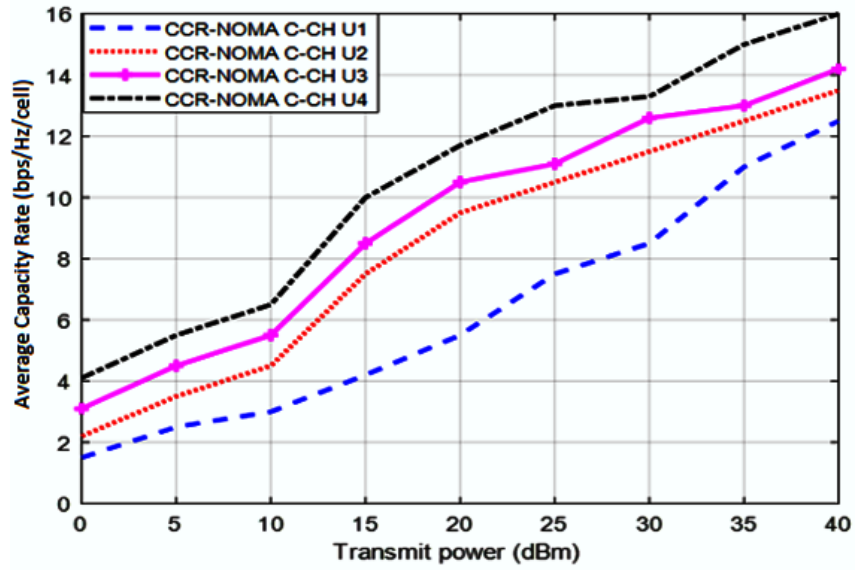


Figure 6.9. Four DL CCR- PD NOMA users' average capacity versus TP with C-CH

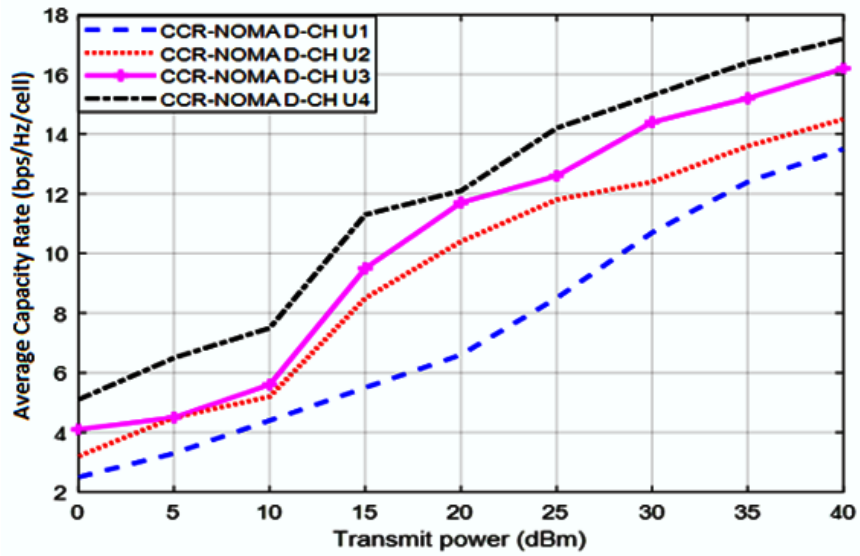


Figure 6.10. Four DL CCR- PD NOMA users average capacity vs. TP with D-CH

Figure 6.11 illustrates the BER vs TP for (U_1 , U_2 , U_3 , and U_4) users at 800 m, 600 m, 300 m, and 100 m with PLCs of 0.6, 0.3, 0.075, and 0.01875 for DL NOMA PD with channel state instability. There is a convergence in performance among all NOMA users' BER, particularly when the TP is between 0 dBm and 12 dBm. Beyond this threshold, the performance of the user improves and becomes distinct. The quick shift in behaviour exhibited by the first user, U_1 , due to attributed to interference from other users, the unstable condition of the channel, and low transmit power. Consequently, this has led to poor performance noticeable during the transient response of program simulation implementation. According to the findings, the BER drops as TP rises. With a BER performance of $7.0e-05$, U_4 the user nearest to the BS topped the list at 40 dBm TP, followed by U_3 , U_2 , and lastly U_1 .

For four distinct users with varied PLCs for DL NOMA PD and system integration with the CCRN via the C-CH, Figure 6.12 shows the BER compared to the TP. There is a consistent alignment in performance between all NOMA users and the initial suggestion of BER, particularly when the TP falls between 7 dBm and 14 dBm. When U_4 crosses the threshold, their performance significantly improves and reaches an excellent level. At TP of 38 dBm, the performance of Users 3 and 1 becomes almost comparable again. The initial user, U_1 , abruptly changed its behaviour due to interference from other users, an unstable channel condition, and limited transmission power. With a TP of 40 dBm and a BER of $9.0e-03$, U_4 performs the best.

Figure 6.13 shows the BER against TP for four users with different PLCs for DL NOMA PD and system combination with the CCRN utilizing the D-CH. There is a strong correlation in performance between all NOMA users and the second proposal of BER, especially when the TP is between 7 dBm and 15 dBm. Upon crossing the barrier, User 4 experiences a substantial improvement in their performance, ultimately achieving an exceptional level. At a level of 34 dBm TP, the performance of U_3 and U_1 becomes nearly equivalent once more. Interference from other users, an unstable channel situation, and restricted transmission power suddenly altered U_1 's behaviour. Consequently, the software simulation execution displayed inadequate performance during the brief response. As a result, the software simulation execution exhibited poor performance during the transient reaction. U_4 has the best BER performance of $1.0e-04$ at a TP of 40 dBm. However, the results that were achieved are superior to those found in [177]-[178]. When comparing the BER performance of the U_4 best user of DL NOMA PD with and integrating the system with CCRN using C-CH, the BER increased by 17%, while when comparing the system with CCR-

NOMA using D-CH, the BER increased by 12%. Because CR demands more difficult actions including channel detection, switching from one channel to another, and false alarms, the reason for the BER grows.

Upon examination of the results, it was determined that the BER performance in NOMA systems was enhanced by the use of techniques such as SIC and efficient allocation of resources. These strategies effectively mitigate the negative effects of channel estimation errors, interference, and system complexity. However, the BER is influenced and heightened by several aspects when it is integrated NOMA network with the CRN. These factors include interference, channel attenuation, limited availability of spectrum, packet size, network size, transmission power and rate, cooperative spectrum sensing, and optimal resource allocation.

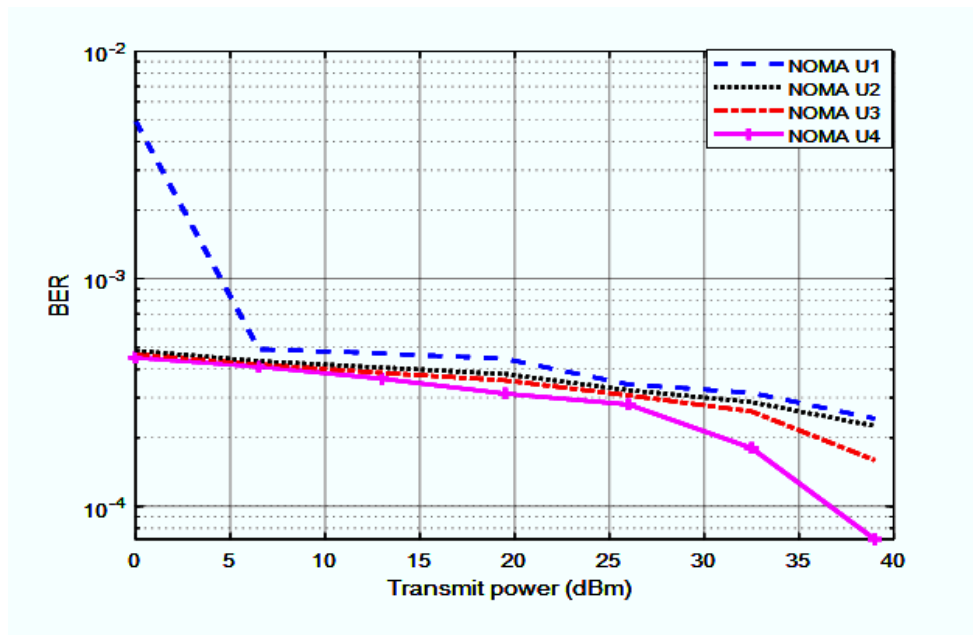


Figure 6.11. BER vs. TP for four DL NOMA PD users

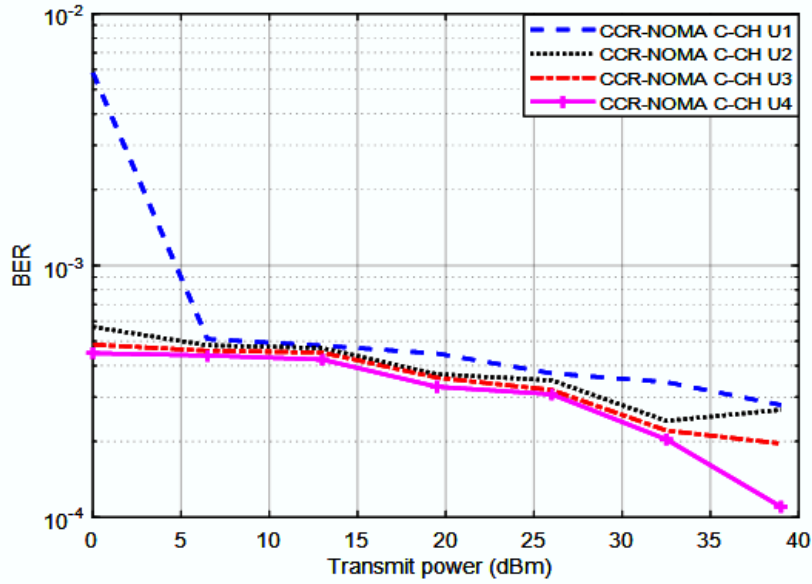


Figure 6.12. BER against TP for four DL CCR-NOMA PD users with C-CH

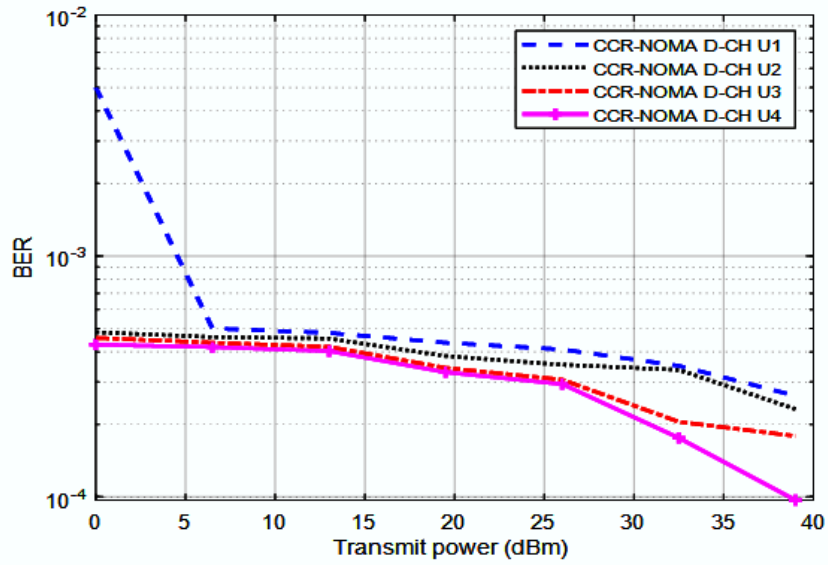


Figure 6.13. BER versus TP for four DL CCR-NOMA PD users with D-CH

6.5.2 MIMO-DL-NOMA Scenario Results

There are four users (U_1 , U_2 , U_3 , and U_4) in Figure 6.14. They are spread out over 800 m, 600 m, 300 m, and 100 m, and their PLCs are 0.6, 0.3, 0.075, and 0.01875. The SE value is unstable, and the TP value is the same for all four. The SE performance of all MIMO NOMA users exhibits variability, as demonstrated. In terms of SE, the fourth user has superior performance compared to the first user. A proportional rise in SE reflects increases in TP. The nearest user to the BS, U_4 , has the best SE values of 12.23 bps/Hz/cell, followed by U_3 , U_2 , and finally U_1 at the TP of 40 dBm. After adopting 64x64 MIMO technology with NOMA, the best user, U_4 , boosted the SE by 8.33 bps/Hz/cell at a TP of 40 dBm when compared with DL NOMA PD.

Four users with different distances and PLCs have their SE compared to their TP in Figure 6.15. Combining the C-CH's CCRN with 64x64 MIMO DL NOMA PD made that possible. We discovered discrepancies in the SE performance across all NOMA users upon implementing the proposal's integration with the MIMO NOMA network. The U_4 that is closest has the best performance, while the U_1 that is farthest has the worst performance. With a TP of 40 dBm, the SE performance is 17.75 bps/Hz/cell for the user closest to the BS U_4 . When using CCRN NOMA (C-CH) 64x64 MIMO technology, U_4 , the top user, experienced a 12.66 bps/Hz/cell improvement in SE at TP of 40 dBm compared to the first scenario.

In order to show the difference between SE and TP for 64x64 MIMO DL NOMA PD along with the CCRN for the D-CH, Figure 6.16 shows four users at various distances and PLCs. We identified inconsistencies in the SE performance of all NOMA users upon implementing the proposal to connect with the MIMO NOMA network. The U_4 that is nearest has the most superior performance, while the U_1 that is farthest has the least satisfactory performance at TP 40 dBm, which is 18.51 bps/Hz/cell. If you compare the best U_4 performing 64x64 MIMO with CCRN NOMA with C-CH to the DL CCR-NOMA PD for the D-CH at 40 dBm TP, the SE got 11.31 bps/Hz/cell better. The examination of the best U_4 's performance revealed this. The actual outcomes, detailed in reference [151], are even more crucial.

5G communications' frequency ranges and applications present spectrum sensing and efficiency challenges and potential in CRNs. Overall SE depends on CRNs' spectrum distribution to primary and secondary users. The simplicity and limits of energy-detecting methods used in CRNs impact spectrum utilization

efficiency. Understanding and improving these features is crucial for optimal network use and quick data transfer in modern wireless communication networks.

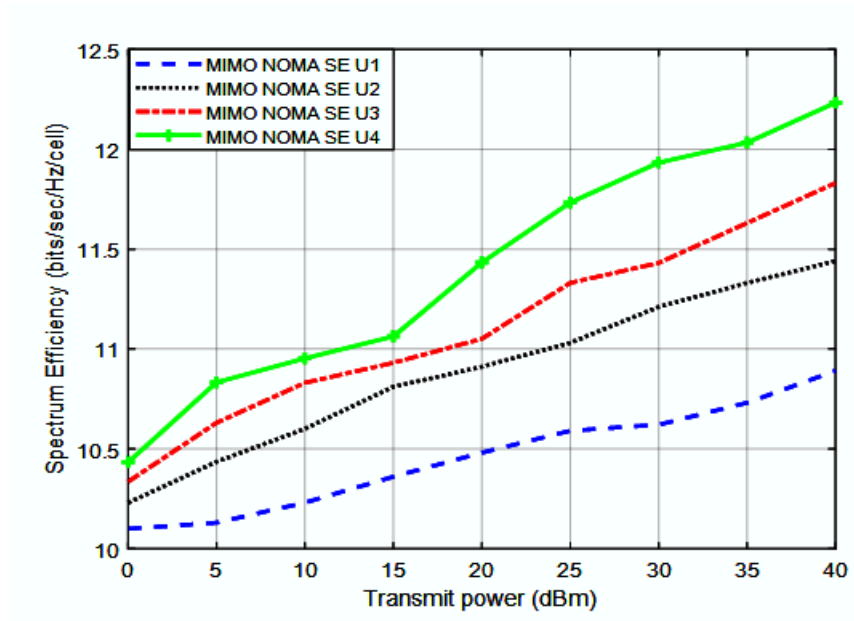


Figure 6.14. SE against TP for four MIMO DL PD NOMA users

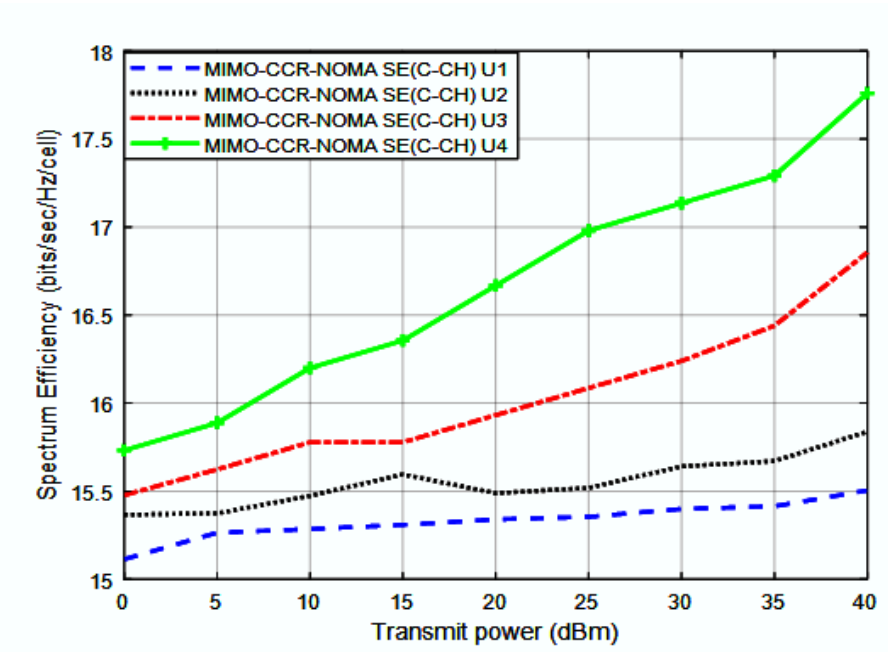


Figure 6.15. SE versus TP for four MIMO DL CCR- PD NOMA users with C-CH

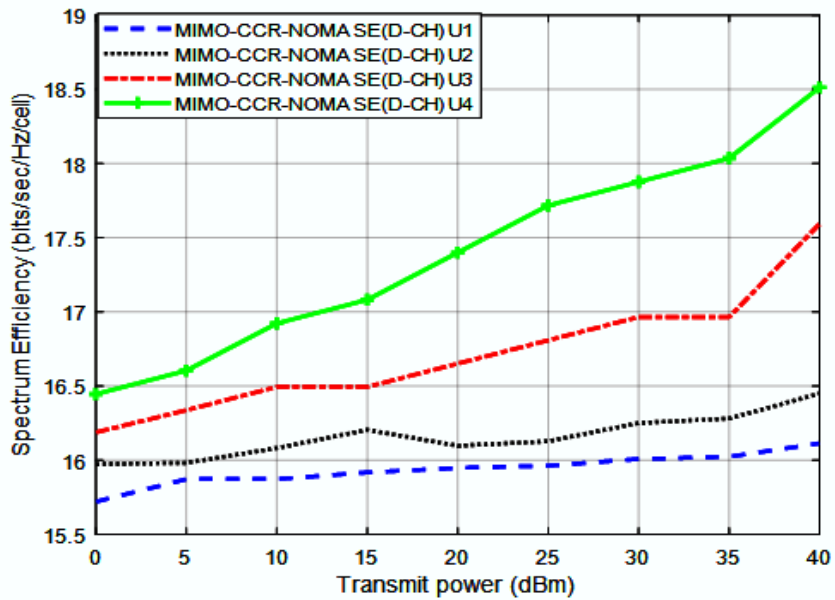


Figure 6.16. SE vs. TP for four MIMO DL CCR- PD NOMA users using D-CH

For DL NOMA PD with 64x64 MIMO, the average capacity vs. TP is as shown in Figure 6.17. There is a noticeable difference in performance capacity among all MIMO NOMA users. The fourth user exhibits the highest overall performance, whereas the first user demonstrates the lowest performance in terms of average capacity. Furthermore, we see a discrepancy in the obtained outcomes due to interference between users, as demonstrated by the quality of the channel. As the TP grew, the average capacity performance also increased. The U_4 achieves the highest average capacity values, operating at 21.5 bps/Hz/cell. As compared to traditional NOMA, U_4 offers a 7.01 bps/Hz/cell improvement in average capacity performance for the identical user. We got a bigger number than [151].

Figure 6.18 displays the average capacity vs. TP for DC-RN with C-CH and DL NOMA PD with 64x64 MIMO. There is a noticeable difference in performance capacity between all MIMO NOMA users, but when the second and third users reach a TP of 12 dBm and up to 17 dBm, there is a great convergence in performance. The fourth user has the best overall performance, while the first user has the worst average capacity. Furthermore, we see variation in the results obtained due to interference between users, as evidenced by the channel quality. Likewise, the average capacity performance increased as TP grew. 25.5 bps/Hz/cell yielded the best results in average capacity performance for U_4 and has an increased average capacity of 11.01 bps/Hz/cell when compared to the same user in standard NOMA. The achieved result exceeds the value of [176].

Figure 6.19 shows the average capacity vs. TP for the CCRN with D-CH and the DL NOMA PD utilizing 64x64 MIMO. After implementing the suggestion to establish the connection with the MIMO NOMA network, the U_4 that is nearest is functioning very well, but the U_1 that is farthest is not performing as well. The average capacity performance of all users has experienced a substantial improvement as compared to the prior model. Moreover, we observe a disparity in the achieved results as a result of interference among users, which was evident in the channel's quality. As measured by average capacity performance, the U_4 excelled at 26.5 bps/Hz/cell. U_4 's average capacity performance is 12.01 bps/Hz/cell higher than that of traditional NOMA for the same user. In comparison to [179], this result is much better.

The findings showed that the MIMO NOMA system with CRN's average capacity is affected by many things, including how power is distributed, how much interference there is, the channel conditions, the number of antennas, the

NOMA parameters, and the CR parameters. By optimizing these characteristics, the average capacity of the system is enhanced.

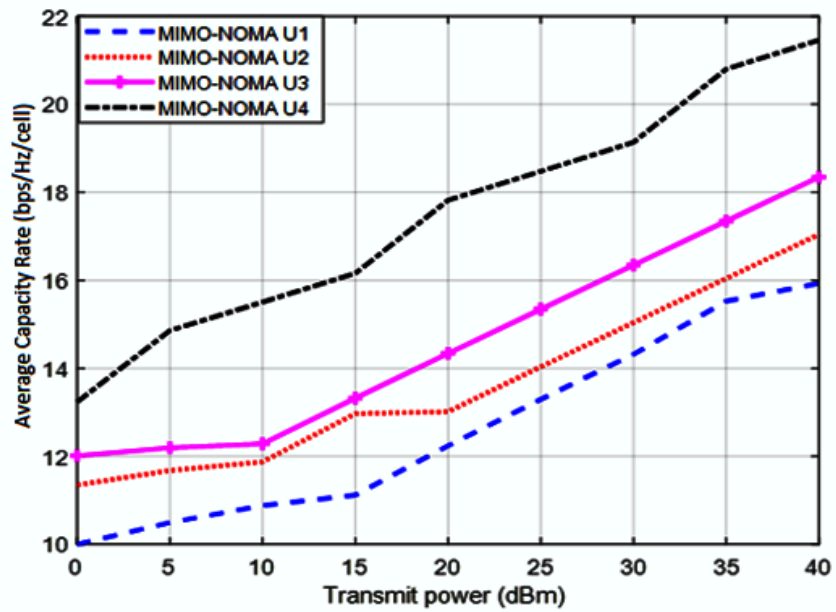


Figure 6.17. Average capacity versus TP for four MIMO DL PD NOMA users

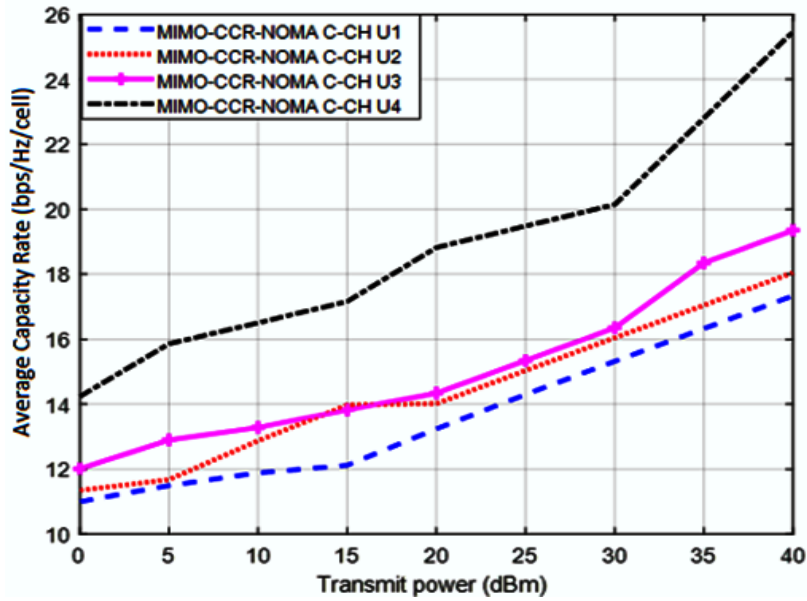


Figure 6.18. Average capacity versus TP for four users MIMO DL CCR- PD NOMA with C-CH

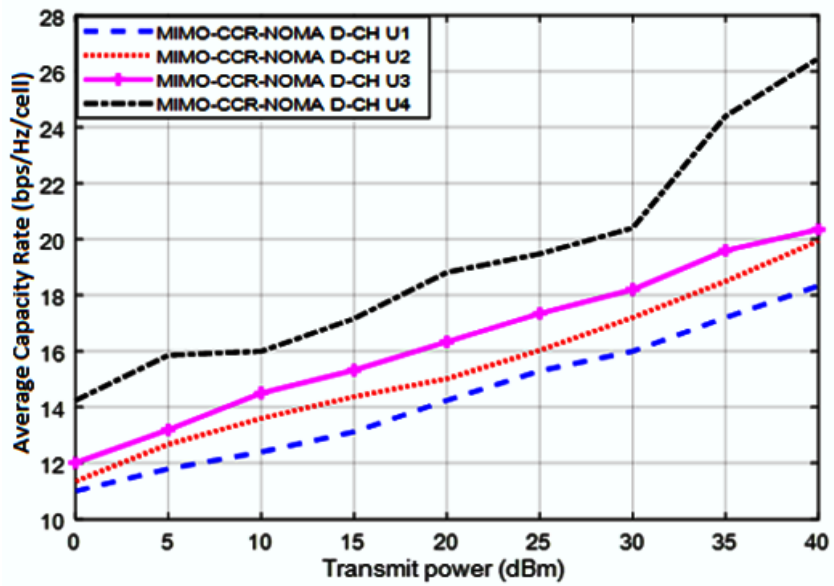


Figure 6.19. Average capacity versus TP for four users MIMO DL CCR- PD NOMA with D-CH

For four users BER is plotted against TP in Figure 6.20. PLCs and user separation distances diverge. Given the fundamentally unstable nature of the channel state, this also holds for 64x64 MIMO NOMA PD. There is a divergence in performance among all MIMO NOMA users from BER. The BER decreased as signal strength increased. U_4 was the closest to the BS, and they have the best BER performance by $1.31e-06$. In comparison to the same user in conventional NOMA, U_4 's BER performance is 94.3% better.

With 64x64 MIMO, the DL NOMA PD, and CCRN integration through C-CH, Figure 6.21 shows the BER as a product of TP for four users with different PLCs and distances between them. There is a variation in performance among all MIMO NOMA users with the proposal method based on the BER. As TP grows, BER reduces, according to the data. The BER performance of U_4 is $1.51e-06$. At BER, U_4 outperforms the identical user in conventional NOMA by 93.7%.

Figure 6.22 plots the BER against the TP for four users connected to the CCRN via D-CH and 64x64 MIMO. There is variability in the performance of all MIMO NOMA users when using the proposed technique, which is based on the BER. Based on the results, U_4 achieved the best BER performance of $1.41e-06$. If we look at U_4 's BER performance and compare it to the same user's performance in classic NOMA, 94% is the boost. The achieved results are superior to those of [151].

Results showed that BER in MIMO NOMA employing CR is affected by numerous parameters, including CSI, which is necessary for optimal performance. A higher BER results from CSI errors. TP influences BER directly. When TP rises, BER falls. MIMO NOMA systems must optimize resource allocation to reduce BER. While CR techniques improve resource allocation, they can also boost BER. The BER rises considerably with additional devices or systems. Beamforming improves signal transmission and reception in MIMO NOMA systems. Optimizing beamforming reduces BER. Spectrum-sharing strategies boost MIMO NOMA spectrum use. Because these parts operate together, improving one benefits the others.

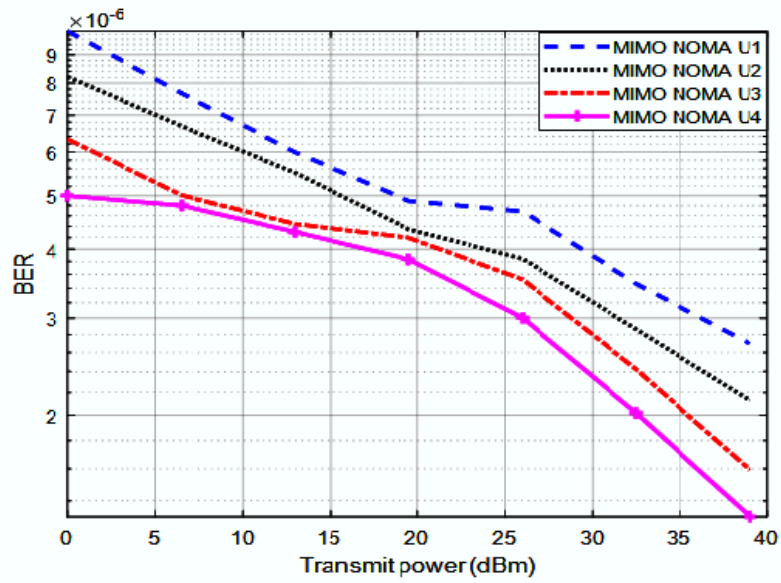


Figure 6.20. BER vs. TP for four MIMO DL NOMA PD users

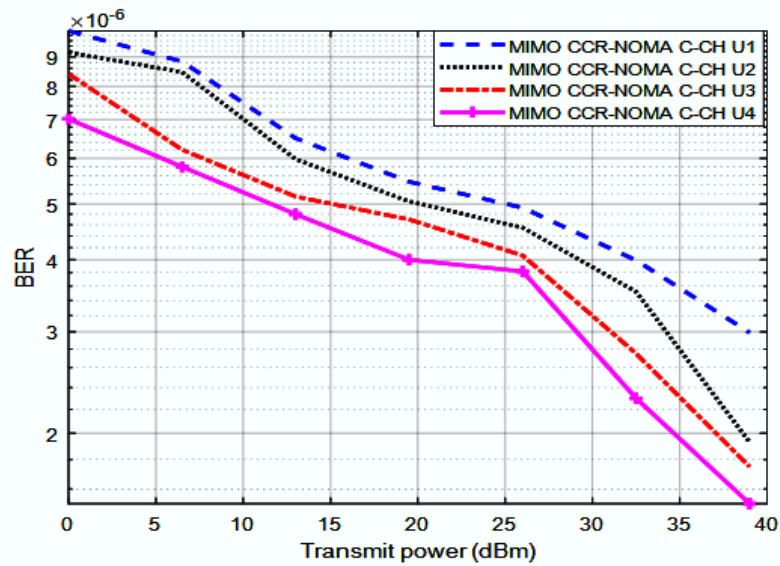


Figure 6.21. BER against TP for four MIMO DL CCR-NOMA PD users with C-CH

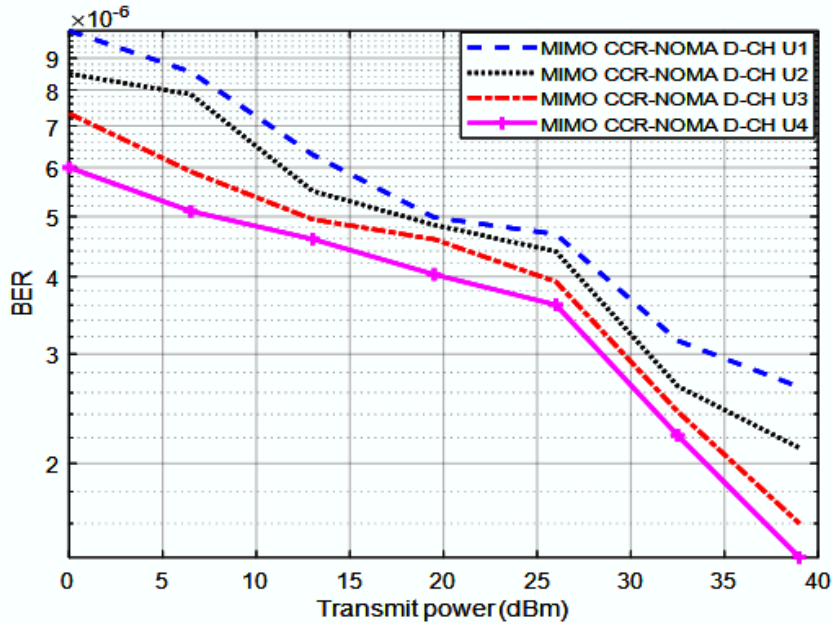


Figure 6.22. BER versus TP for four MIMO DL CCR-NOMA PD users with D-CH

6.5.3 Massive MIMO-DL-NOMA Scenario Results

At different distances and different PLCs, Figure 6.23 shows SE versus TP for four users in a 128x128 M-MIMO DL NOMA PD. It is common for SE to increase when TP increases. After executing the plan to integrate with the M-MIMO NOMA network, it was found that there is a difference in the SE performance of all NOMA users. The U₄ in closest proximity exhibits the most superior performance, whilst the U₁ situated at the greatest distance demonstrates the least satisfactory performance. At 40 dBm, SE performance is assessed by U₄ at 33.89 bps/Hz/cell. The top user, the U₄, obtained an improvement of 29.99 bps/Hz/cell at SE at 40 dBm TP when DL NOMA PD with 128x128 M-MIMO technology was compared with NOMA.

With the CCRN using C-CH, Figure 6.24 shows a comparison of SE and TP for 128x128, DL, NOMA, and PD integration. We discovered that the SE performance of all NOMA users varied while executing the proposal to join the M-MIMO NOMA network. As far as performance goes, the nearest U₄ is at the top, while the furthest U₁ is last. With 50.12 bps/Hz/cell, the user U₄ is operating at 40 dBm of TP. Compared to DL CCR-NOMA PD, the SE for the C-CH rose by 45.03 bits/sec/Hz/cell after applying 128x128 M-MIMO technology with NOMA.

The DL M-MIMO NOMA PD and the CCRN D-CH are shown in Figure 6.25. They show the SE versus TP for four users who are at different distances and have different power placement factors. The execution of the plan to merge with the M-MIMO NOMA network revealed differences in the SE performance of all NOMA users. At 40 dBm and 53.29 bps/Hz/cell, U_4 , the user closest to the BS, has the best SE performance. The SE was improved by 46.09 bps/Hz/cell at 40 dBm when using 128x128 M-MIMO technology with NOMA. The top user in the test, the D-CH, experienced this improvement with the DL CCR-NOMA PD. These results are significantly better than the SE performance reported in the literature [180]–[181].

In 5G M-MIMO systems, DL scheduling optimizes frequency spectrum usage. User grouping and power distribution greatly impact spectrum utilization in M-MIMO NOMA systems with CRN. M-MIMO cognitive cooperative relaying simplifies CRN cooperative relaying, improving SE. SE is affected by CRN design and implementation, which includes complete spectrum sharing. Honing these characteristics maximizes M-MIMO systems' SE. Important to meet rising cellular data demand.

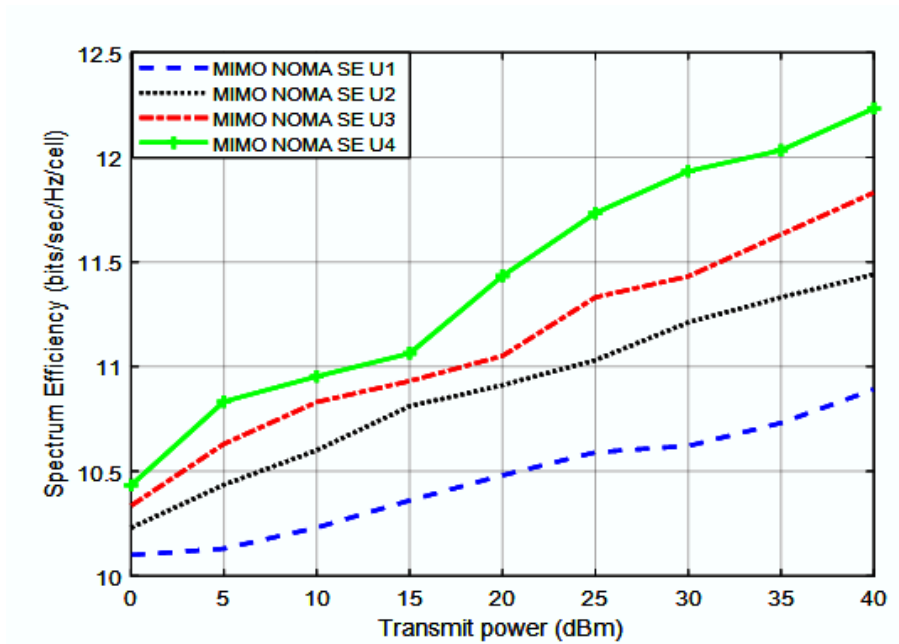


Figure 6.23. SE against TP for four M-MIMO DL PD NOMA users

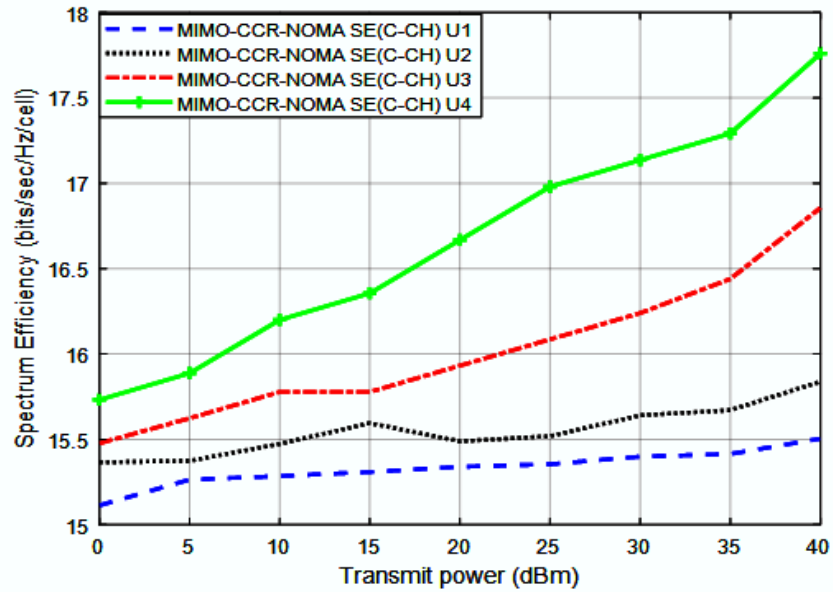


Figure 6.24. SE versus TP for four M-MIMO DL CCR- PD NOMA users with C-CH

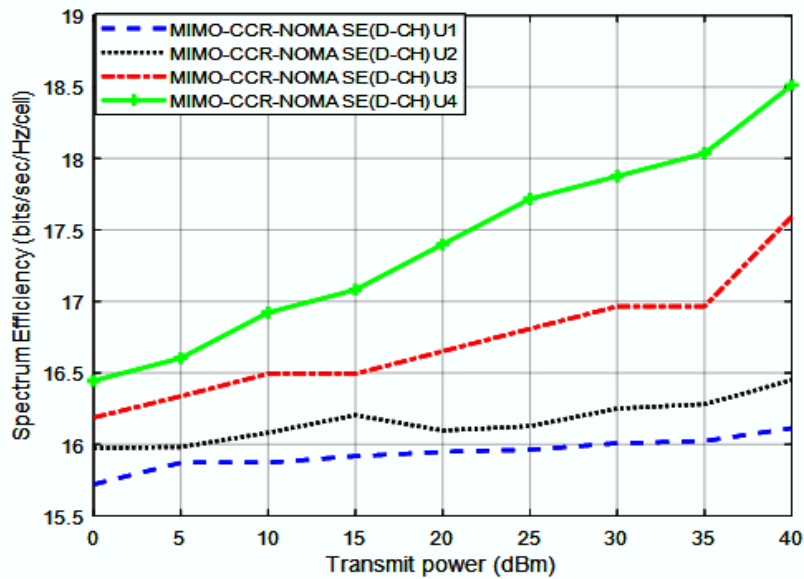


Figure 6.25. SE vs. TP for four M-MIMO DL CCR- PD NOMA users using D-CH

As a function of TP, Figure 6.26 displays the results for four users in DL NOMA PD utilizing 128x128 M-MIMO. When comparing all M-MIMO NOMA users, a clear disparity in average capacity performance emerges. Compared to its rivals, the U_4 excels thanks to its 40 dBm operating level and average capacity of 31.5 bps/Hz/cell. U_4 has an improved average capacity of 10 bps/Hz/cell compared to 64x64 MIMO NOMA and 17 bps/Hz/cell compared to standard NOMA. The results presented here demonstrate a significant improvement when contrasted with those in [182].

Figure 6.27 shows the ideal setup with 128x128 M-MIMO, DL NOMA PD, and CCRN C-CH. The proposed system significantly improves the average capacity performance compared to all other M-MIMO NOMAs. For four users at various PLCs and distances, U_4 realised an average capacity vs. TP of 35.5 bps/Hz/cell. The results for U_4 with 64x64 MIMO CCR-NOMA with C-CH are different from those for conventional CCR-NOMA with C-CH. The average capacity for U_4 goes up by 10 bps/Hz/cell and 21 bps/Hz/cell.

In Figure 6.28, you can see how the average capacity changes with TP for four users with various PLCs and distances when 128x128 M-MIMO, DL NOMA PD, and CCRN with D-CH are used. All M-MIMO NOMAs utilizing the proposed method exhibit significantly different average capacity performance. With a performance upgrade of 39.5 bps/Hz/cell, U_4 surpassed all competitors. As compared to 64x64 MIMO-NOMA and normal NOMA, U_4 's average capacity rate is 25 bps/Hz/cell higher.

The analysis found that antenna count, multi-user interference, SE, active users, transmit power, and CR technology impact M-MIMO NOMA with CRN average capacity. Optimizing M-MIMO NOMA with CRN systems is difficult due to the complex interplay of various parameters. However, understanding these factors can optimize system capacity and performance.

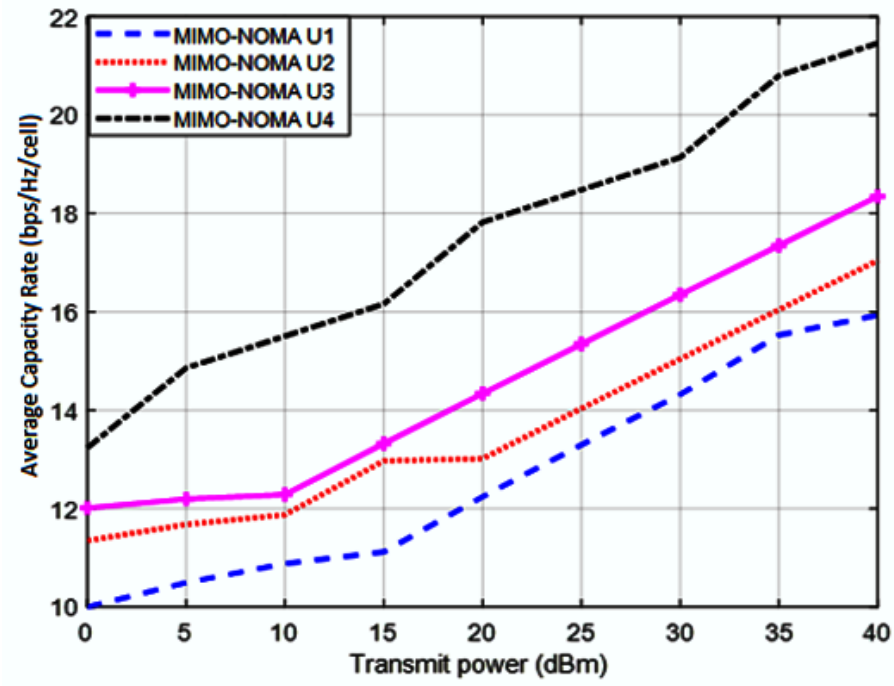


Figure 6.26. Average capacity versus TP for four M-MIMO DL PD NOMA users

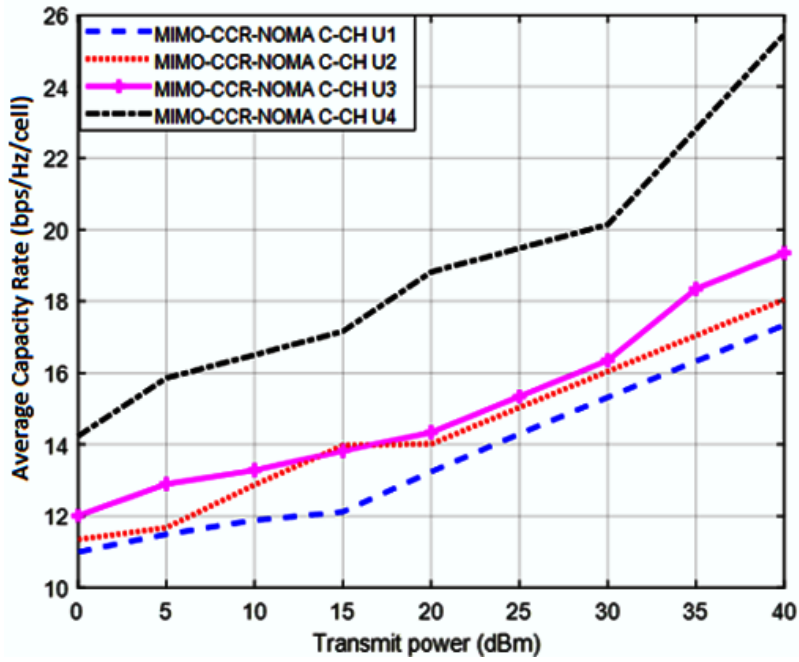


Figure 6.27. Average capacity versus TP for four users M-MIMO DL CCR- PD NOMA with C-CH

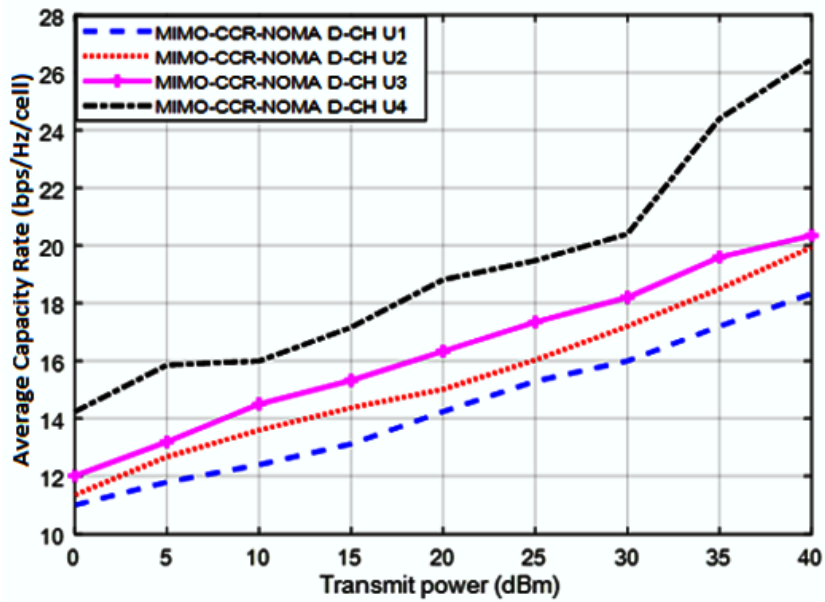


Figure 6.28. Average capacity versus TP for four users M-MIMO DL CCR- PD NOMA with D-CH

The correlation between BER and TP for four users is shown in Figure 6.29. There is a wide range of user-PLC distances. This rule applies to 128x128 MIMO NOMA PD. As the transmitted power increases, the BER drops. According to the BER, there is a variation in performance among all M-MIMO NOMA users. Because of their proximity to the BS, User 4 by $2.0e-08$ had the best BER performance. U_4 's BER performance is 98% better than that of the same user in standard NOMA.

Figure 6.30 shows the BER vs. TP for four users utilizing 128x128 MIMO, DL CCR-NOMA PD, and the C-CH. The users employ a variety of PLCs and distances. When using the BER-based proposal approach, performance varies among all M-MIMO NOMA users. At $2.9e-08$, U_4 's BER performance was the poorest. In terms of BER, U_4 outperforms the same user in conventional NOMA by a whopping 97.5%.

The graph in Figure 6.31 shows the BER vs. TP for four users with various PLCs and distances. It uses 128x128 MIMO, DL CCR-NOMA PD, and the C-CH. When using the BER-based proposal method, all M-MIMO NOMA users experience different levels of performance. With a score of $2.5 e-08$, U_4 stands out when examining BER performance. In ordinary NOMA, the identical user's BER performance is 97.7 times higher than in U_4 . Having said that, the results were better than those in [11].

The study examined interference, spectrum availability, power allocation, detection, and decoding as BER factors in M-MIMO NOMA with CR. More research is needed to determine how these factors affect BER in this system.

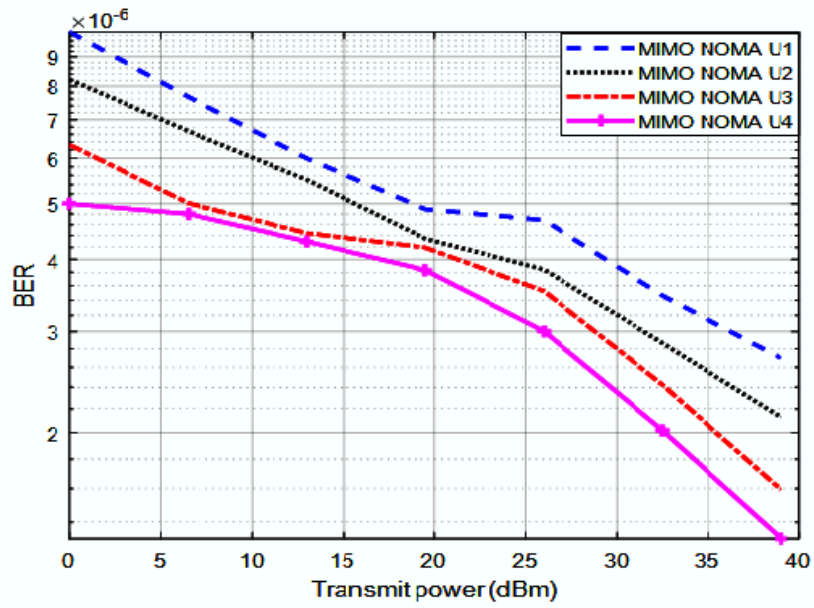


Figure 6.29. BER vs. TP for four M-MIMO DL NOMA PD users

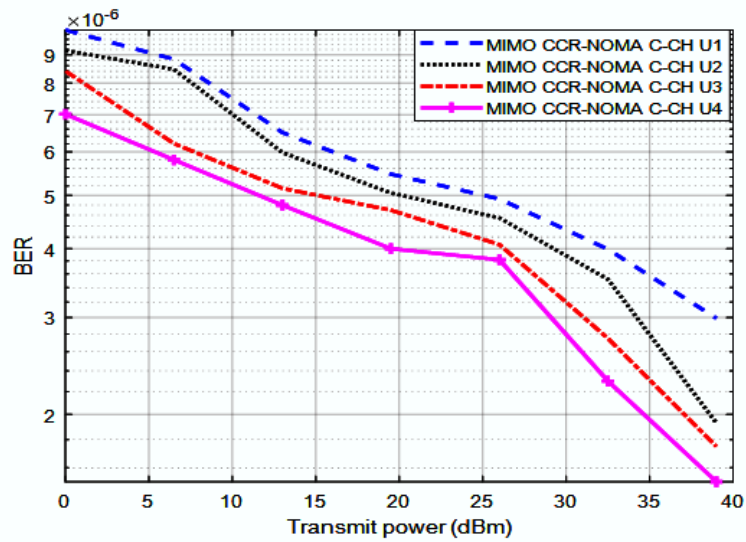


Figure 6.30. BER against TP for four M-MIMO DL CCR-NOMA PD users with C-CH

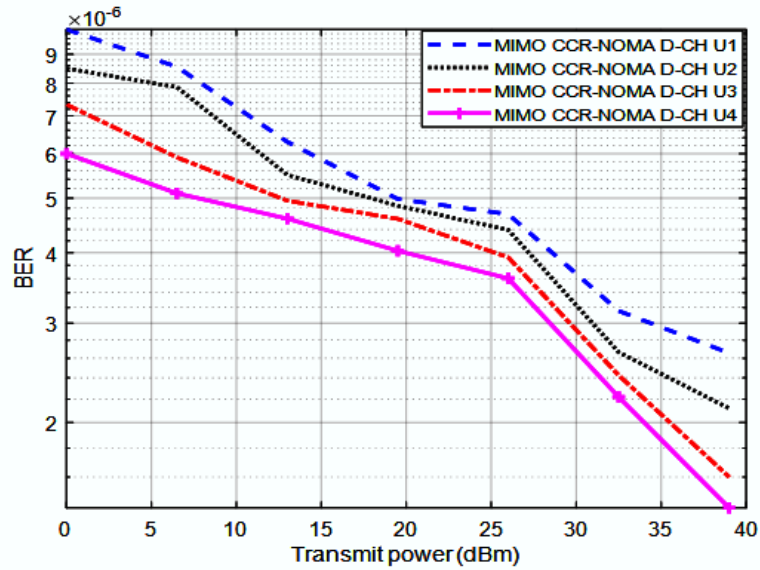


Figure 6.31. BER versus TP for four M-MIMO DL CCR-NOMA PD users with D-CH

6.6. Summary

In a 5G network with 64x64 MIMO and 128x128 M-MIMO integrated with the CCRN, this study showed how well DL NOMA PD performed in terms of SE, average capacity, and BER. One approach made it possible for users to access CCRN channels through the competition channel (C-CH), while the other made it possible for the CCRN to fulfil all channel demands of users through the dedicated channel (D-CH), irrespective of their location, PLCs, or TP.

While assessing performance, we paid close attention to the SIC, unstable channels, and AWGN when Rayleigh fading was present. The DL NOMA study found that integrating CCRN with 64x64 MIMO or 128x128 M-MIMO greatly enhanced SE, average capacity, and BER. When using DL NOMA, 5.1 bps/Hz/cell when using the CCRN with C-CH, and 7.2 bps/Hz/cell when using the CCRN with D-CH are the ideal SE performance for user U₄ at 40 dBm TP. At 40 dBm TP, the SE performance of DL 64x64 MIMO NOMA with CCRN (D-CH) improved by 65%, the SE performance of DL NOMA with CCRN (C-CH) grew by 64%, and the SE performance of DL NOMA with CCRN (U₄) improved by 51%. At 40 dBm TP, the SE performance was 85% better with DL 128x128 M-MIMO NOMA with CCRN (C-CH), 86% better with DL 128x128

M-MIMO NOMA with CCRN (D-CH), and 79% better with DL NOMA with best user U_4 .

U_4 attains an average capacity performance of 14.5 bps/Hz/cell for DL NOMA, 21.5 bps/Hz/cell for 64x64 MIMO DL NOMA, and 31.5 bps/Hz for 128x128 M-MIMO DL NOMA when tested at 40 dBm TP. U_4 average capacity performance was enhanced by 4% when DL NOMA was used in conjunction with the CCRN and C-CH; by 27% when 64x64 MIMO DL NOMA was used in conjunction with the CCRN and C-CH; and by 42% when 128x128 M-MIMO DL NOMA was used in conjunction with the CCRN and C-CH. In terms of average capacity performance, 64x64MIMO DL NOMA with CCRN (D-CH) increased it by 29%, 128x128 M-MIMO DL NOMA with CCRN (D-CH) improved it by 46%, and DL NOMA with CCRN (D-CH) enhanced it for U_4 by 9%.

The best BER performance for DL NOMA, DL CCR-NOMA with C-CH, and DL CCR-NOMA with D-CH, when considering the best U_4 and a TP of 40 dBm, is $7.0e-05$, $9.0e-03$, and $1.0e-04$, respectively. In contrast, 64x64 DL NOMA brought a BER reduction of 94.3% for BER U_4 , 93.7% for 64x64 MIMO DL NOMA with CCRN and C-CH, and 94% for 64x64 MIMO DL NOMA with CCRN and C-CH. Using C-CH, 128x128 M-MIMO DL NOMA with CCRN lowered BER by 97.5% for the best U_4 , while D-CH, 128x128 M-MIMO DL NOMA with CCRN, decreased BER by 97.7%. Integrating DL NOMA, DL MIMO NOMA, and DL M-MIMO NOMA with the recommended systems resulted in a higher BER when compared to the best user U_4 .

This is due to the fact that CR is required to handle increasingly intricate tasks, such as channel detection, channel switching, and error handling. Results in SE, average capacity, and BER were significantly enhanced when CCRN was used in conjunction with 64x64 MIMO and 128x128 M-MIMO DL NOMA systems.

CHAPTER SEVEN

Summary and Conclusion

7.1 Introduction

This chapter provides a summary and conclusion to the entire research, as well as suggestions and recommendations for additional research.

7.2 Summary

5G is a fifth-generation wireless network provides enhanced data transfer rates, reduced response time, and greater connectivity than its predecessors. However, its adoption and implementation is not without challenges. The main obstacles and challenges facing 5G technology are the scarcity of spectrum at small frequencies, while high-frequency versions are short-range and affected by objects such as trees and buildings, necessitating the construction of many facilities. Cell towers to avoid signal path loss.

The study explores the concept of spectrum scarcity, proposes solutions utilizing innovative methods and technologies, and views the spectrum as a valuable and limited resource.

Multiplexing allows several users to communicate across a single wired or wireless channel, which is explained in the first portion of this thesis along with access techniques. For a long time, research into wireless networking has centred on these technologies. The study of NOMA and spectrum sharing has several elements, including aims, problem statements, research objectives, scope, constraints, and definitions of essential terminologies.

The second chapter focuses on doing a literature study and discussing the essential ideas of OMA, NOMA, and cooperative NOMA. It also explores the concept of 5G, CR principles, CR-NOMA, MIMO, M-MIMO, and perimeter parameters for wireless communications and QoS.

The third chapter of the study examines the design and simulation of a 5G network, specifically examining the DL and UL PD NOMA techniques. All sorts of distances, SNRs, and BWs were factored into the calculations, both with and without 64x64 MIMO. The goal was to examine UL NOMA's performance

regarding average capacity and OP and to assess DL PD NOMA's performance about BER and SE.

Furthermore, the study's fourth chapter assessed the average sum-rate performance using TDMA and SC-NOMA and introduced two kinds of couplings in PD DL NOMA.

The fifth chapter analysed the impact of different power location coefficients (PLCs) of remote users on cooperative DL NOMA PD and DL NOMA PD. Additionally, it evaluated cooperative DL NOMA PD with and without MIMO as well as M-MIMO, taking into account OP against SNR.

A 5G network with 64x64 MIMO and 128x128 M-MIMO linked to the CCRN was shown to function effectively in the sixth chapter by DL NOMA PD. First, the CCRN could provide users' channel demands through the dedicated channel (D-CH), and second, users may get CCRN channels through the competition channel (C-CH). We looked at three performance metrics: SE average capacity, and BER.

7.3 Conclusion

In order to enhance SE, average capacity, and BER, this thesis introduces the DL NOMA PD for the 5G network in conjunction with 64x64 MIMO and 128x128 M-MIMO technologies integrated with CCRN. The novel approach involves accessing CCRN channels through the C-CH or D-CH to meet users' channel needs. Chapter 4 covered 5G network performance, including DL PD NOMA's impact on BER and SE, OP, and average capacity, under a range of conditions including distance, PLCs, TPs, and BWs, and with and without 64x64 MIMO. In addition, the acquired results for SE and BER were found to be superior when compared with [157] for DL NOMA, while the results for OP and average capacity were better when compared with [159]-[162]-[163] for UL NOMA. Findings from chapter five, Near-Far User Problems, demonstrate that the first strategy achieves a better average rate when pairing local users with distant users. Even with the second scheme's near-near, far-far pairing, NOMA still outperforms TDMA and SC-NOMA on average sum rate, albeit not as significantly. The effects of PLCs used by distant users on cooperative DL NOMA PD and DL NOMA were examined in Chapter 5. The OP and SNR were compared, and MIMO and M-MIMO systems of varying dimensions were introduced into the cooperative DL NOMA system. The dimensions for M-MIMO were 128x128, 256x256, and 512x512, while for MIMO they were

16x16, 32x32, and 64x64. The results demonstrate that the OP's performance rate surpasses that of the results obtained in [163]-[164]-[166]. Two separate methods were demonstrated in Chapter Six to improve the DL NOMA PD performance in 5G networks in terms of SE, average capacity, and BER. Two methods that were used in these techniques were CCRN and 64x64 MIMO and 128x128 M-MIMO, which stand for coordinated channel and resource allocation. There was an improvement over [11]-[182]-[181]. The results demonstrate a noteworthy enhancement in the quality of service across all proposed scenarios. Tables and figures display an extensive collection of quantitative data from the research. According to the study, the proposed methods are effective in mitigating the challenges of spectrum scarcity and improving performance quality in 5G networks.

7.4 Future Research

From the results obtained the researcher suggests the following recommendation for future works

- The study reveals that the SE of DL-NOMA is influenced by several parameters, including user distribution, power allocation coefficients, number of users, transmission power, BW, channel conditions, and SIC. These parameters can have intricate interactions, and enhancing the SE of the DL-NOMA method in the future needs a more thorough and meticulous investigation to devise sophisticated algorithms and strategies for its efficient management.
- NOMA power fields are widely used in the scientific community, but the second type, the code field (CD) NOMA, has not been adequately addressed and will therefore be the focus of future research.
- Two, the outcomes demonstrated that pairing NOMA with other access strategies yields beneficial outcomes; hence, this feature will be the subject of future studies and will be explored in greater depth using more realistic settings.
- Multi-band NOMA (MC-NOMA) is an improved version of SC-NOMA that uses multiple carriers to accommodate multiple users. MC-NOMA provides superior system capacity, low latency, and wide-range communications compared to SC-NOMA. MC-NOMA enables multiplexing of users in the power and frequency domains, resulting in more efficient use of resources. Therefore, it will be an important area for future studies.

- Spectrum sharing is a solution to spectrum shortages. Combining CCRN and NOMA worked well. Maintaining the same research method while merging cooperative NOMA technology, with AI, is the goal.
- The problem of restricted spectrum in the upcoming sixth-generation (6G) wireless communication systems is both major and pressing. Spectrum scarcity refers to the situation when there is a restricted quantity of radio frequency (RF) spectrum available, which is a vital resource for wireless communication systems. The demand for wireless communication services, such as mobile broadband, and crucial communications, is steadily growing. Consequently, we plan to use the recommended methodologies and concentrate on honing them to discover the most advantageous resolutions to this dilemma.

List of Publications

Published Papers

S/N	Title	Journal	Index of journal	Remarks
1.	Impact of Power and Bandwidth on the Capacity Rate and Number of Users In SC-NOMA	Journal of Harbin Institute Technology	Scopus, Q3	Published 2021
2.	BER Performance of NOMA Downlink for AWGN and Rayleigh Fading Channels in (SIC).	EAI Endorsed Transactions on Mobile Communications and Applications	Web of Science	Published 2022
3.	Modeling of NOMA-MIMO-Based Power Domain for 5G Network under Selective Rayleigh Fading Channels.	Energies- MDPI	Scopus, Q1	Published 2022
4.	Design of Power Location Coefficient System for 6G Downlink Cooperative NOMA Network.	Energies- MDPI	Scopus, Q1	Published 2022
5.	Capacity Evaluation of NOMA Uplink with Rayleigh Fading Channels.	University of Science and Technology Scientific Journal	Web of Science	Published 2022
6.	Outage Probability Analysis of NOMA Uplink with Rayleigh Fading Channels.	University of Science and Technology Scientific Journal	Web of Science	Published 2022

7.	Enhancing NOMA's spectrum efficiency in a 5G network through cooperative spectrum sharing.	Electronics- MDPI	Scopus, Q2	Published 2023
8.	Enhancement of Outage Probability for Down Link Cooperative Non-orthogonal multiple access in a 5G Network.	International Journal of Electrical and Computer Engineering (IJECE)	Scopus, Q2	Published 2023
9.	Improving 6G Network Spectrum Efficiency with Non-Cooperative and Cooperative Spectrum Sharing Using NOMA and Massive-MIMO	EAI Endorsed Transactions on Mobile Communications and Applications	Web of Science	Published 2023

Communication Articles

S/N	Title	Journal	Index of journal	Remarks
1.	Survey on Advanced Spectrum Sharing Using Cognitive Radio Technique.	ICT Systems and Sustainability. Advances in Intelligent Systems and Computing, Springer.	Scopus	2020
2.	Overview of Cognitive Radio Networks.	International Conference on Robotics and Artificial Intelligence (RoAI).	Scopus	2020
3.	Review of NOMA with Spectrum Sharing Technique.	ICT with Intelligent Applications. Smart Innovation, Systems and Technologies, Springer	Scopus	2021
4.	Survey on NOMA and Spectrum Sharing Techniques in 5G.	IEEE International Conference on Smart Information Systems and Technologies (SIST).	Scopus	2021
5.	Average Rate Performance for Pairing Downlink NOMA Networks Schemes.	International Conference on Smart Information Systems and Technologies (SIST).	Scopus	2022
6.	BER Improvement of Cooperative Spectrum Sharing of NOMA in 5G Network.	2023 IEEE 3rd International Maghreb Meeting of the Conference on Sciences and Techniques of Automatic Control	Scopus	2023

		and Computer Engineering.		
7.	NOMA Cooperative Spectrum Sharing Average Capacity Improvement in 5G Network.	2023 IEEE 3rd International Maghreb Meeting of the Conference on Sciences and Techniques of Automatic Control and Computer Engineering.	Scopus	2023
8.	Enhancing the Efficient Use of Spectrum in 5G Networks via Uncooperative and Cooperative Spectrum Sharing with NOMA and MIMO	Ubiquitous Technology in Communication and Artificial Intelligence - (UTCA-2023)	Scopus	2023
9.	Improving 5G Networks' Average Capacity and BER by Using Uncooperative Underlay and Cooperative Interweave Cognitive Radio NOMA and MIMO	International Conference on Information and Communication Technology for Competitive Strategies, Springer (2023).	Scopus	2023
10.	6G Networks Capacity Improvement Based on Massive MIMO for Cognitive Radio NOMA	4th International Conference on Artificial Intelligence and Data Engineering (AIDE) – 2023	Scopus	2023
11.	Capacity Enhancement Based	2024 IEEE 4th International	Scopus	2024

	on mMIMO for Cognitive Radio NOMA in Future 6G Networks.	Maghreb Meeting of the Conference on Sciences and Techniques of Automatic Control and Computer Engineering (MI-STA 2024).		
12.	Enhancing the Average Capacity of 6G Networks by Utilizing NOMA and mMIMO with Spectrum Sharing Modes.	ICT4SD CONFERENCE.	Scopus	2024

References

- [1] Z. Chen, Z. Ding, X. Dai and R. Zhang, "An Optimization Perspective of the Superiority of NOMA Compared to Conventional OMA," in *IEEE Transactions on Signal Processing*, vol. 65, no. 19, pp. 5191-5202, 1 Oct.1, 2017, doi: 10.1109/TSP.2017.2725223.
- [2] P. V. Reddy et al, "Analytical Review on OMA vs. NOMA and Challenges Implementing NOMA," 2021 2nd International Conference on Smart Electronics and Communication (ICOSEC), pp. 552-556, 2021, doi:10.1109/ICOSEC51865.2021.9591629.
- [3] M. Vaezi, H. Poor, "NOMA: An Information-Theoretic Perspective," In *Multiple Access Techniques for 5G Wireless Networks and Beyond*, " Springer, Cham, 2019, doi:10.1007/978-3-319-92090-0_5.
- [4] T. Kebede, Y. Wondie, J. Steinbrunn, H. B. Kassa and K. T. Kornegay, "Multi-Carrier Waveforms and Multiple Access Strategies in Wireless Networks: Performance, Applications, and Challenges," in *IEEE Access*, vol. 10, pp. 21120-21140, 2022, doi: 10.1109/ACCESS.2022.3151360.
- [5] B. Wang, K. Wang, Z. Lu, T. Xie and J. Quan, "Comparison study of non-orthogonal multiple access schemes for 5G," 2015 IEEE International Symposium on Broadband Multimedia Systems and Broadcasting, 2015, pp. 1-5, doi: 10.1109/BMSB.2015.7177186.
- [6] A. F. M. Shahen Shah, "A Survey From 1G to 5G Including the Advent of 6G: Architectures, Multiple Access Techniques, and Emerging Technologies," 2022 IEEE 12th Annual Computing and Communication Workshop and Conference (CCWC), Las Vegas, NV, USA, 2022, pp. 1117-1123, doi: 10.1109/CCWC54503.2022.9720781.
- [7] D. Galda, H. Rohling, E. Costa, H. Haas and E. Schulz, "A low complexity transmitter structure for OFDM-FDMA uplink systems," *Vehicular Technology Conference. IEEE 55th Vehicular Technology Conference. VTC Spring 2002 (Cat. No.02CH37367)*, 2002, pp. 1737-1741 vol.4, doi: 10.1109/VTC.2002.1002918.
- [8] A. F. M. S. Shah, A. N. Qasim, M. A. Karabulut, H. Ilhan and M. B. Islam, "Survey and Performance Evaluation of Multiple Access Schemes for Next-Generation Wireless Communication Systems," in *IEEE Access*, vol. 9, pp. 113428-113442, 2021, doi: 10.1109/ACCESS.2021.3104509.
- [9] T. -H. Vu, T. -V. Nguyen, D. B. da Costa and S. Kim, "Performance Analysis and Deep Learning Design of Underlay Cognitive NOMA-Based CDRT Networks With Imperfect SIC and Co-Channel Interference," in *IEEE Transactions on*

- Communications, vol. 69, no. 12, pp. 8159-8174, Dec. 2021, doi: 10.1109/TCOMM.2021.3110209.
- [10] A. Celik, M. -C. Tsai, R. M. Radaydeh, F. S. Al-Qahtani and M. -S. Alouini, "Distributed Cluster Formation and Power-Bandwidth Allocation for Imperfect NOMA in DL-HetNets," in IEEE Transactions on Communications, vol. 67, no. 2, pp. 1677-1692, Feb. 2019, doi: 10.1109/TCOMM.2018.2879508.
- [11] M. Hassan, M. Singh, and Kh. Hamid , "BER Performance of NOMA Downlink for AWGN and Rayleigh Fading Channels in (SIC)," in MCA, EAI, 2022, doi: 10.4108/eai.20-6-2022.174227.
- [12] F. Schaich and T. Wild, "Waveform contenders for 5G — OFDM vs. FBMC vs. UFMF," 2014 6th International Symposium on Communications, Control and Signal Processing (ISCCSP), 2014, pp. 457-460, doi: 10.1109/ISCCSP.2014.6877912.
- [13] A. Alqahtani, E. Alsusa, A. Al-Dweik and M. Al-Jarrah, "Performance Analysis for Downlink NOMA Over α - μ Generalized Fading Channels," in IEEE Transactions on Vehicular Technology, vol. 70, no. 7, pp. 6814-6825, July 2021, doi: 10.1109/TVT.2021.3082917.
- [14] O. Maraqa, A. S. Rajasekaran, S. Al-Ahmadi, H. Yanikomeroglu and S. M. Sait, "A Survey of Rate-Optimal Power Domain NOMA With Enabling Technologies of Future Wireless Networks," in IEEE Communications Surveys & Tutorials, vol. 22, no. 4, pp. 2192-2235, Fourth quarter 2020, doi: 10.1109/COMST.2020.3013514.
- [15] Liaqat, M., Noordin, K.A., Abdul Latef, T. et al, " Power-domain non orthogonal multiple access (PD-NOMA) in cooperative networks: an overview. Wireless Network," 26, 181–203 (2020, doi:10.1007/s11276-018-1807-z.
- [16] L. Dai, B. Wang, Z. Ding, Z. Wang, S. Chen and L. Hanzo, "A Survey of Non-Orthogonal Multiple Access for 5G," in IEEE Communications Surveys & Tutorials, vol. 20, no. 3, pp. 2294-2323, thirdquarter 2018, doi: 10.1109/COMST.2018.2835558.
- [17] Z. Elsaraf, F. A. Khan and Q. Z. Ahmed, "Deep Learning Based Power Allocation Schemes in NOMA Systems: A Review," 2021 26th International Conference on Automation and Computing (ICAC), 2021, pp. 1-6, doi: 10.23919/ICAC50006.2021.9594173.
- [18] Z. Q. Al-Abbasi and D. K. C. So, "Power allocation for sum rate maximization in non-orthogonal multiple access system," 2015 IEEE 26th Annual International Symposium on Personal, Indoor, and Mobile Radio Communications (PIMRC), 2015, pp. 1649-1653, doi: 10.1109/PIMRC.2015.7343563.

- [19] M. Hassan, M. Singh, and K. Hamid, "Review of NOMA with Spectrum Sharing Technique," In: Senjyu, T., Mahalle, P.N., Perumal, T., Joshi, A. (eds) *ICT with Intelligent Applications, Smart Innovation, Systems and Technologies*, vol 248. Springer, Singapore. 2022, doi:10.1007/978-981-16-4177-0_16.
- [20] D. Cohen, S. Tsiper and Y. C. Eldar, "Analog-to-Digital Cognitive Radio: Sampling, Detection, and Hardware," in *IEEE Signal Processing Magazine*, vol. 35, no. 1, pp. 137-166, Jan. 2018, doi: 10.1109/MSP.2017.2740966.
- [21] M. R. Hassan, G. C. Karmakar, J. Kamruzzaman and B. Srinivasan, "Exclusive Use Spectrum Access Trading Models in Cognitive Radio Networks: A Survey," in *IEEE Communications Surveys & Tutorials*, vol. 19, no. 4, pp. 2192-2231, Fourthquarter 2017, doi: 10.1109/COMST.2017.2725960.
- [22] F. Hu, B. Chen and K. Zhu, "Full Spectrum Sharing in Cognitive Radio Networks Toward 5G: A Survey," in *IEEE Access*, vol. 6, pp. 15754-15776, 2018, doi: 10.1109/ACCESS.2018.2802450.
- [23] A. Aissioui, A. Ksentini, A. M. Gueroui and T. Taleb, "On Enabling 5G Automotive Systems Using Follow Me Edge-Cloud Concept," in *IEEE Transactions on Vehicular Technology*, vol. 67, no. 6, pp. 5302-5316, June 2018, doi: 10.1109/TVT.2018.2805369.
- [24] S. Onoe, "1.3 Evolution of 5G mobile technology toward 1 2020 and beyond," 2016 *IEEE International Solid-State Circuits Conference (ISSCC)*, 2016, pp. 23-28, doi: 10.1109/ISSCC.2016.7417891.
- [25] S. Zhang, "An Overview of Network Slicing for 5G," in *IEEE Wireless Communications*, vol. 26, no. 3, pp. 111-117, June 2019, doi: 10.1109/MWC.2019.1800234.
- [26] M. A. Inamdar and H. V. Kumaraswamy, "Energy Efficient 5G Networks: Techniques and Challenges," 2020 *International Conference on Smart Electronics and Communication (ICOSEC)*, pp. 1317-1322, 2020, doi: 10.1109/ICOSEC49089.2020.9215362.
- [27] M. Zebari, A. Zebari, and Al-zebari, "FUNDAMENTALS OF 5G CELLULAR NETWORKS: A REVIEW," *Journal of Information Technology and Informatics*, 1(1), 1-5, 2021, doi:/10.6084.
- [28] Kabalci, Y, "5G Mobile Communication Systems: Fundamentals, Challenges, and Key Technologies," In: Kabalci, E, Kabalci, Y. (eds) *Smart Grids and Their Communication Systems, Energy Systems in Electrical Engineering*, Springer, Singapore, 2019, doi:10.1007/978-981-13-1768-2_10.
- [29] Q. -V. Pham et al., "A Survey of Multi-Access Edge Computing in 5G and Beyond: Fundamentals, Technology Integration, and State-of-the-Art," in *IEEE Access*, vol. 8, pp. 116974-117017, 2020, doi: 10.1109/ACCESS.2020.3001277.

- [30] M. Abd-Elnaby, G. Sedhom, M. El-Rabaie, and M. Elwekeil, "NOMA for 5G and beyond: literature review and novel trends," *Wireless Netw.*, 2022, doi:10.1007/s11276-022-03175-7.
- [31] A. Amanna and J. H. Reed, "Survey of cognitive radio architectures," *Proceedings of the IEEE SoutheastCon 2010 (SoutheastCon)*, 2010, pp. 292-297, doi: 10.1109/SECON.2010.5453869.
- [32] J. Mitola III, "Cognitive Radio Architecture. In: Arslan, H. (eds) *Cognitive Radio, Software Defined Radio, and Adaptive Wireless Systems*," Springer, Dordrecht, 2007, doi:10.1007/978-1-4020-5542-3_3.
- [33] M. R. Manesh, M. S. Apu, N. Kaabouch and W. -C. Hu, "Performance evaluation of spectrum sensing techniques for cognitive radio systems," *2016 IEEE 7th Annual Ubiquitous Computing, Electronics & Mobile Communication Conference (UEMCON)*, 2016, pp. 1-7, doi: 10.1109/UEMCON.2016.7777829.
- [34] E. U. Ogbodo, D. Dorrell and A. M. Abu-Mahfouz, "Cognitive Radio Based Sensor Network in Smart Grid: Architectures, Applications and Communication Technologies," in *IEEE Access*, vol. 5, pp. 19084-19098, 2017, doi: 10.1109/ACCESS.2017.2749415.
- [35] M. Hassan, M. Singh, K. Hamid, "Overview of Cognitive Radio Networks," Published under licence by IOP Publishing Ltd *Journal of Physics: Conference Series*, International Conference on Robotics and Artificial Intelligence (RoAI) 2020 28-29 December 2020, Chennai, India, vol. 1831, 2020, doi:10.1088/1742-6596/1831/1/012013.J.
- [36] Thomas and P. Menon, "A survey on spectrum handoff in cognitive radio networks," *2017 International Conference on Innovations in Information, Embedded and Communication Systems (ICIIECS)*, pp.1-4, 2017, doi: 10.1109/ICIIECS.2017.8275896.
- [37] M. Hassan, M. Singh, K. Hamid, "Survey on Advanced Spectrum Sharing Using Cognitive Radio Technique," In: Tuba, M., Akashe, S., Joshi, A. (eds) *ICT Systems and Sustainability. Advances in Intelligent Systems and Computing*, vol.1270. Springer, Singapore, 2021, doi:10.1007/978-981-15-8289-9_62.
- [38] S. Arzykulov, G. Naurzybayev, T. A. Tsiftsis and M. Abdallah, "Outage Performance of Underlay CR-NOMA Networks," *2018 10th International Conference on Wireless Communications and Signal Processing (WCSP)*, pp.1-6, 2018, doi: 10.1109/WCSP.2018.8555600.
- [39] D. -T. Do, A. -T. Le and B. M. Lee, "NOMA in Cooperative Underlay Cognitive Radio Networks Under Imperfect SIC," in *IEEE Access*, vol. 8, pp. 86180-86195, 2020, doi: 10.1109/ACCESS.2020.2992660.

- [40] I. Budhiraja, S. Tyagi, S. Tanwar, N. Kumar and M. Guizani, "CR-NOMA Based Interference Mitigation Scheme for 5G Femtocells Users," 2018 IEEE Global Communications Conference (GLOBECOM), 2018, pp. 1-6, doi: 10.1109/GLOCOM.2018.8647354.
- [41] Y.Qiao, Y. He, L. Zhang, , J.YangZhou, "Performance Analysis of Multiple Primary Users CR-NOMA Networks Under Partial Relay Selection, " In: Kountchev, R., Mahanti, A., Chong, S., Patnaik, S., Favorskaya, M. (eds) *Advances in Wireless Communications and Applications. Smart Innovation, Systems and Technologies*, vol 191. Springer, Singapore. 2021, doi:10.1007/978-981-15-5879-5_11.
- [42] Z. Ding, X. Lei, G. K. Karagiannidis, R. Schober, J. Yuan and V. K. Bhargava, "A Survey on Non-Orthogonal Multiple Access for 5G Networks: Research Challenges and Future Trends," in *IEEE Journal on Selected Areas in Communications*, vol. 35, no. 10, pp. 2181-2195, Oct. 2017, doi: 10.1109/JSAC.2017.2725519.
- [43] Andrea Goldsmith. *Wireless communications*. Cambridge university press, 2005.
- [44] Y. Saito, A. Benjebbour, Y. Kishiyama and T. Nakamura, "System-Level Performance of Downlink Non-Orthogonal Multiple Access (NOMA) under Various Environments," 2015 IEEE 81st Vehicular Technology Conference (VTC Spring), 2015, pp. 1-5, doi: 10.1109/VTCSpring.2015.7146120. 2013.
- [45] Peng Wang, Jun Xiao, and Li Ping, "Comparison of orthogonal and nonorthogonal approaches to future wireless cellular systems," *IEEE Vehicular Technology Magazine*, 1(3):4–11, 2006.
- [46] Y. Cai, Z. Qin, F. Cui, G. Ye Li, and J. A McCann, " Modulation and multiple access for 5g networks. *IEEE Communications Surveys & Tutorials*, " 20(1):629–646, 2017.
- [47] G. Miao, J. Zander, K. Sung, and S. Slimane, "Fundamentals of mobile data networks, " Cambridge University Press, 2016.
- [48] SD Icev, "Time division multiple access (TDMA) applicable for mobile satellite communications," In 21st International Crimean Conference" Microwave & Telecommunication Technology"(CriMiCo 2011), pages 365–367, 2011.
- [49] J. J. Caffery and G. L. Stuber, "Overview of radiolocation in CDMA cellular systems," in *IEEE Communications Magazine*, vol. 36, no. 4, pp. 38-45, April 1998, doi: 10.1109/35.667411.
- [50] A. Singh and P. Singh, "Effect of erroneous power control on the performance of overloaded cellular UCDS-CDMA," 2013 IEEE International Conference on Electronics, Computing and Communication Technologies, 2013, pp. 1-6, doi: 10.1109/CONECCT.2013.6469305.

- [51] S. Hara and R. Prasad, "Overview of multicarrier CDMA," in *IEEE Communications Magazine*, vol. 35, no. 12, pp. 126-133, Dec. 1997, doi: 10.1109/35.642841.
- [52] TS Rappaport, BD Woerner, JH Reed, "Wireless personal communications: The evolution of personal communications systems," 2012
- [53] D. Stamatelos and A. Ephremides, "Multiple access capability of indoor wireless networks using spatial diversity," 5th IEEE International Symposium on Personal, Indoor and Mobile Radio Communications, Wireless Networks - Catching the Mobile Future., 1994, pp. 1271-1275 vol.4, doi: 10.1109/WNCMF.1994.529457.
- [54] Aarab, M.N., Chakkor, O, "MIMO-OFDM for Wireless Systems: An Overview," In: Ezziyyani, M. (eds) *Advanced Intelligent Systems for Sustainable Development (AI2SD'2019)*, AI2SD 2019, Lecture Notes in Networks and Systems, vol 92. Springer, Cham, 2020, doi:10.1007/978-3-030-33103-0_19.
- [55] H. Yin and S. Alamouti, "OFDMA: A Broadband Wireless Access Technology," 2006 IEEE Sarnoff Symposium, 2006, pp. 1-4, doi: 10.1109/SARNOF.2006.4534773.
- [56] X. Lin et al., "5G New Radio: Unveiling the Essentials of the Next Generation Wireless Access Technology," in *IEEE Communications Standards Magazine*, vol. 3, no. 3, pp. 30-37, September 2019, doi: 10.1109/MCOMSTD.001.1800036.
- [57] D. Skordoulis, Q. Ni, H. -h. Chen, A. P. Stephens, C. Liu and A. Jamalipour, "IEEE 802.11n MAC frame aggregation mechanisms for next-generation high-throughput WLANs," in *IEEE Wireless Communications*, vol. 15, no. 1, pp. 40-47, February 2008, doi: 10.1109/MWC.2008.4454703.
- [58] G. L. Stuber, J. R. Barry, S. W. McLaughlin, Ye Li, M. A. Ingram and T. G. Pratt, "Broadband MIMO-OFDM wireless communications," in *Proceedings of the IEEE*, vol. 92, no. 2, pp. 271-294, Feb. 2004, doi: 10.1109/JPROC.2003.821912.
- [59] Harish Viswanathan and Marcus Weldon. The past, present, and future of mobile communications. *Bell Labs Technical Journal*, 19:8–21, 2014.
- [60] A. Anwar, B.Ch. Seet, M. A. Haasan, X. J. Li, "A Survey on Application of Non-Orthogonal Multiple Access to Different Wireless Networks," 2019, *Electronics* 8, no. 11: 1355, doi:10.3390/electronics8111355.
- [61] B. Kimy et al., "Non-orthogonal Multiple Access in a Downlink Multiuser Beamforming System," *MILCOM 2013 - 2013 IEEE Military Communications Conference*, 2013, pp. 1278-1283, doi: 10.1109/MILCOM.2013.218.
- [62] H. Lei et al., "On Secure NOMA Systems With Transmit Antenna Selection Schemes," in *IEEE Access*, vol. 5, pp. 17450-17464, 2017, doi: 10.1109/ACCESS.2017.2737330.

- [63] H. Nikopour and H. Baligh, "Sparse code multiple access," 2013 IEEE 24th Annual International Symposium on Personal, Indoor, and Mobile Radio Communications (PIMRC), 2013, pp. 332-336, doi: 10.1109/PIMRC.2013.6666156.
- [64] Z. ElSaraf, F. Khan, and Q. Ahmed, "Performance analysis of codedomain noma in 5g communication systems," Proceedings of the 2018 ELEKTRO, Mikulov, Czech Republic, pages 21–23, 2018.
- [65] F. Alavi, K. Cumanan, Z. Ding and A. G. Burr, "Robust Beamforming Techniques for Non-Orthogonal Multiple Access Systems with Bounded Channel Uncertainties," in IEEE Communications Letters, vol. 21, no. 9, pp. 2033-2036, Sept. 2017, doi: 10.1109/LCOMM.2017.2702580.
- [66] L. Zhu, J. Zhang, Z. Xiao, X. Cao and D. O. Wu, "Optimal User Pairing for Downlink Non-Orthogonal Multiple Access (NOMA)," in IEEE Wireless Communications Letters, vol. 8, no. 2, pp. 328-331, April 2019, doi: 10.1109/LWC.2018.2853741.
- [67] F. Liu and M. Petrova, "Dynamic Power Allocation for Downlink Multi-Carrier NOMA Systems," in IEEE Communications Letters, vol. 22, no. 9, pp. 1930-1933, Sept. 2018, doi: 10.1109/LCOMM.2018.2852655.
- [68] A. Rawat, R. Kaushik, and A. Tiwari, "AN OVERVIEW OF MIMO OFDM SYSTEM FOR WIRELESS COMMUNICATION, " International Journal of Technical Research & Science, vol. 6, October 2021 doi:10.30780/IJTRS.V06.I10.001.
- [69] H. Mathur, T. Deepa, "A Survey on Advanced Multiple Access Techniques for 5G and Beyond Wireless Communications," Wireless Pers Commun 118, 1775–1792 (2021), doi:10.1007/s11277-021-08115-w
- [70] M. Hassan, M. Singh and K. Hamid, "Survey on NOMA and Spectrum Sharing Techniques in 5G," 2021 IEEE International Conference on Smart Information Systems and Technologies (SIST), 2021, pp. 1-4, doi: 10.1109/SIST50301.2021.9465962.
- [71] I. Budhiraja et al., "A Systematic Review on NOMA Variants for 5G and Beyond," in IEEE Access, vol. 9, pp. 85573-85644, 2021, doi: 10.1109/ACCESS.2021.3081601.
- [72] R. Vannithamby and S. Talwar, "Towards 5G: Applications, requirements & candidate technologies, "1st ed. Chichester, West Susses, United Kingdom: John Wiley & Sons Inc., 2017.
- [73] Z. Ding et al., "Application of Non-Orthogonal Multiple Access in LTE and 5G Networks," in IEEE Communications Magazine, vol. 55, no. 2, pp. 185-191, February 2017, doi: 10.1109/MCOM.2017.1500657CM.

- [74] Z. Ding, P. Fan and H. V. Poor, "Impact of User Pairing on 5G Nonorthogonal Multiple-Access Downlink Transmissions," in *IEEE Transactions on Vehicular Technology*, vol. 65, no. 8, pp. 6010-6023, Aug. 2016, doi: 10.1109/TVT.2015.2480766.
- [75] S. M. R. Islam, M. Zeng, O. A. Dobre and K. -S. Kwak, "Resource Allocation for Downlink NOMA Systems: Key Techniques and Open Issues," in *IEEE Wireless Communications*, vol. 25, no. 2, pp. 40-47, April 2018, doi: 10.1109/MWC.2018.1700099.
- [76] Z. Q. Al-Abbasi and D. K. C. So, "Resource Allocation in Non-Orthogonal and Hybrid Multiple Access System With Proportional Rate Constraint," in *IEEE Transactions on Wireless Communications*, vol. 16, no. 10, pp. 6309-6320, Oct. 2017, doi: 10.1109/TWC.2017.2721936.
- [77] W. Liang, Z. Ding, Y. Li and L. Song, "User Pairing for Downlink Non-Orthogonal Multiple Access Networks Using Matching Algorithm," in *IEEE Transactions on Communications*, vol. 65, no. 12, pp. 5319-5332, Dec. 2017, doi: 10.1109/TCOMM.2017.2744640.
- [78] Z. Ding, Z. Yang, P. Fan and H. V. Poor, "On the Performance of Non-Orthogonal Multiple Access in 5G Systems with Randomly Deployed Users," in *IEEE Signal Processing Letters*, vol. 21, no. 12, pp. 1501-1505, Dec. 2014, doi: 10.1109/LSP.2014.2343971.
- [79] A. Benjebbour, K. Saito, A. Li, Y. Kishiyama and T. Nakamura, "Non-orthogonal multiple access (NOMA): Concept, performance evaluation and experimental trials," 2015 International Conference on Wireless Networks and Mobile Communications (WINCOM), pp. 1-6, 2015, doi: 10.1109/WINCOM.2015.7381343.
- [80] C. Cordeiro, K. Challapali, D. Birru and Sai Shankar, "IEEE 802.22: the first worldwide wireless standard based on cognitive radios," First IEEE International Symposium on New Frontiers in Dynamic Spectrum Access Networks, 2005. DySPAN 2005, 2005, pp. 328-337, doi: 10.1109/DYSPAN.2005.1542649.
- [81] R. V. Prasad, P. Pawelczak, J. A. Hoffmeyer and H. S. Berger, "Cognitive functionality in next generation wireless networks: standardization efforts," in *IEEE Communications Magazine*, vol. 46, no. 4, pp. 72-78, April 2008, doi: 10.1109/MCOM.2008.4481343.
- [82] A. Shakeel, H. Riaz, A. Iqbal, I. Khan, Q. ul Hasan, and Sh. Malik, "Analysis of Efficient Spectrum Handoff in a Multi-Class Hybrid Spectrum Access Cognitive Radio Network Using Markov Modelling," *Sensors* 19, no. 19: 4120, 2019, doi:10.3390/s19194120.

- [83] M. Hassan, M. Singh, Kh. Hamid, R. Saeed, M. Abdelhaq, and R. Alsaqour, "Design of Power Location Coefficient System for 6G Downlink Cooperative NOMA Network," *Energies*, 2022, 15(19), 6996; doi:10.3390/en15196996.
- [84] Recommendation ITU-R M.2083-0. IMT Vision—Framework and Overall Objectives of the Future Development of IMT for 2020 and Beyond. Available online: <http://www.itu.int/rec/R-REC-M.20830-201509-I/en> (accessed on 29 September 2017).
- [85] <https://enclass.hiclc.com/portal/#/planLearning/en/21091502-2306-1995-eda6-5f8a024b4227>.
- [86] F. K. Jondral, "Cognitive Radio: A Communications Engineering View," in *IEEE Wireless Communications*, vol. 14, no. 4, pp. 28-33, August 2007, doi: 10.1109/MWC.2007.4300980.
- [87] F. Khozeimeh and S. Haykin, "Brain-Inspired Dynamic Spectrum Management for Cognitive Radio Ad Hoc Networks," in *IEEE Transactions on Wireless Communications*, vol. 11, no. 10, pp. 3509-3517, October 2012, doi: 10.1109/TWC.2012.081312.111538.
- [88] T. Cui, F. Gao and A. Nallanathan, "Optimization of Cooperative Spectrum Sensing in Cognitive Radio," in *IEEE Transactions on Vehicular Technology*, vol. 60, no. 4, pp. 1578-1589, May 2011, doi: 10.1109/TVT.2011.2116815.
- [89] F. Chiti, R. Fantacci and A. Tani, "Performance Evaluation of an Adaptive Channel Allocation Technique for Cognitive Wireless Sensor Networks," in *IEEE Transactions on Vehicular Technology*, vol. 66, no. 6, pp. 5351-5363, June 2017, doi: 10.1109/TVT.2016.2621140.
- [90] H. Kim and K. G. Shin, "Efficient Discovery of Spectrum Opportunities with MAC-Layer Sensing in Cognitive Radio Networks," in *IEEE Transactions on Mobile Computing*, vol. 7, no. 5, pp. 533-545, May 2008, doi: 10.1109/TMC.2007.70751.
- [91] S. Stotas and A. Nallanathan, "On the Throughput and Spectrum Sensing Enhancement of Opportunistic Spectrum Access Cognitive Radio Networks," in *IEEE Transactions on Wireless Communications*, vol. 11, no. 1, pp. 97-107, January 2012, doi: 10.1109/TWC.2011.111611.101716.
- [92] T. Wang, L. Song, Z. Han and W. Saad, "Overlapping coalitional games for collaborative sensing in cognitive radio networks," 2013 *IEEE Wireless Communications and Networking Conference (WCNC)*, 2013, pp. 4118-4123, doi: 10.1109/WCNC.2013.6555237.
- [93] K. M. Thilina, K. W. Choi, N. Saquib and E. Hossain, "Machine Learning Techniques for Cooperative Spectrum Sensing in Cognitive Radio Networks,"

- in IEEE Journal on Selected Areas in Communications, vol. 31, no. 11, pp. 2209-2221, November 2013, doi: 10.1109/JSAC.2013.131120.
- [94] S. P. Herath, N. Rajatheva and C. Tellambura, "On the energy detection of unknown deterministic signal over Nakagami channels with selection combining," 2009 Canadian Conference on Electrical and Computer Engineering, 2009, pp. 745-749, doi: 10.1109/CCECE.2009.5090228.
- [95] S. Jayram, K. Ouahada, G. Singh, F. Mekuria, A. Pitsillides and S. Rimer, "Stochastically Resonant Spectrum Sensing Signal-to-Noise Ratio Improvements for Dynamic Spectrum Access Cognitive Radios," 2019 Fifth International Conference on Image Information Processing (ICIIP), 2019, pp. 425-430, doi: 10.1109/ICIIP47207.2019.8985904.
- [96] H. Zheng and L. Cao, "Device-centric spectrum management," First IEEE International Symposium on New Frontiers in Dynamic Spectrum Access Networks, 2005. DySPAN 2005., 2005, pp. 56-65, doi: 10.1109/DYSPAN.2005.1542617.
- [97] V. Kanodia, A. Sabharwal and E. Knightly, "MOAR: a multi-channel opportunistic auto-rate media access protocol for ad hoc networks," First International Conference on Broadband Networks, pp. 600-610, 2004, doi: 10.1109/BROADNETS.2004.46.
- [98] B. Debaillie, C. Desset and F. Louagie, "A Flexible and Future-Proof Power Model for Cellular Base Stations," 2015 IEEE 81st Vehicular Technology Conference (VTC Spring), 2015, pp. 1-7, doi: 10.1109/VTCSpring.2015.7145603.
- [99] P. Skokowski, K. Malon, J. M. Kelner, J. Dolowski, J. Lopatka and P. Gajewski, "Adaptive channels' selection for hierarchical cluster based cognitive radio networks," 2014 8th International Conference on Signal Processing and Communication Systems (ICSPCS), pp. 1-6, 2014, doi: 10.1109/ICSPCS.2014.7021123.
- [100] K. Akabane, H. Shiba, M. Matsui and K. Uehara, "An Autonomous Adaptive Base Station that Supports Multiple Wireless Network Systems," 2007 2nd IEEE International Symposium on New Frontiers in Dynamic Spectrum Access Networks, 2007, pp. 85-88, doi: 10.1109/DYSPAN.2007.18.
- [101] H. S. Mehta and S. A. Zekavat, "Dynamic Resource Allocation via Clustered MC-CDMA in Multi-Service Ad-Hoc Networks: Achieving Low Interference Temperature," 2007 2nd IEEE International Symposium on New Frontiers in Dynamic Spectrum Access Networks, 2007, pp. 266-269, doi: 10.1109/DYSPAN.2007.42.

- [102]N. Zhao, F. R. Yu, H. Sun and M. Li, "Adaptive Power Allocation Schemes for Spectrum Sharing in Interference-Alignment-Based Cognitive Radio Networks," in *IEEE Transactions on Vehicular Technology*, vol. 65, no. 5, pp. 3700-3714, May 2016, doi: 10.1109/TVT.2015.2440428.
- [103]S. K. Sharma, E. Lagunas, S. Chatzinotas and B. Ottersten, "Application of Compressive Sensing in Cognitive Radio Communications: A Survey," in *IEEE Communications Surveys & Tutorials*, vol. 18, no. 3, pp. 1838-1860, thirdquarter 2016, doi: 10.1109/COMST.2016.2524443.
- [104]B. Jabbari, R. Pickholtz and M. Norton, "Dynamic spectrum access and management [Dynamic Spectrum Management]," in *IEEE Wireless Communications*, vol. 17, no. 4, pp. 6-15, August 2010, doi: 10.1109/MWC.2010.5547916.
- [105]J. Wang, M. Dong, B. Liang, G. Boudreau and H. Abou-zeid, "Distributed Coordinated Precoding for MIMO Cellular Network Virtualization," in *IEEE Transactions on Wireless Communications*, vol. 21, no. 1, pp. 106-120, Jan. 2022, doi: 10.1109/TWC.2021.3094061.
- [106]J. Iqbal, M. A. Iqbal, A. Ahmad, M. Khan, A. Qamar and K. Han, "Comparison of Spectral Efficiency Techniques in Device-to-Device Communication for 5G," in *IEEE Access*, vol. 7, pp. 57440-57449, 2019, doi: 10.1109/ACCESS.2019.2914486.
- [107]M. B. H. Weiss, K. Werbach, D. C. Sicker and C. E. C. Bastidas, "On the Application of Blockchains to Spectrum Management," in *IEEE Transactions on Cognitive Communications and Networking*, vol. 5, no. 2, pp. 193-205, June 2019, doi: 10.1109/TCCN.2019.2914052.
- [108]S. Agarwal and S. De, "eDSA: Energy-Efficient Dynamic Spectrum Access Protocols for Cognitive Radio Networks," in *IEEE Transactions on Mobile Computing*, vol. 15, no. 12, pp. 3057-3071, 1 Dec. 2016, doi: 10.1109/TMC.2016.2535405.
- [109]Y. Lu, X. Huang, K. Zhang, S. Maharjan and Y. Zhang, "Communication-Efficient Federated Learning and Permissioned Blockchain for Digital Twin Edge Networks," in *IEEE Internet of Things Journal*, vol. 8, no. 4, pp. 2276-2288, 15 Feb.15, 2021, doi: 10.1109/JIOT.2020.3015772.
- [110]N. Pratas, N. Marchetti, N. R. Prasad, A. Rodrigues and R. Prasad, "Centralized Cooperative Spectrum Sensing for Ad-Hoc Disaster Relief Network Clusters," 2010 *IEEE International Conference on Communications*, 2010, pp. 1-5, doi: 10.1109/ICC.2010.5502710.

- [111]K. Sultan, "Best Relay Selection Schemes for NOMA Based Cognitive Relay Networks in Underlay Spectrum Sharing," in *IEEE Access*, vol. 8, pp. 190160-190172, 2020, doi: 10.1109/ACCESS.2020.3031631.
- [112]M. Bouabdellah et al., "Cooperative Energy Harvesting Cognitive Radio Networks With Spectrum Sharing and Security Constraints," in *IEEE Access*, vol. 7, pp. 173329-173343, 2019, doi: 10.1109/ACCESS.2019.2955205.
- [113]L. Lv, J. Chen and Q. Ni, "Cooperative Non-Orthogonal Multiple Access in Cognitive Radio," in *IEEE Communications Letters*, vol. 20, no. 10, pp. 2059-2062, Oct. 2016, doi: 10.1109/LCOMM.2016.2596763.
- [114]Y. Liu, Z. Ding, M. ElKashlan and J. Yuan, "Nonorthogonal Multiple Access in Large-Scale Underlay Cognitive Radio Networks," in *IEEE Transactions on Vehicular Technology*, vol. 65, no. 12, pp. 10152-10157, Dec. 2016, doi: 10.1109/TVT.2016.2524694.
- [115]L. Lv, Q. Ni, Z. Ding and J. Chen, "Application of Non-Orthogonal Multiple Access in Cooperative Spectrum-Sharing Networks Over Nakagami- m Fading Channels," in *IEEE Transactions on Vehicular Technology*, vol. 66, no. 6, pp. 5506-5511, June 2017, doi: 10.1109/TVT.2016.2627559.
- [116]L. Lv, J. Chen, Q. Ni and Z. Ding, "Design of Cooperative Non-Orthogonal Multicast Cognitive Multiple Access for 5G Systems: User Scheduling and Performance Analysis," in *IEEE Transactions on Communications*, vol. 65, no. 6, pp. 2641-2656, June 2017, doi: 10.1109/TCOMM.2017.2677942.
- [117]Y. Chen, L. Wang and B. Jiao, "Cooperative multicast non-orthogonal multiple access in cognitive radio," 2017 *IEEE International Conference on Communications (ICC)*, 2017, pp. 1-6, doi: 10.1109/ICC.2017.7996607.
- [118]J. Zhou, W. Cheng and L. Liang, "OAM Transmission in Sparse Multipath Environments with Fading," *ICC 2020 - 2020 IEEE International Conference on Communications (ICC)*, 2020, pp. 1-6, doi: 10.1109/ICC40277.2020.9149057.
- [119]W. Labidi, C. Deppe and H. Boche, "Identification for Multi-Antenna Gaussian Channels," *WSA 2021; 25th International ITG Workshop on Smart Antennas*, 2021, pp. 1-6.
- [120]G. Nauryzbayev and E. Alsusa, "Identifying the maximum DoF region in the three-cell compounded MIMO network Identifying the maximum DoF region in the three-cell compounded MIMO network," 2016 *IEEE Wireless Communications and Networking Conference*, 2016, pp. 1-5, doi: 10.1109/WCNC.2016.7564829.
- [121]A. Ksendzov, "A three-dimensional mobile-to-mobile MIMO channel model including fading correlation and pattern diversity," 2016 *5th Mediterranean*

- Conference on Embedded Computing (MECO), 2016, pp. 268-272, doi: 10.1109/MECO.2016.7525758.
- [122] Y. Tang, Y. Huang, M. Wen, L. -L. Yang and C. -B. Chae, "A Molecular Spatio-Temporal Modulation Scheme for MIMO Communications," 2021 IEEE Wireless Communications and Networking Conference (WCNC), 2021, pp. 1-6, doi: 10.1109/WCNC49053.2021.9417557.
- [123] G. Kaddoum, Y. Nijssure and H. Tran, "Generalized Code Index Modulation Technique for High-Data-Rate Communication Systems," in IEEE Transactions on Vehicular Technology, vol. 65, no. 9, pp. 7000-7009, Sept. 2016, doi: 10.1109/TVT.2015.2498040.
- [124] C. Shi, L. Ding, F. Wang, S. Salous and J. Zhou, "Joint Target Assignment and Resource Optimization Framework for Multitarget Tracking in Phased Array Radar Network," in IEEE Systems Journal, vol. 15, no. 3, pp. 4379-4390, Sept. 2021, doi: 10.1109/JSYST.2020.3025867.
- [125] H. Park and T. Hwang, "Energy efficiency of sensing-based spectrum sharing technique for cognitive radio systems," 2016 IEEE International Conference on Communications (ICC), 2016, pp. 1-6, doi: 10.1109/ICC.2016.7511211.
- [126] G. Barb and M. Ottesteanu, "4G/5G: A Comparative Study and Overview on What to Expect from 5G," 2020 43rd International Conference on Telecommunications and Signal Processing (TSP), 2020, pp. 37-40, doi: 10.1109/TSP49548.2020.9163402.
- [127] A. Sousa de Sena, D. Benevides da Costa, Z. Ding and P. H. J. Nardelli, "Massive MIMO-NOMA Networks With Multi-Polarized Antennas," in IEEE Transactions on Wireless Communications, vol. 18, no. 12, pp. 5630-5642, Dec. 2019, doi: 10.1109/TWC.2019.2937868.
- [128] Q. -U. -A. Nadeem, A. Kammoun and M. -S. Alouini, "Elevation Beamforming With Full Dimension MIMO Architectures in 5G Systems: A Tutorial," in IEEE Communications Surveys & Tutorials, vol. 21, no. 4, pp. 3238-3273, Fourthquarter 2019, doi: 10.1109/COMST.2019.2930621.
- [129] K. Hosseini, W. Yu and R. S. Adve, "Large-Scale MIMO Versus Network MIMO for Multicell Interference Mitigation," in IEEE Journal of Selected Topics in Signal Processing, vol. 8, no. 5, pp. 930-941, Oct. 2014, doi: 10.1109/JSTSP.2014.2327594.
- [130] K. Senel, H. V. Cheng, E. Björnson and E. G. Larsson, "What Role can NOMA Play in Massive MIMO?," in IEEE Journal of Selected Topics in Signal Processing, vol. 13, no. 3, pp. 597-611, June 2019, doi: 10.1109/JSTSP.2019.2899252.

- [131]S. Bhandari and S. Joshi, "Cognitive Radio Technology in 5G Wireless Communications," 2018 2nd IEEE International Conference on Power Electronics, Intelligent Control and Energy Systems (ICPEICES), Delhi, India, 2018, pp. 1115-1120, 2018.
- [132]L. Lv, J. Chen, Q. Ni, Z. Ding and H. Jiang, "Cognitive Non-Orthogonal Multiple Access with Cooperative Relaying: A New Wireless Frontier for 5G Spectrum Sharing," in IEEE Communications Magazine, vol. 56, no. 4, pp. 188-195, April 2018.
- [133]Z. Shi, W. Gao, S. Zhang, J. Liu and N. Kato, "AI-Enhanced Cooperative Spectrum Sensing for Non-Orthogonal Multiple Access," in IEEE Wireless Communications, vol. 27, no. 2, pp. 173-179, April 2020.
- [134]S. Sodagari and H. Jafarkhani, "Enhanced Spectrum Sharing and Cognitive Radio Using Asynchronous Primary and Secondary Users," in IEEE Communications Letters, vol. 22, no. 4, pp. 832-835, April 2018.
- [135]P. K. Sangdeh, H. Pirayesh, A. Quadri and H. Zeng, "A Practical Spectrum Sharing Scheme for Cognitive Radio Networks: Design and Experiments," in IEEE/ACM Transactions on Networking, vol. 28, no. 4, pp. 1818-1831, Aug. 2020.
- [136]P. K. Sangdeh, H. Pirayesh, H. Zeng and H. Li, "A Practical Underlay Spectrum Sharing Scheme for Cognitive Radio Networks," IEEE INFOCOM 2019 - IEEE Conference on Computer Communications, Paris, France, pp. 2521-2529, 2019.
- [137]V. Kumar, B. Cardiff and M. F. Flanagan, "Fundamental Limits of Spectrum Sharing for NOMA-Based Cooperative Relaying Under a Peak Interference Constraint," in IEEE Transactions on Communications, vol. 67, no. 12, pp. 8233-8246, Dec. 2019.
- [138]P. Kansal, A. Kumar and M. Gangadharappa, "Cognitive Radio based Spectrum Sharing technique for 5G system," 2020 7th International Conference on Signal Processing and Integrated Networks (SPIN), Noida, India, pp. 332-337, 2020.
- [139]W. Zhang, C. Wang, X. Ge and Y. Chen, "Enhanced 5G Cognitive Radio Networks Based on Spectrum Sharing and Spectrum Aggregation," in IEEE Transactions on Communications, vol. 66, no. 12, pp. 6304-6316, Dec. 2018.
- [140]S. K. Sharma, T. E. Bogale, L. B. Le, S. Chatzinotas, X. Wang and B. Ottersten, "Dynamic Spectrum Sharing in 5G Wireless Networks With Full-Duplex Technology: Recent Advances and Research Challenges," in IEEE Communications Surveys & Tutorials, vol. 20, no. 1, pp. 674-707, First quarter 2018.

- [141]S. Arzykulov, T. A. Tsiftsis, G. Nauryzbayev and M. Abdallah, "Outage Performance of Cooperative Underlay CR-NOMA With Imperfect CSI," in *IEEE Communications Letters*, vol. 23, no. 1, pp. 176-179, Jan. 2019.
- [142]S. Singh, M. Bansa, "Performance analysis of non-orthogonal multiple access assisted cooperative relay system with channel estimation errors and imperfect successive interference cancellation," *Transactions on Emerging Telecommunications Technologies*, vol. 32, Issue 12, July 2022, doi:10.1002/dac.5304.
- [143]K. Srinivasarao, S. Maruthu, "Outage analysis of cooperative NOMA system with imperfect successive interference cancellation and channel state information over Rayleigh fading channel," *International Journal of Communication Systems*, 20 July 2022, doi:10.1002/dac.5304.
- [144]A. Celik, F. S. Al-Qahtani, R. M. Radaydeh and M. -S. Alouini, "Cluster Formation and Joint Power-Bandwidth Allocation for Imperfect NOMA in DL-HetNets," *GLOBECOM 2017 - 2017 IEEE Global Communications Conference*, 2017, pp. 1-6, doi: 10.1109/GLOCOM.2017.8254637.
- [145]J. Zeng et al., "Investigation on Evolving Single-Carrier NOMA Into Multi-Carrier NOMA in 5G," in *IEEE Access*, vol. 6, pp. 48268-48288, 2018, doi: 10.1109/ACCESS.2018.2868093.
- [146]S. M. R. Islam, N. Avazov, O. A. Dobre and K. S. Kwak, "Power-Domain Non-Orthogonal Multiple Access (NOMA) in 5G Systems: Potentials and Challenges," in *IEEE Communications Surveys & Tutorials*, vol. 19, no. 2, pp. 721-742, Secondquarter 2017, doi: 10.1109/COMST.2016.2621116.
- [147]R. Alsaqour, E. S. Ali, R. A. Mokhtar, R. A. Saeed, H. Alhumyani and M. Abdelhaq, "Efficient Energy Mechanism in Heterogeneous WSNs for Underground Mining Monitoring Applications," in *IEEE Access*, vol. 10, pp. 72907-72924, 2022, doi: 10.1109/ACCESS.2022.3188654.
- [148]T. Balachander, M.B.M. Krishnan, "Efficient Utilization of Cooperative Spectrum Sensing (CSS) in Cognitive Radio Network (CRN) Using Non-orthogonal Multiple Access (NOMA)," *Wireless Pers Commun* 127, 2189–2210 (2022). doi:10.1007/s11277-021-08776-
- [149]T. Perarasi, G. Nagarajan, R. Gayathri, M. Leeban Moses, "Evaluation of cooperative spectrum sensing with filtered bank multi carrier utilized for detecting in cognitive radio network," vol33, Issue7, First published: 15 March 2022, doi:10.1002/ett.4478.
- [150]A. S. Parihar, P. Swami, V. Bhatia and Z. Ding, "Performance Analysis of SWIPT Enabled Cooperative-NOMA in Heterogeneous Networks Using Carrier

- Sensing," in *IEEE Transactions on Vehicular Technology*, vol. 70, no. 10, pp. 10646-10656, Oct. 2021, doi: 10.1109/TVT.2021.3110806.
- [151] P. Thakur, and G. Singh, "Performance analysis of MIMO-based CR–NOMA communication systems", vol.14, pp. 2677-2686,01 October 2020, doi:10.1049/iet-com.2019.0988.
- [152] M. Hassan, M. Singh, K. Hamid, R. Saeed, M. Abdelhaq, R. Alsaqour, " Modeling of NOMA-MIMO-Based Power Domain for 5G Network under Selective Rayleigh Fading Channels, " *Energies*. 2022; 15(15):5668. doi:10.3390/en15155668.
- [153] A.M. Mukhtar, R.A. Saeed, R.A. Mokhtar, E.S. Ali, H. Alhumyani, " Performance Evaluation of Downlink Coordinated Multipoint Joint Transmission under Heavy IoT Traffic Load, " *Wirel. Commun. Mob. Comput.* 2022, 2022, 6837780.
- [154] D.T. Do, T.L. Nguyen, S. Ekin, Z. Kaleem, M. Voznak, "Joint user grouping and decoding order in uplink/downlink MISO/SIMO-NOMA, " *IEEE Access* 2020, 8, 143632–143643.
- [155] M.S. Elbamby, M. Bennis, W. Saad, M. Debbah, M. Latva-Aho, "Resource optimization and power allocation in in-band full duplex-enabled non-orthogonal multiple access networks, " *IEEE J. Sel. Areas Commun.* 2017, 35, 2860–2873.
- [156] N.M. Elfatih, M.K. Hasan, Z. Kamal, D. Gupta, R.A Saeed, E.S Ali, M.S. Hosain, " Internet of vehicle's resource management in 5G networks using AI technologies: Current status and trends, " *IET Commun.* 2022, 16, 400–420.
- [157] J. W. Kim, S. Y. Shin and V. C. M. Leung, "Performance Enhancement of Downlink NOMA by Combination With GSSK," in *IEEE Wireless Communications Letters*, vol. 7, no. 5, pp. 860-863, Oct. 2018, doi: 10.1109/LWC.2018.2833469.
- [158] D. Shen, C. Wei, X. Zhou, L. Wang, C. Xu, "Photon Counting Based Iterative Quantum Non-Orthogonal Multiple Access with Spatial Coupling, " In *Proceedings of the 2018 IEEE Global Communications Conference (GLOBECOM)*, Abu Dhabi, United Arab Emirates, 9–13 December 2018; pp. 1–6.
- [159] J. Choi, " Minimum power multicast beamforming with superposition coding for multiresolution broadcast and application to NOMA systems, " *IEEE Trans. Commun.* 2015, 63, 791–800.
- [160] R.A. Mokhtar, R.A. Saeed, H. Alhumyani, " Cooperative Fusion Architecture-based Distributed Spectrum Sensing Under Rayleigh Fading Channel, " *Wirel. Pers. Commun.* 2022, 124, 839–865.

- [161]M. Hassan, M. Singh and K. Hamid, " IMPACT OF POWER AND BANDWIDTH ON THE CAPACITY RATE AND NUMBER OF USERS IN SC-NOMA," VOL. Publisher Harbin Gongye Daxue, 53 NO. 9 (2021).
- [162]M. Hassan, M. Singh and K. Hamid, "Average Rate Performance for Pairing Downlink NOMA Networks Schemes," 2022 International Conference on Smart Information Systems and Technologies (SIST), Nur-Sultan, Kazakhstan, 2022, pp. 1-4, doi: 10.1109/SIST54437.2022.9945815.
- [163]Y.T. Abdelrahman, R.A. Saeed, A. El-Tahir, "Multiple Physical Layer Pipes performance for DVB-T2, " In Proceedings of the 2017 International Conference on Communication, Control, Computing and Electronics Engineering (ICCCCEE), Khartoum, Sudan, 16–18 January 2017; pp. 1–7.
- [164]T. Nguyen, D.T. Do, " Novel multiple access for cooperative networks with nakagami-m fading: system model and performance analysis," Indonesian Journal of Electrical Engineering and Computer Science 2020, 19, 233-240.
- [165]H.T. Van, T.A. Vo, D.H. Le, M.Q. Phu, H.S. Nguyen, " Outage performance analysis of non-orthogonal multiple access systems with RF energy harvesting," International Journal of Electrical and Computer Engineering 2021, 11, 4135.
- [166]Z. Ding, M. Peng, H.V. Poor, "Cooperative non-orthogonal multiple access in 5G systems," IEEE Communications Letters 2015, 19, 1462-1465.
- [167]Y. Zhang, H. Wang, Q. Yang, Z. Ding, " Secrecy sum rate maximization in non-orthogonal multiple access, " IEEE Communications Letters 2016, 20, 930-933.
- [168]Z. Ding, P. Fan, H.V. Poor, " Random beamforming in millimeter-wave NOMA networks," IEEE access 2017, 5, 7667-7681.
- [169]M. Aldababsa, O. Kucur, "Outage and ergodic sum-rate performance of cooperative MIMO-NOMA with imperfect CSI and SIC," International Journal of Communication Systems, Vol33, Issue11, 25 July 2020, doi:10.1002/dac.4405.
- [170]S. Mondal, D. Sanjay, S. Kundu, "Outage analysis for NOMA-based energy harvesting relay network with imperfect CSI and transmit antenna selection," IET Communications, Vol14, Issue14, Pages 2240-2249, August 2020 , doi:10.1049/iet-com.2019.0841.
- [171]S. Shashank, S. Muralikrishnan, K. Sheetal, "Outage Probability of Uplink Cell-Free Massive MIMO Network with Imperfect CSI Using Dimension-Reduction Method, Information Theory," Feb 2021, version, v2, doi:10.48550/arXiv.2101.07737.
- [172]S.amal, M.Rihan, S.Hussin, A.Zaghloul, A.Salem, "Multiple access in cognitive radio networks: from orthogonal and non-orthogonal to rate-splitting," IEEE Access, 2021, 9, pp. 95569-95584.

- [173] M. Hamdi, R. Saeed, A. Abbas, "Downlink scheduling in 5G massive MIMO," *Journal of Engineering and Applied Sciences*, 2018, 13(6), pp. 1376-1381.
- [174] K. L. A. Yau, J. Qadir; C. Wu; M. A. Imran and M. H. Ling. Cognition-Inspired 5G Cellular Networks: A Review and the Road Ahead," in *IEEE Access*, 2018, vol. 6, pp. 35072-35090, doi: 10.1109/ACCESS.2018.2849446.
- [175] MS. Van Nguyen, DT. Do, Z.D Zaharis, "Enabling Full-duplex in MEC Networks Using Uplink NOMA in Presence of Hardware Impairments," *Wireless Pers Commun*, 2021, 120, vol. 120, pp. 1945–1973. <https://doi.org/10.1007/s11277-021-08102-1>.
- [176] M. Cheng; W. Lin and T. Matsumoto, "Down-Link NOMA With Successive Refinement for Binary Symmetric Source Transmission," in *IEEE Transactions on Communications*, vol. 68, no. 12, pp. 7927-7937, Dec. 2020, doi: 10.1109/TCOMM.2020.3022400.
- [177] DT. Do and CB. Le, "Ergodic capacity computation in cognitive radio aided non-orthogonal multiple access systems," *Bulletin of Electrical Engineering and Informatics*, vol. 11, no. 1, February 2022, pp. 270-277, doi: 10.11591/eei.v11i1.3297.
- [178] K. Ferdi ; K. Hakan, "The error performance analysis of the decode-forward relay-aided-NOMA systems and a power allocation scheme for user fairness," *Journal of the Faculty of Engineering and Architecture of Gazi University*, 2020, 35. 97-108, doi:10.17341/gazimmfd.441452.
- [179] W. Han; X. Ma; D. Tang and N. Zhao, "Study of SER and BER in NOMA Systems," in *IEEE Transactions on Vehicular Technology*, 2021, vol. 70, no. 4, pp. 3325-3340, doi: 10.1109/TVT.2021.3062890.
- [180] A. A. Amin and S. Y. Shin, "Capacity Analysis of Cooperative NOMA-OAM-MIMO Based Full-Duplex Relaying for 6G," in *IEEE Wireless Communications Letters*, 2021, vol. 10, no. 7, pp. 1395-1399, doi: 10.1109/LWC.2021.3068654.
- [181] M. Zeng; A. Yadav; O. A. Dobre; G. I. Tsiropoulos and H. V, "Poor. Capacity Comparison Between MIMO-NOMA and MIMO-OMA With Multiple Users in a Cluster," in *IEEE Journal on Selected Areas in Communications*, 2017, vol. 35, no. 10, pp. 2413-2424, doi: 10.1109/JSAC.2017.2725879.
- [182] B. Mona, S. Elmustafa, A. Rashid, "Ultra-Massive mimo in thz communications, Book: Next generation wireless terahertz communication networks," CRC group, Taylor & Francis Group, USA, 2020.
- [183] W. A. Al-Hussaibi and F. H. Ali, "Efficient User Clustering, Receive Antenna Selection, and Power Allocation Algorithms for Massive MIMO-NOMA Systems," in *IEEE Access*, 2019, vol. 7, pp. 31865-31882, doi: 10.1109/ACCESS.2019.2902331.